



HAL
open science

Propagation des ondes dans les plaques multicouches : le modèle du Bending-Gradient et la méthode des développements asymptotiques

Nadine Bejjani

► **To cite this version:**

Nadine Bejjani. Propagation des ondes dans les plaques multicouches : le modèle du Bending-Gradient et la méthode des développements asymptotiques. Autre. Université Paris-Est; Université Saint-Joseph (Beyrouth). Ecole supérieure d'ingénieurs de Beyrouth, 2019. Français. NNT : 2019PESC1025 . tel-02915304

HAL Id: tel-02915304

<https://pastel.hal.science/tel-02915304>

Submitted on 14 Aug 2020

HAL is a multi-disciplinary open access archive for the deposit and dissemination of scientific research documents, whether they are published or not. The documents may come from teaching and research institutions in France or abroad, or from public or private research centers.

L'archive ouverte pluridisciplinaire **HAL**, est destinée au dépôt et à la diffusion de documents scientifiques de niveau recherche, publiés ou non, émanant des établissements d'enseignement et de recherche français ou étrangers, des laboratoires publics ou privés.

Propagation des ondes dans les plaques multicouches : le modèle du Bending-Gradient et la méthode des développements asymptotiques.

THÈSE

présentée et soutenue publiquement le Lundi 2 décembre 2019

pour l'obtention du grade du

Docteur de l'Université Paris-Est
et
Docteur de l'Université Saint-Joseph - Liban
(Spécialité Mathématiques)

par

Nadine BEJJANI

Composition du jury

<i>Président :</i>	SAYAH Toni
<i>Rapporteurs :</i>	BOUTIN Claude SEPPECHER Pierre
<i>Examineur :</i>	LEBEE Arthur
<i>Directeur de Thèse :</i>	SAB Karam
<i>Co-Directeur de Thèse :</i>	BODGI Joanna

Remerciements

J'aimerais tout d'abord remercier chaleureusement mon directeur de thèse, Professeur Karam SAB, qui m'a intégrée au sein de son équipe et m'a octroyé sa confiance. Je lui adresse ma gratitude pour le temps accordé, sa gentillesse, son exigence, sa rigueur scientifique et les nombreux encouragements prodigués.

Un très grand merci à ma co-directrice de thèse, Docteur Joanna BODGI pour son encadrement, son attention et ses sages conseils qui m'ont permis de mener à bien ce travail.

Je souhaite exprimer ma profonde reconnaissance au Docteur Arthur LEBEE pour ses conseils avisés, son enthousiasme, sa disponibilité et son implication tout au long de ce travail. J'ai pris un grand plaisir à travailler avec lui.

Je tiens à remercier cordialement M. Claude BOUTIN et M. Pierre SEPPECHER, respectivement Professeurs à L'École Nationale Des Travaux Publics de L'Etat et à l'Université de Toulon et du Var, pour avoir accepté d'être rapporteurs de ce travail.

Mes vifs remerciements s'adressent également à Professeur Toni SAYAH qui a accepté de présider mon jury de thèse.

Je remercie Pierre MARGERIT pour l'aide qu'il m'a offerte dans la partie concernant les éléments finis et pour ses résultats que j'ai utilisés comme référence dans mon travail.

Je souhaite exprimer ici tout le plaisir que j'ai eu à travailler au sein du laboratoire Navier. Que tous ses membres en soient remerciés, en particulier Marie-Françoise KASPI pour sa gentillesse remarquable et son affection.

Je remercie également les doctorants en France et au Liban qui m'ont cotoyé pendant ma thèse et avec qui j'ai partagé des moments inoubliables.

Mes remerciements vont aussi à mes proches et mes amis qui, avec cette question fréquente, "quand est-ce que tu vas soutenir ta thèse?", bien que stressante, ont été à mes côtés pour me remonter le moral durant toutes ces années.

Je dédie cette thèse à ma famille, mon père et ma mère sans lesquels je n'en serais pas là aujourd'hui. Leur soutien inconditionnel et leur présence dans les moments difficiles m'ont été indispensables.

Résumé

Cette thèse est consacrée à la modélisation de la propagation des ondes planes dans les plaques multicouches infinies, dans le cadre de l'élasticité linéaire. L'objet du travail est de trouver une approximation analytique ou semi-analytique des relations de dispersion des ondes lorsque le rapport de l'épaisseur de la plaque sur la longueur d'onde est petit. Ces relations de dispersion, liant la fréquence angulaire et le nombre d'onde, fournissent des informations clés sur les caractéristiques de propagation des différents modes. On propose dans cette thèse deux modélisations : le modèle du Bending-Gradient et la méthode des développements asymptotiques. La pertinence de ces méthodes est testée en comparant leurs prédictions à celles des théories de plaques bien connues, et à des résultats de référence obtenus par la méthode des éléments finis. Au préalable, dans la première partie de la thèse, une justification mathématique de la théorie du Bending-Gradient dans le cadre statique est réalisée à l'aide des méthodes variationnelles. Il s'agit d'abord d'identifier les espaces mathématiques dans lesquels les problèmes variationnels du Bending-Gradient sont bien posés. Puis, des théorèmes d'existence et d'unicité des solutions correspondantes sont ensuite formulés et prouvés. La deuxième partie est consacrée à la formulation des équations du mouvement du Bending-Gradient. Des simulations numériques sont effectuées pour plusieurs types d'empilements, permettant ainsi de tester la validité du modèle pour la modélisation de la propagation des ondes de flexion. La troisième partie est dédiée à l'analyse asymptotique des équations tridimensionnelles du mouvement, menée à bien grâce à la méthode des développements asymptotiques, le petit paramètre étant le rapport de l'épaisseur sur la longueur d'onde. En supposant que les champs tridimensionnels s'écrivent comme des séries en puissance du petit paramètre, on obtient une succession de problèmes à résoudre en cascade. La validité de cette méthode est évaluée par comparaison avec la méthode des éléments finis.

Abstract

This thesis is dedicated to the modelling of plane wave propagation in infinite multilayered plates, in the context of linear elasticity. The aim of this work is to find an analytical or semi-analytical approximation of the wave dispersion relations when the ratio of the thickness to the wavelength is small. The dispersion relations, linking the angular frequency and the wave number, provide key information about the propagation characteristics of the wave modes. Two methods are proposed in this thesis : the Bending-Gradient model and the asymptotic expansion method. The relevance of these methods is tested by comparing their predictions to those of well-known plate theories, and to reference results computed using the finite element method. Preliminarily, the first part of the thesis is devoted to the mathematical justification of the Bending-Gradient theory in the static framework using variational methods. The first step is to identify the mathematical spaces in which the variational problems of the Bending-Gradient are well posed. A series of existence and uniqueness theorems of the corresponding solutions are then formulated and proved. The second part is dedicated to the formulation of the equations of motion of the Bending-Gradient theory. Numerical simulations are realized for different types of layer stacks to assess the ability of this model to correctly predict the propagation of flexural waves. The third part is concerned with the asymptotic analysis of the three-dimensional equations of motion, carried out using the asymptotic expansion method, the small parameter being the ratio of the thickness to the wavelength. Assuming that the three-dimensional fields can be written as expansions in power of the small parameter, a series of problems which can be solved recursively is obtained. The validity of this method is evaluated by comparison with the finite element method.

Table des matières

Résumé	ii
Abstract	iii
Table des figures	viii
Liste des tableaux	ix

Introduction	1
---------------------	----------

Chapitre 1	
The Bending-Gradient Theory for Thick Plates : Existence and Uniqueness Results	3

1.1	Introduction	4
1.2	Notations and preliminaries	6
1.2.1	Tensors	6
1.2.2	Functional spaces	8
1.3	The Bending-Gradient problem	11
1.3.1	The 3D configuration	11
1.3.2	The Bending-Gradient theory	13
1.3.2.1	Generalized stresses	13
1.3.2.2	Generalized displacements	14

1.3.2.3	Equilibrium equations	15
1.3.2.4	Constitutive equations	15
1.3.2.5	Summary of the Bending-Gradient plate theory	16
1.3.2.6	Minimum of the potential energy	17
1.3.2.7	Minimum of the complementary energy	17
1.4	Mathematical formulation of the Bending-Gradient problem for a fully clamped plate	18
1.4.1	Stress formulation	18
1.4.2	Well-posedness of the stress formulation	19
1.4.3	Well-posedness of the displacement formulation	20
1.4.3.1	Coercivity of the bilinear form a	21
1.4.3.2	Existence and uniqueness of the solution to (1.52)	22
1.4.4	Relation between the stress and the displacement formulations	23
1.5	Mathematical formulation of the Bending-Gradient problem for a loaded plate with free boundary conditions	25
1.5.1	Formulation of the problem	25
1.5.2	Coercivity of the bilinear form \check{a}	28
1.5.3	Well-posedness of the minimization problem for free boundary conditions	31
1.5.4	Equivalence to a stress formulation	32
1.6	Simple Support Boundary Conditions	33
1.7	Formulation of the Bending-Gradient theory in the general case	34
1.7.1	Stress formulation	36
1.7.2	Displacement formulation	37
1.8	Regularization of the shear force compliance tensor	38
1.8.1	The regularized problem	38
1.8.2	Convergence of the regularized solution	38
1.9	Conclusion	41

Chapitre 2**The Bending-Gradient theory for flexural wave propagation in composite plates****42**

2.1	Introduction	43
2.2	Notations	44
2.3	The Bending-Gradient Model for the equilibrium of thick plates	45
2.3.1	The 3D plate configuration	45
2.3.2	The Bending-Gradient equations	46
2.3.3	Homogeneous plates	47
2.3.4	Projection of the Bending-Gradient plate model	48
2.3.4.1	The Shear Compliance Projection (SCP)	48
2.3.4.2	The Shear Stiffness Projection (SSP)	49
2.3.5	Kelvin Notations	49
2.3.6	The reduction method	51
2.4	Propagation of plane waves in an anisotropic plate	53
2.4.1	Exact dispersion curves for guided waves	53
2.4.1.1	Three-dimensional equations of motion	53
2.4.1.2	Resolution by means of Finite Element Analysis	54
2.4.2	Plate models dispersion curves	55
2.4.2.1	Bending-Gradient equations of motion	55
2.4.2.2	Implementation of plate dispersion equations	56
2.4.2.3	Reissner-Mindlin and Kirchhoff-Love plate models	59
2.5	Numerical Results and Verification	59
2.6	Conclusion	65

Chapitre 3 On asymptotic expansions for modelling wave propagation in composite plates	66
---	-----------

3.1	Introduction	67
3.2	Notations	69
3.3	Propagation of plane waves in composite plates	69
3.3.1	Exact dispersion curves for guided waves	69
3.3.1.1	Three-dimensional equations of motion	69
3.3.1.2	Resolution by means of Finite Element Analysis	72
3.4	The asymptotic expansion method	72
3.4.1	The asymptotic expansion framework	72
3.4.1.1	Scaling	73
3.4.1.2	Expansion	74
3.4.2	Cascade resolution	75
3.4.2.1	The case of in-plane membranal waves : $\alpha_0 \neq 0$ and $V_3^{-1} = 0$	79
3.4.2.2	The case of flexural (or bending) waves : $\alpha_0 = 0$ and $V_3^{-1} \neq 0$	84
3.5	Numerical results	88
3.5.1	Flexural waves	89
3.5.2	In-plane membranal waves	95
3.5.2.1	Longitudinal waves	96
3.5.2.2	In-plane shear waves	96
3.6	Conclusion	100

Conclusions et perspectives	103
------------------------------------	------------

Annexes

Bibliographie	113
----------------------	------------

Table des figures

1.1	The 3D configuration	12
2.1	The 3D configuration	46
2.2	Comparison of the dispersion curves for a $[0^\circ, 90^\circ]_s$ ply	61
2.3	Comparison of the dispersion curves for a $[-30^\circ, 30^\circ]_s$ ply	61
2.4	Comparison of the dispersion curves for a $[0^\circ, -45^\circ, 90^\circ, 45^\circ]_s$ ply	62
2.5	Comparison of the dispersion curves for a $[\text{GFRP}, \text{Al}, \text{GFRP}, \text{Al}]_s$ ply	64
3.1	Comparison of the flexural dispersion curves for a $[0^\circ, 90^\circ]_s$ ply	90
3.2	Comparison of the flexural dispersion curves for a $[0^\circ, 90^\circ]_s$ ply	91
3.3	Comparison of the flexural dispersion curves for a $[-30^\circ, 30^\circ]_s$ ply	92
3.4	Comparison of the flexural dispersion curves for a $[0^\circ, -45^\circ, 90^\circ, 45^\circ]_s$ ply	93
3.5	Comparison of the flexural dispersion curves for a $[\text{GFRP}, \text{Al}, \text{GFRP}, \text{Al}]_s$ ply	94
3.6	Comparison of longitudinal dispersion curves for a $[0^\circ, 90^\circ]_s$ ply	96
3.7	Comparison of longitudinal dispersion curves for a $[-30^\circ, 30^\circ]_s$ ply	97
3.8	Comparison of longitudinal dispersion curves for a $[0^\circ, -45^\circ, 90^\circ, 45^\circ]_s$ ply	97
3.9	Comparison of longitudinal dispersion curves for a $[\text{GFRP}, \text{Al}, \text{GFRP}, \text{Al}]_s$ ply	98
3.10	Comparison of longitudinal dispersion curves for a $[\text{GFRP}, \text{Al}, \text{GFRP}, \text{Al}]_s$ ply	98
3.11	Comparison of in-plane shear dispersion curves for a $[0^\circ, 90^\circ]_s$ ply	99
3.12	Comparison of in-plane shear wave dispersion curves for a $[-30^\circ, 30^\circ]_s$ ply	99
3.13	Comparison of in-plane shear wave dispersion curves for a $[0^\circ, -45^\circ, 90^\circ, 45^\circ]_s$ ply	100
3.14	Comparison of in-plane shear dispersion curves for a $[\text{GFRP}, \text{Al}, \text{GFRP}, \text{Al}]_s$ ply	101

Liste des tableaux

2.1	Elastic properties of the laminate, E and G in Pa , ρ in kg/m^3	60
2.2	Relative error of plate models compared to finite element results with $h/\lambda = 0.3$	62
2.3	Relative error of plate models compared to finite element results for a $[0^\circ, -45^\circ, 90^\circ, 45^\circ]_s$ ply with $h/\lambda = 0.3$	63
2.4	Elastic properties of epoxy-glass fiber composite material Renno et al. (2013), E and G in Pa , ρ in kg/m^3	63
2.5	Elastic properties of aluminium material Liu et al. (2016), E and G in Pa , ρ in kg/m^3	64
2.6	Relative error of plate models compared to finite element results with $h/\lambda = 0.3$ for a $[0^\circ, 0^\circ, 90^\circ, 0^\circ]_s$ ply	64
3.1	Elastic properties of the laminate, E and G in Pa , ρ in kg/m^3 (Lebée and Sab, 2015; Pagano, 1969)	89
3.2	Elastic properties of epoxy-glass fiber composite material, E and G in Pa , ρ in kg/m^3 (Renno et al., 2013)	89
3.3	Elastic properties of aluminium material, E and G in Pa , ρ in kg/m^3 (Liu et al., 2016)	95

Introduction

La propagation des ondes est l'un des phénomènes physiques les plus usuels, dont l'importance pratique est considérable, étant à la base de la transmission d'informations diverses dans notre environnement quotidien (propagation de la lumière, du son, d'ondes radios, ...). C'est un domaine très vaste ayant des applications dans plusieurs disciplines.

En géophysique par exemple, les tremblements de terre sont détectés en mesurant les ondes qu'ils créent. Les ondes sont aussi utilisées pour les prospections du pétrole et du gaz et pour étudier la structure géologique de la Terre.

Une autre application très commune des ondes est le contrôle non destructif (CND) visant à déceler la présence de failles dans une structure sans avoir à altérer les propriétés physiques de celle-ci. Le contrôle non destructif est capital pour les industries de fabrication comme l'industrie pétrolière (pipelines, réservoirs, ...), l'aéronautique (ailes d'avion, pièces moteurs, ...), l'industrie nucléaire (tube d'échangeur de chaleur, générateur de vapeur,...).

Nombreux sont les efforts qui ont été déployés dans le domaine des structures et des matériaux visant à modéliser correctement la propagation des ondes dans les plaques élastiques. Cet intérêt a été suscité notamment par l'expansion récente de l'utilisation des matériaux composites dans l'aéronautique, les constructions navales, le transport automobile ou dans le bâtiment, du fait des nombreux avantages qu'ils offrent par rapport aux matériaux métalliques conventionnels. On cite en premier leur formidable durabilité et leur bonne résistance à la fatigue, à la corrosion et à la plupart des conditions environnementales, ce qui leur permet de garder indéfiniment leurs structures. Les matériaux composites sont aussi caractérisés par un grand rapport raideur/masse qui permet un allègement conséquent des structures, notamment recherché dans les domaines précités. Cependant, leur usage intensif reste limité par la nécessité de localiser les défauts ou les dégradations lors de leur fabrication et donc de s'assurer de leur intégrité.

Plusieurs sont les paramètres structuraux qui influent sur le comportement mécanique et dynamique des plaques composites : la nature des matériaux constitutifs (propriétés chimiques, densité), les épaisseurs relatives des différentes couches et leurs séquences d'empilement. Etant hétérogènes et fortement anisotropes, la caractérisation des propriétés mécaniques des structures composites et la prédiction de leur réponse dynamique représentent un enjeu important.

Dans ce travail, deux approches principales sont proposées pour étudier la propagation des ondes élastiques dans les plaques composites infinies. De plus, une évaluation du compro-

mis entre la simplicité et l'exactitude de ces approches pour le problème de propagation des ondes est présentée.

La première se place dans le cadre de la modélisation du problème 3D par un problème 2D et est basée sur un nouveau modèle de plaque en statique, créé récemment au laboratoire Navier, connu sous le nom du Bending-Gradient. Ce modèle peut être considéré comme une extension aux plaques hétérogènes du modèle de Reissner-Mindlin.

Nous consacrons tout d'abord le chapitre 1 à une justification mathématique détaillée de la théorie du Bending-Gradient dans le cadre statique par le biais des méthodes variationnelles. Les définitions principales des champs statiques et cinématiques ainsi que les équations du Bending-Gradient sont expliquées en détail. Dans notre étude, on se concentre en particulier sur les plaques encastées et libres. La première étape consiste à expliciter les formulations variationnelles en contrainte et en déplacement du problème en se basant sur le principe du minimum de l'énergie potentielle et celui de l'énergie complémentaire. Nous définissons ensuite les espaces fonctionnels appropriés, dans lesquels ces formulations sont bien posées. Enfin, des théorèmes d'existence et d'unicité de la solution du problème sont formulés et prouvés.

Le chapitre 2 concerne l'évaluation de la validité de la théorie du Bending-Gradient pour la modélisation de la propagation des ondes de flexion dans des plaques symétriques, hétérogènes et anisotropes. Les équations régissant la propagation des ondes dans ces structures sont formulées en premier en tenant compte des déformations du cisaillement transverse et en négligeant les effets d'inertie en rotation. Nous détaillons ensuite la résolution et l'implémentation de ces équations. Des simulations numériques sont effectuées pour plusieurs types d'empilements. La pertinence du modèle est testée en comparant les résultats obtenus à ceux prédits à partir de la méthode des éléments finis spectraux. Nous présentons aussi les résultats obtenus pour le modèle de Kirchhoff-Love et la théorie de déformation en cisaillement du premier ordre.

La deuxième approche s'inspire des travaux de Lebée and Sab (2013) et consiste à mettre en oeuvre la méthode des développements asymptotiques pour l'étude de la propagation des ondes planes dans les plaques composites élancées.

Le chapitre 3 débute par un rappel des équations tridimensionnelles du mouvement. Les champs tridimensionnels, solutions de ces équations, sont recherchés sous la forme d'un développement asymptotique en puissance croissante d'un petit paramètre, égal au rapport de l'épaisseur sur la longueur d'onde. Le problème initial se décompose alors en une série de problèmes simplifiés dont la résolution permet de déterminer des approximations successives de la solution. La performance de la méthode des développements asymptotiques est évaluée en la comparant à la méthode des éléments finis et aux théories de plaque de Kirchhoff-Love, de déformation en cisaillement du premier ordre et du Bending-Gradient.

Nous terminons enfin par une conclusion générale qui comporte les résultats essentiels établis dans ce travail de thèse et nous proposons quelques perspectives de recherche.

Chapitre 1

The Bending-Gradient Theory for Thick Plates : Existence and Uniqueness Results

*Ce chapitre vise à exploiter les méthodes variationnelles afin de donner une justification mathématique de la théorie du Bending-Gradient en statique. On présente tout d'abord les définitions des contraintes et des déformations généralisées ainsi que les équations de compatibilité, les équations d'équilibre et les équations constitutives du Bending-Gradient. On passe ensuite à formuler les problèmes variationnels en déplacement et en contrainte. Le principe est de montrer l'existence et l'unicité des solutions de ces problèmes pour tous types de conditions aux bords. Ce chapitre a été publié dans la revue *Journal of Elasticity* sous la référence *Bejjani et al. (2018)*.*

Abstract

This paper is devoted to the mathematical justification of the Bending-Gradient theory which is considered as the extension of the Reissner-Mindlin theory (or the First Order Shear Deformation Theory) to heterogeneous plates. In order to rigorously assess the well-posedness of the Bending-Gradient problems, we first assume that the compliance tensor related to the generalized shear force is positive definite. We define the functional spaces to which the variables of the theory belong, then state and prove the existence and uniqueness theorems of solutions of the Bending-Gradient problems for clamped and free plates, as well as for simply supported plates. The obtained results are afterward extended to the general case, i.e., when the compliance tensor related to generalized shear forces is not definite.

1.1 Introduction

Plates are three-dimensional structures with a small dimension compared to the other two dimensions. Numerous approaches were suggested in order to replace the three-dimensional problem by a two-dimensional problem while guaranteeing accuracy of the three-dimensional fields' information. The passage from the 3D problem to a 2D plate theory is known as dimensional reduction. It also makes the theory easier to understand and to deal with. Every two-dimensional plate theory is indeed judged based on how well its solution approximates the corresponding three-dimensional problem. The most common dimensionally reduced theories of thin plates are the Kirchhoff-Love and the Reissner-Mindlin theories. The mathematical justification of these plate theories is hence interesting and has a long history. It has been a challenging subject to engineers and mathematicians throughout the past centuries. Two distinct ways to justify two-dimensional plate theories are either by using asymptotic expansions or by using variational techniques.

The Kirchhoff-Love theory, known also as the classical theory of plates, is an extension of Euler-Bernoulli beam theory. It dates back to 1888 and is based on the assumption that straight lines normal to the mid-plane of the plate remain normal after deformation. Morgenstern was the first to prove in 1959 that the Kirchhoff theory is correct for thin plates, i.e., when the thickness approaches zero (see Morgenstern (1959)). His analysis was performed using the two-energies principle of Prager and Synge, known also as the hypercircle theorem (Prager and Synge (1947)). Next, Ciarlet and Destuynder established rigorous error estimates between the solution of the 3D elastic problem and its limit (see Ciarlet and Destuynder (1979); G. Ciarlet (1990)). Later on, another mathematical justification of the Kirchhoff-Love theory was established by Ciarlet using convergence theorems as the thickness of the plate approaches zero (see G. Ciarlet (1997) for more details).

Due to its normality assumption, the classical plate theory neglects deformations caused by transverse shear. This leads to considerable errors when applied to moderately thick plates. Reissner (1976), Hencky (1947) and Bollé (1947) independently developed plate bending formulations trying to eliminate the above-mentioned deficiency of Kirchhoff-Love plate theory and gathered here under the usual denomination Reissner-Mindlin theories. To this aim, they released Kirchhoff's normality constraint, i.e., straight lines normal to the mid-plane of the plate undergo an independent rotation after deformation. This allowed them to take into account shear deformations through the thickness of the plate. The Reissner-Mindlin theory is often called the first-order shear deformation theory (FOSDT). This theory was proved to have a wider range of applicability than the Kirchhoff-Love theory particularly for clamped plates of small to moderate thickness when transverse shear plays a significant role (see Reissner (1985) and Hughes (2000)). According to Reissner (1985), the Reissner-Mindlin theory is also preferred because it better represents boundary conditions since it can distinguish between hard and soft simple support conditions.

There is a vast literature regarding Reissner-Mindlin theory. Indeed, The Kirchhoff-Love

theory is the limit model of the Reissner-Mindlin theory when the thickness of the plate goes to 0. This limit behavior enforces a jump of regularity of the solution and the emergence of boundary layers which required specific numerical treatments (see for instance Arnold and Falk (1996); Alessandrini et al. (1999); Arnold et al. (2002); Braess et al. (2009)). Furthermore, rigorous derivations of the Reissner-Mindlin model as well as proof of higher-order convergence of the Reissner-Mindlin remain under discussion (see Braess et al. (2009); Paroni et al. (2007); Neff and Hong (2009) among others).

Reissner-Mindlin's theory is widely used in applied mechanics since it works well for homogeneous plates. However, applying it directly to laminated plates leads to discontinuous transverse shear distributions in addition to incorrect estimation of the deflection compared to exact solutions. In recent decades, many studies have been conducted in order to try to capture correctly the effects of transverse shear deformations (see M. Whitney (1972); Reddy (1989); Noor and Malik (2000); Diaz et al. (2001); Carrera (2002)). Recently, motivated and inspired by the ideas and techniques presented in Reissner (1945), A. Lebée and K. Sab derived a new plate theory called the Bending-Gradient theory for thick heterogeneous plates (Lebée and Sab (2011)). This theory replaces the classical Reissner-Mindlin out-of-plane shear force by a generalized shear force related to the first gradient of the bending moment. The Bending-Gradient theory is hence considered as an extension to laminated plates of the Reissner-Mindlin plate theory. A. Lebée and K. Sab also demonstrated that the Bending-Gradient theory cannot be reduced to a Reissner-Mindlin theory unless the plate under consideration is homogeneous (see Lebée and Sab (2011)). The new theory was compared to the Reissner-Mindlin theory and to full 3D (Pagano (1969, 1970)) exact solutions in Lebée and Sab (2011). They came up with the conclusion that their new theory gives good prediction of deflection, shear stress distributions and in-plane displacement distributions in any material configuration. They also extended their new theory, which was originally designed for laminated plates, to in-plane periodic plates and they applied it to sandwich panels (see Lebée and Sab (2012a) and Lebée and Sab (2012b)), as well as space frames (Lebée and Sab (2013)). Finally, the Bending-Gradient theory was justified through asymptotic expansions Lebée and Sab (2013).

We concentrate in this paper on the mathematical justification of this theory by means of variational methods. The main emphasis is put on clamped and free plates. We are principally concerned with identifying mathematical spaces in which the corresponding variational problems are well-defined, in order to formulate existence and uniqueness theorems for the solutions of these problems. For full details on the Bending-Gradient theory, we refer to Sab and Lebée (2015).

The paper proceeds as follows. Section 3.2 provides a brief review of tensor calculus and necessary notions that will be needed in this work. Furthermore, it recalls some well-known definitions in addition to theorems and results which are essential for the problems that we want to consider. In Section 1.3, we set briefly the 3D elastic problem for a clamped plate then we summarize synthetically the Bending-Gradient problem. We propose next in Section 1.4 a proper mathematical framework for the Bending-Gradient theory. Section

1.4.1 is devoted to the stress formulation of the new plate theory then to the proof of its well-posedness (Theorem 1). In Section 1.4.3, we present a displacement formulation which is based on the minimum potential energy principle. In Section 1.5, we study the problem with free boundary conditions and prove that it admits a unique solution (Theorem 4). In Section 1.6, we discuss the problem when the plate is simply supported. It should be underlined that throughout Sections 1.4-1.6, we treat the particular case where the compliance tensor related to the gradient of the bending moment is positive definite. In Section 1.7, we extend the obtained results to the general case and provide corresponding stress and displacement formulations. Section 1.8 is intended to provide a regularization of the Bending-Gradient problem and to study the convergence of the regularized solution to the exact solution of the problem in the general case. Finally, we conclude in Section 3.6 with some final remarks.

1.2 Notations and preliminaries

In this section, we introduce our notations and we recall some existing results which are crucial for our analysis.

1.2.1 Tensors

Throughout this paper, we shall assume that all vector spaces are over \mathbb{R} . First, second, third, fourth and sixth rank tensors are denoted by $\underline{\mathbf{X}}$, $\underline{\underline{\mathbf{X}}}$, $\underline{\underline{\underline{\mathbf{X}}}}$, $\underline{\underline{\underline{\underline{\mathbf{X}}}}}$, $\underline{\underline{\underline{\underline{\underline{\mathbf{X}}}}}}$, respectively. They comply with specific symmetries detailed in the following. Note that these notations are used for both $2D$ and $3D$ tensors. For tensor components, we use Greek indices to represent $2D$ tensors ($\alpha, \beta, \gamma, \dots = 1, 2$) and Latin indices to represent $3D$ tensors ($i, j, k, \dots = 1, 2, 3$). For example, (X_{ij}) denotes the $3D$ tensor $\underline{\underline{\underline{\mathbf{X}}}}$ whereas $(X_{\alpha\beta})$ designates the $2D$ tensor $\underline{\underline{\mathbf{X}}}$. For simplicity purposes, we adopt the Einstein summation convention on repeated indices when manipulating expressions involving tensors.

The transpose operation ${}^T \bullet$ is applied to any order tensors as follows : $({}^T X)_{\alpha\beta\dots\psi\omega} = X_{\omega\psi\dots\beta\alpha}$. Four symbols are defined : (\cdot) , $(:)$, $(\dot{:})$ and $(\ddot{:})$ for contraction on, respectively, one, two, three and four indices. By convention, the closest indices are successively summed together in contraction products. Thus, $\underline{\underline{\underline{\mathbf{X}}}} : \underline{\underline{\underline{\mathbf{Y}}}} = (X_{\alpha\beta\gamma\delta\lambda\mu} Y_{\mu\lambda\delta})$ and $\underline{\underline{\underline{\mathbf{X}}}} \cdot \underline{\underline{\mathbf{Y}}} = (X_{\alpha\beta\gamma} Y_{\gamma})$ is different from $\underline{\underline{\mathbf{Y}}} \cdot \underline{\underline{\underline{\mathbf{X}}}} = (Y_{\alpha} X_{\alpha\beta\gamma})$.

The identity for $2D$ vectors is $\underline{\underline{\delta}} = (\delta_{\alpha\beta})$ where $\delta_{\alpha\beta}$ is Kronecker symbol ($\delta_{\alpha\beta} = 1$ if $\alpha = \beta$, $\delta_{\alpha\beta} = 0$ otherwise). The identity for $2D$ symmetric second order tensors is $\underline{\underline{\dot{\delta}}}$ where $i_{\alpha\beta\gamma\delta} = \frac{1}{2} (\delta_{\alpha\gamma}\delta_{\beta\delta} + \delta_{\alpha\delta}\delta_{\beta\gamma})$. The reader might easily check that $\underline{\underline{\dot{\delta}}} : \underline{\underline{\dot{\delta}}} = \underline{\underline{\dot{\delta}}}$, $\underline{\underline{\dot{\delta}}} : \underline{\underline{\dot{\delta}}} = 3/2 \underline{\underline{\delta}}$ and $\underline{\underline{\dot{\delta}}} \dot{\dot{:}} \underline{\underline{\dot{\delta}}} = 3$.

The gradient of a scalar field X writes $\underline{\underline{\nabla}} X = (X_{,\beta})$ while the gradient of a vector or a higher-order tensor fields writes $\underline{\underline{\mathbf{X}}} \otimes \underline{\underline{\nabla}} = (X_{\alpha\beta,\gamma})$, for instance, where \otimes is the

dyadic product. The divergence of a vector field or a second order tensor field is noted $\underline{\mathbf{X}} \cdot \underline{\nabla} = (X_{\alpha,\alpha})$ and $\underline{\mathbf{X}} \cdot \underline{\nabla} = (X_{\alpha\beta,\beta})$, respectively.

Let $\underline{\mathbb{R}}$, $\underline{\mathbb{R}}$ and $\underline{\mathbb{R}}$ be the spaces of $2D$ first, second and third rank tensors which comply with the following symmetries :

$$(1.1) \quad \underline{\mathbb{R}} = \{ \underline{\mathbf{X}} = (X_{\alpha\beta}) \in \mathbb{R}^4 \mid X_{\alpha\beta} = X_{\beta\alpha} \},$$

$$(1.2) \quad \underline{\mathbb{R}} = \{ \underline{\mathbf{X}} = (X_{\alpha\beta\gamma}) \in \mathbb{R}^8 \mid X_{\alpha\beta\gamma} = X_{\beta\alpha\gamma} \}$$

The spaces $\underline{\mathbb{R}}$ and $\underline{\mathbb{R}}$ are respectively endowed with the following scalar products :

$${}^t \underline{\mathbf{X}} : \underline{\mathbf{X}}' = X_{\alpha\beta} X'_{\alpha\beta}$$

and

$${}^t \underline{\mathbf{X}} : \underline{\mathbf{X}}' = X_{\alpha\beta\gamma} X'_{\alpha\beta\gamma}.$$

Any $2D$ third-rank tensor $\underline{\mathbf{X}}$ in $\underline{\mathbb{R}}$ can be orthogonally decomposed into a spherical part $\underline{\mathbf{X}}^s$ and a deviatoric¹ part $\underline{\mathbf{X}}^d$ as :

$$\underline{\mathbf{X}} = \underline{\mathbf{X}}^s + \underline{\mathbf{X}}^d$$

where

$$X_{\alpha\beta\gamma}^s = \frac{1}{3} (X_{\alpha\nu\lambda} \delta_{\nu\lambda} \delta_{\beta\gamma} + X_{\beta\nu\lambda} \delta_{\nu\lambda} \delta_{\alpha\gamma}).$$

One can easily check the following properties :

$${}^t \underline{\mathbf{X}}^s : \underline{\mathbf{X}}^d = 0, \quad \underline{\mathbf{X}}^d : \underline{\delta} = 0.$$

Note that any tensor of the form

$$(1.3) \quad \underline{\mathbf{X}} = \underline{\mathbf{i}} \cdot \underline{\mathbf{X}}$$

where $\underline{\mathbf{X}} \in \underline{\mathbb{R}}$, is a purely spherical tensor. Conversely, for any given $\underline{\mathbf{X}} \in \underline{\mathbb{R}}$, there exists a unique vector $\underline{\mathbf{X}}^s$ extracted from its spherical part such that (1.3) is satisfied for $\underline{\mathbf{X}}^s$. This vector is given by :

$$(1.4) \quad \underline{\mathbf{X}}^s = \frac{2}{3} \underline{\mathbf{X}} : \underline{\delta} = \frac{2}{3} \underline{\mathbf{X}}^s : \underline{\delta}$$

1. Whereas the spherical and deviatoric part of a second rank tensor is conventional, this denomination is understood here for the two last indices of a third rank tensor.

1.2.2 Functional spaces

Let ω be a bounded, connected, open subset of \mathbb{R}^2 with a Lipschitz-continuous boundary. We denote by $C^\infty(\omega)$ the space of infinitely differentiable functions on ω and by $D(\omega)$ the subspace of functions with compact support in ω . We further refer to $D'(\omega)$ as the space of distributions on ω . The fundamental Sobolev space $L^2(\omega)$ is the space of square integrable functions on ω . For each integer $m \geq 1$, $H^m(\omega)$ and $H_0^1(\omega)$ denote the usual Sobolev spaces. To avoid ambiguity, we will use the tensorial notations as mentioned in section 1.2.1. Namely, $\underline{\mathbf{L}}^2(\omega)$, $\underline{\mathbf{L}}^2(\omega)$ and $\underline{\mathbf{L}}^2(\omega)$ denote, respectively, the space of vector fields, symmetric second rank fields and symmetric third rank fields having their components in $L^2(\omega)$. The associated norms are defined as :

$$\|\underline{\mathbf{a}}\|_{\underline{\mathbf{L}}^2(\omega)}^2 = \int_{\omega} \underline{\mathbf{a}} \cdot \underline{\mathbf{a}}, \quad \|\underline{\mathbf{a}}\|_{\underline{\mathbf{L}}^2(\omega)}^2 = \int_{\omega} \underline{\mathbf{a}} : \underline{\mathbf{a}}, \quad \|\underline{\mathbf{a}}\|_{\underline{\mathbf{L}}^2(\omega)}^2 = \int_{\omega} {}^T \underline{\mathbf{a}} : \underline{\mathbf{a}}.$$

Here, we have used the fact that tensors $\underline{\mathbf{a}}$ of $\underline{\mathbf{L}}^2(\omega)$ are symmetric, i.e., ${}^T \underline{\mathbf{a}} = \underline{\mathbf{a}}$. The well-posedness of the Bending-Gradient problems relies on some intermediate theorems and results which we state here as Lemmas. First, Lemma 1 to Lemma 4 have been already established for three-dimensional tensor fields in Sab et al. (2015) and their straightforward extension to the case of two-dimensional tensors will not be detailed. Then, Lemma 5 is an original contribution which will be proved below.

Lemma 1. *The set defined by*

$$(1.5) \quad \underline{\mathbf{H}}(div, \omega) = \{ \underline{\mathbf{\Phi}} \in \underline{\mathbf{L}}^2(\omega); \quad \underline{\mathbf{\Phi}} \cdot \underline{\mathbf{\nabla}} \in \underline{\mathbf{L}}^2(\omega) \}$$

equipped with the scalar product

$$(1.6) \quad \langle \underline{\mathbf{\Phi}}_1, \underline{\mathbf{\Phi}}_2 \rangle_{\underline{\mathbf{H}}(div, \omega)} = \int_{\omega} {}^T \underline{\mathbf{\Phi}}_1 : \underline{\mathbf{\Phi}}_2 + (\underline{\mathbf{\Phi}}_1 \cdot \underline{\mathbf{\nabla}}) : (\underline{\mathbf{\Phi}}_2 \cdot \underline{\mathbf{\nabla}})$$

and its associated norm $\|\bullet\|_{\underline{\mathbf{H}}(div, \omega)}$ is a Hilbert space.

We now give an appropriate sense to the Dirichlet boundary condition related to $\underline{\mathbf{H}}(div, \omega) : \underline{\mathbf{\Phi}} \cdot \underline{\mathbf{n}} = 0$. It is well-known that we can define the trace of $\underline{\mathbf{H}}^1(\omega)$ tensors on $\partial\omega$. However, the trace of a tensor belonging to $\underline{\mathbf{L}}^2(\omega)$ is not defined. Since $\underline{\mathbf{\Phi}} \in \underline{\mathbf{H}}(div, \omega)$, it is less regular than a $\underline{\mathbf{H}}^1(\omega)$ tensor. Nevertheless, we can set its normal trace $\underline{\mathbf{\Phi}} \cdot \underline{\mathbf{n}}$ to zero in the following weak sense : Let $\underline{\mathbf{\Phi}}$ in $\underline{\mathbf{C}}^\infty(\omega)$ and $\underline{\mathbf{M}}$ in $\underline{\mathbf{C}}^\infty(\omega)$ be smooth fields, we have :

$$(1.7) \quad \int_{\omega} \underline{\mathbf{M}} : (\underline{\mathbf{\Phi}} \cdot \underline{\mathbf{\nabla}}) + {}^T(\underline{\mathbf{M}} \otimes \underline{\mathbf{\nabla}}) : \underline{\mathbf{\Phi}} = \int_{\partial\omega} \underline{\mathbf{M}} : (\underline{\mathbf{\Phi}} \cdot \underline{\mathbf{n}})$$

Since (1.7) holds true for any given $\underline{\mathbf{M}}$ on $\partial\omega$, imposing $\underline{\mathbf{\Phi}} \cdot \underline{\mathbf{n}} = 0$ is thus equivalent to imposing :

$$(1.8) \quad \int_{\omega} \underline{\mathbf{M}} : (\underline{\mathbf{\Phi}} \cdot \underline{\mathbf{\nabla}}) + {}^T(\underline{\mathbf{M}} \otimes \underline{\mathbf{\nabla}}) : \underline{\mathbf{\Phi}} = 0$$

for all $\underline{\mathbf{M}} \in \underline{\mathbf{C}}^\infty(\omega)$. The following definition is hence very natural.

Lemma 2. *The set defined by :*

$$(1.9) \quad \underline{\mathbf{H}}_0(\operatorname{div}, \omega) = \{ \underline{\Phi} \in \underline{\mathbf{H}}(\operatorname{div}, \omega); \text{ (1.8) holds true for all } \underline{\mathbf{M}} \in \underline{\mathbf{H}}^1(\omega) \}$$

is a closed subspace of $\underline{\mathbf{H}}(\operatorname{div}, \omega)$ equipped with its norm $\|\bullet\|_{\underline{\mathbf{H}}(\operatorname{div}, \omega)}$. Hence, $\underline{\mathbf{H}}_0(\operatorname{div}, \omega)$ endowed with the scalar product $\langle \bullet, \bullet \rangle_{\underline{\mathbf{H}}(\operatorname{div}, \omega)}$ is a Hilbert space.

Lemma 3. *Let $(\underline{\Phi}_k)_{k \in \mathbb{N}^*}$ be a sequence of third-rank tensors defined over $\underline{\mathbf{H}}_0(\operatorname{div}, \omega)$. We denote by $\underline{\Phi}_k^{\text{d}}$ the deviatoric part of $\underline{\Phi}_k$. If $\underline{\Phi}_k$ satisfies*

$$\|\underline{\Phi}_k \cdot \underline{\nabla}\|_{\underline{\mathbf{L}}^2(\omega)} + \|\underline{\Phi}_k^{\text{d}}\|_{\underline{\mathbf{L}}^2(\omega)} \leq \frac{C}{k}$$

where C is a strictly positive constant, then $\underline{\Phi}_k$ strongly converges to zero in $\underline{\mathbf{H}}(\operatorname{div}, \omega)$.

Lemma 4. *There exists a strictly positive constant C such that, for all $\underline{\Phi} \in \underline{\mathbf{H}}(\operatorname{div}, \omega)$, there exists a two-dimensional rigid motion vector field $\underline{\mathbf{r}}$ of the form :*

$$(1.10) \quad \underline{\mathbf{r}}(x_1, x_2) = (u - wx_2, v + wx_1),$$

such that :

$$(1.11) \quad \|\underline{\Phi}^{\text{s}} - \underline{\mathbf{r}}\|_{\underline{\mathbf{L}}^2(\omega)} \leq C \left(\|\underline{\Phi} \cdot \underline{\nabla}\|_{\underline{\mathbf{L}}^2(\omega)}^2 + \|\underline{\Phi}^{\text{d}}\|_{\underline{\mathbf{L}}^2(\omega)}^2 \right)^{1/2}$$

Here, (u, v) and w are respectively the in-plane rotation vector and the global out-of-plane twist of the rigid motion field $\underline{\mathbf{r}}$, $\underline{\Phi}^{\text{d}}$ denotes the deviatoric part of $\underline{\Phi}$ and $\underline{\Phi}^{\text{s}}$ is the vector field associated to the spherical part of $\underline{\Phi}$ through (1.4).

Lemma 5. *Assume that for each integer k , there exists a vector field $\underline{\mathbf{r}}_k$ of the form (1.10)*

$$\underline{\mathbf{r}}_k(x_1, x_2) = (u_k - w_k x_2, v_k + w_k x_1)$$

and a scalar field W_k in $H^1(\omega)$ such that :

$$(1.12) \quad \|\underline{\mathbf{r}}_k + \underline{\nabla} W_k\|_{\underline{\mathbf{L}}^2(\omega)} \longrightarrow 0$$

as k goes to infinity. Then, $w_k \longrightarrow 0$ and there exists a sequence of real numbers denoted by z_k such that :

$$(1.13) \quad \|W_k + u_k x_1 + v_k x_2 + z_k\|_{H^1(\omega)} \longrightarrow 0.$$

Moreover, if W_k is in $H_0^1(\omega)$ for all k , then $(u_k, v_k) \longrightarrow (0, 0)$ and

$$(1.14) \quad \|W_k\|_{H_0^1(\omega)} \longrightarrow 0.$$

Démonstration. Let us decompose \mathbf{r}_k into two terms $\mathbf{r}_k = \mathbf{r}_k^{(u,v)} + \mathbf{r}_k^w$ with $\mathbf{r}_k^{(u,v)} = (u_k, v_k)$ and $\mathbf{r}_k^w = (-w_k x_2, w_k x_1)$. Then, the limit (1.12) can be written as :

$$(1.15) \quad \|\underline{\mathbf{r}}_k^w + \underline{\nabla} (W_k + u_k x_1 + v_k x_2)\|_{\underline{\mathbf{L}}^2(\omega)} \longrightarrow 0$$

Assume first that the origin point $(0,0)$ is inside the domain ω . Since ω is open, there exists a disc D_ρ in ω of radius ρ centered at $(0,0)$. We have,

$$(1.16) \quad \begin{aligned} \|\underline{\mathbf{r}}_k^w + \underline{\nabla} (W_k + u_k x_1 + v_k x_2)\|_{\underline{\mathbf{L}}^2(\omega)}^2 &\geq \|\underline{\mathbf{r}}_k^w + \underline{\nabla} (W_k + u_k x_1 + v_k x_2)\|_{\underline{\mathbf{L}}^2(D_\rho)}^2 = \\ &\|\underline{\mathbf{r}}_k^w\|_{\underline{\mathbf{L}}^2(D_\rho)}^2 + \|\underline{\nabla} (W_k + u_k x_1 + v_k x_2)\|_{\underline{\mathbf{L}}^2(D_\rho)}^2 + \int_{D_\rho} 2\underline{\mathbf{r}}_k^w \cdot \underline{\nabla} (W_k + u_k x_1 + v_k x_2) \end{aligned}$$

Integrating by parts the last term in the above right-hand side yields :

$$(1.17) \quad \begin{aligned} \int_{D_\rho} 2\underline{\mathbf{r}}_k^w \cdot \underline{\nabla} (W_k + u_k x_1 + v_k x_2) &= - \int_{D_\rho} 2(\underline{\mathbf{r}}_k^w \cdot \underline{\nabla}) (W_k + u_k x_1 + v_k x_2) \\ &+ \int_{\partial D_\rho} 2(\underline{\mathbf{r}}_k^w \cdot \underline{\mathbf{n}}) (W_k + u_k x_1 + v_k x_2) = 0 \end{aligned}$$

because $\underline{\mathbf{r}}_k^w \cdot \underline{\nabla} = 0$ in the bulk and $\underline{\mathbf{r}}_k^w \cdot \underline{\mathbf{n}} = 0$ at the boundary where $\underline{\mathbf{n}}$ denotes the outer normal to D_ρ . Moreover, by a simple calculus, we obtain that $\|\underline{\mathbf{r}}_k^w\|_{\underline{\mathbf{L}}^2(D_\rho)}^2 = \frac{\pi}{2} \rho^4 w_k^2$. Consequently, by the limit (1.15), we prove that $w_k \longrightarrow 0$ when the origin point is inside ω .

Now, if the origin point $(0,0)$ is not inside the domain ω , we can make the change of variables

$$(x_1, x_2) = (x'_1, x'_2) + (c_1, c_2)$$

where (c_1, c_2) is a point inside the domain ω and (x'_1, x'_2) belongs to the translated domain ω' . Then, we define on the domain ω' the fields :

$$\underline{\mathbf{r}}'_k(x'_1, x'_2) = \underline{\mathbf{r}}_k(x_1, x_2) = (u'_k - w'_k x'_2, v'_k + w'_k x'_1)$$

and

$$W'_k(x'_1, x'_2) = W_k(x_1, x_2)$$

with

$$(u'_k, v'_k, w'_k) = (u_k - w_k c_2, v_k + w_k c_1, w_k).$$

Then, by construction, the origin point $(0,0)$ is inside the domain ω' . Applying the above result to the fields $\underline{\mathbf{r}}'_k$ and W'_k , we prove that $w_k \longrightarrow 0$ in the general case and, consequently, the limit (1.15) becomes :

$$(1.18) \quad \|\underline{\nabla} W_k + \underline{\mathbf{r}}_k^{(u,v)}\|_{\underline{\mathbf{L}}^2(\omega)} = \|\underline{\nabla} (W_k + u_k x_1 + v_k x_2)\|_{\underline{\mathbf{L}}^2(\omega)} \longrightarrow 0,$$

Using the well-known Poincaré inequality, we prove that there exists a sequence of real numbers denoted by z_k such that (1.13).

In the special case where W_k is in $H_0^1(\omega)$ for all k , then using standard integration by parts gives :

$$(1.19) \quad \left\| \underline{\nabla} W_k + \underline{\mathbf{r}}_k^{(u,v)} \right\|_{\underline{\mathbf{L}}^2(\omega)}^2 = \left\| \underline{\nabla} W_k \right\|_{\underline{\mathbf{L}}^2(\omega)}^2 + \left\| \underline{\mathbf{r}}_k^{(u,v)} \right\|_{\underline{\mathbf{L}}^2(\omega)}^2$$

Hence, the limit (1.18) implies $(u_k, v_k) \rightarrow (0, 0)$ and (1.14) by the Poincaré inequality. \square

1.3 The Bending-Gradient problem

In this section, we first set the 3D laminated plate configuration. Then, we provide an overview of its reduction to a 2D problem according to the Bending-Gradient theory. The definitions of the generalized stresses and strains of this theory are recalled, as well as the compatibility conditions, the equilibrium equations and the constitutive equations. We finally present the variational formulations of this linear problem without specifying the functional spaces to which must belong the unknown kinematic and static fields.

1.3.1 The 3D configuration

The physical space is endowed with an orthonormal reference $(O, \underline{\mathbf{e}}_1, \underline{\mathbf{e}}_2, \underline{\mathbf{e}}_3)$ where O is the origin and $\underline{\mathbf{e}}_i$ is the base vector in direction $i \in \{1, 2, 3\}$. We consider a linear elastic plate occupying the 3D domain $\Omega = \omega \times]-\frac{t}{2}, \frac{t}{2}[$, where $\omega \subset \mathbb{R}^2$ is the middle surface of the plate and t its thickness. The boundary of the domain, denoted by $\partial\Omega$, is decomposed into three parts (Figure 2.1) :

$$(1.20) \quad \begin{aligned} \partial\Omega &= \partial\Omega_{\text{lat}} \cup \partial\Omega_3^+ \cup \partial\Omega_3^-, \\ \text{with } \partial\Omega_{\text{lat}} &= \partial\omega \times \left] -\frac{t}{2}, \frac{t}{2} \right[\quad \text{and} \quad \partial\Omega_3^\pm = \omega \times \left\{ \pm \frac{t}{2} \right\}. \end{aligned}$$

where $\partial\omega$ is the boundary of ω .

Focusing only on out-of-plane loadings, the plate is subjected to forces per unit surface on $\partial\Omega_3^\pm$ of the form :

$$(1.21) \quad \underline{\mathbf{T}}^\pm(x_1, x_2) = \left(0, 0, \frac{1}{2}p(x_1, x_2) \right),$$

where p is a given function on ω .

In the following, we assume that there are no body forces and that the plate is fully clamped on its lateral boundary $\partial\Omega_{\text{lat}}$.

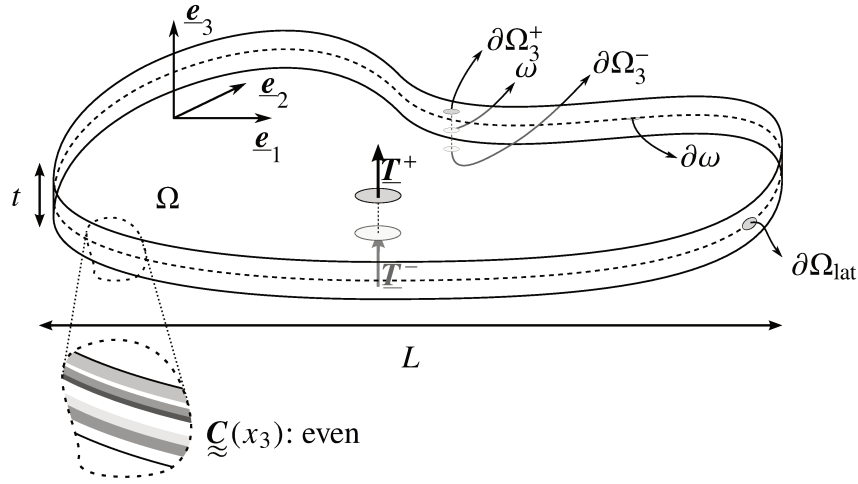


FIGURE 1.1 – The 3D configuration

The fourth-rank 3D elasticity stiffness tensor (C_{ijkl}) has both the minor and major symmetries $C_{ijkl} = C_{jikl} = C_{klij}$ and it is positive definite. Its inverse is called the 3D elastic compliance tensor and is denoted by (S_{ijkl}). The tensor (S_{ijkl}) possesses the same symmetries as (C_{ijkl}) and it is also positive definite.

We suppose that the constitutive material is invariant with respect to translations in the (x_1, x_2) plane. Therefore, C_{ijkl} does not depend on (x_1, x_2) and is an even function of x_3 :

$$(1.22) \quad C_{ijkl}(x_3) = C_{ijkl}(-x_3).$$

Furthermore, we have that :

$$(1.23) \quad C_{3\alpha\beta\gamma} = C_{\alpha 333} = 0.$$

In this case, the constitutive material is said to be monoclinic.

The following notations are needed for the partial compliance tensors :

$$(1.24) \quad \underline{\underline{\mathcal{S}}}^\sigma = (S_{\alpha\beta\gamma\delta}), \quad \underline{\underline{\mathcal{C}}}^\sigma = \left(\underline{\underline{\mathcal{S}}}^\sigma\right)^{-1}, \quad \underline{\underline{\mathcal{S}}}^\gamma = (4S_{\alpha 333}),$$

where $\underline{\underline{\mathcal{S}}}^\sigma$ corresponds to plane stress compliance, $\underline{\underline{\mathcal{C}}}^\sigma$ to plane stress stiffness and $\underline{\underline{\mathcal{S}}}^\gamma$ to transverse shear compliance.

The 3D elastic problem is to find in Ω a displacement field $\underline{\mathbf{u}}$, a stress tensor field $\underline{\underline{\boldsymbol{\sigma}}}$ and a strain tensor field $\underline{\underline{\boldsymbol{\varepsilon}}}$, solution of the following equations :

$$\begin{aligned} (1.25a) & \quad \underline{\underline{\boldsymbol{\sigma}}} \cdot \underline{\nabla} = 0 \quad \text{on } \Omega, \\ (1.25b) & \quad \underline{\underline{\boldsymbol{\sigma}}} = \underline{\underline{\mathcal{C}}}(x_3) : \underline{\underline{\boldsymbol{\varepsilon}}} \quad \text{on } \Omega, \\ (1.25c) & \quad \underline{\underline{\boldsymbol{\sigma}}} \cdot \pm \underline{\mathbf{e}}_3 = \underline{\mathbf{T}}^\pm \quad \text{on } \partial\Omega_3^\pm, \\ (1.25d) & \quad \underline{\underline{\boldsymbol{\varepsilon}}} = \frac{1}{2} (\underline{\mathbf{u}} \otimes \underline{\nabla} + \underline{\nabla} \otimes \underline{\mathbf{u}}) \quad \text{on } \Omega, \\ (1.25e) & \quad \underline{\mathbf{u}} = 0 \quad \text{on } \partial\Omega_{\text{lat}}. \end{aligned}$$

1.3.2 The Bending-Gradient theory

We now introduce the main definitions and equations of the Bending-Gradient theory, which main purpose is to replace the full 3D model by a reduced 2D plate theory and to be able to reconstruct the 3D solution fields from the 2D solution fields.

Following the ideas of Reissner (1945) for homogeneous plates, Lebée and Sab Lebée and Sab (2011) derived a new plate theory, called the Bending-Gradient theory, suitable for heterogeneous plates. In this theory, the full gradient of the bending moment is considered as a generalized shear stress. Note that this theory cannot be reduced to a Reissner-Mindlin theory in the general case. However, it is turned into a Reissner-Mindlin theory when the plate under consideration is homogeneous (see Sab and Lebée (2015), Lebée and Sab (2015), Lebée and Sab (2015) for more details). This shift between theories is directly related to the positive definiteness of the generalized shear constitutive tensor defined in the following. In this section and up to Section 1.7 it is assumed that the generalized shear constitutive tensor is positive definite. Section 1.7 will treat the case when the definiteness is lost.

1.3.2.1 Generalized stresses

The Bending-Gradient theory generalized stresses are :

- The bending moment tensor $\underline{\underline{M}}$ related to the 3D local stress (σ_{ij}) by :

$$\underline{\underline{M}} = (M_{\alpha\beta}) = (\langle x_3 \sigma_{\alpha\beta} \rangle)$$

where the integration through the thickness is noted $\langle \bullet \rangle : \int_{-\frac{t}{2}}^{\frac{t}{2}} f(x_3) dx_3 = \langle f \rangle$. We keep in mind that the second-order tensor $\underline{\underline{M}}$ has the following symmetry :

$$M_{\alpha\beta} = M_{\beta\alpha}.$$

- The generalized shear force, denoted by $\underline{\underline{R}}$ and defined as the gradient of the bending moment :

$$\underline{\underline{R}} = \underline{\underline{M}} \otimes \underline{\underline{\nabla}}.$$

In terms of components, this relation is written as $R_{\alpha\beta\gamma} = M_{\alpha\beta,\gamma}$. Note that the 2D third-order tensor $R_{\alpha\beta\gamma}$ complies with the following symmetry :

$$R_{\alpha\beta\gamma} = R_{\beta\alpha\gamma}.$$

Remark 1. The usual transverse shear force $\underline{\underline{Q}}$ is defined from the 3D stress field $\underline{\underline{\sigma}}$ as follows :

$$\underline{\underline{Q}} = (Q_\alpha) = (\langle \sigma_{\alpha 3} \rangle)$$

It is interesting to note that the 3D equilibrium equations enforce the following relation between $\underline{\underline{Q}}$ and $\underline{\underline{R}}$:

$$(1.26) \quad \underline{\underline{Q}} = \underline{\underline{i}} : \underline{\underline{R}} = \underline{\underline{M}} \cdot \underline{\underline{\nabla}}$$

which can be written in terms of components as :

$$(1.27) \quad Q_\alpha = R_{\alpha\beta\beta} = M_{\alpha\beta,\beta}$$

1.3.2.2 Generalized displacements

The Bending-Gradient generalized displacements are $(W, \underline{\Phi})$. The scalar W is called the out-of-plane displacement of the plate (or deflection) and $\underline{\Phi}$ is the generalized rotation tensor. The 2D third-order tensor $\underline{\Phi}$ complies with the following symmetry :

$$\Phi_{\alpha\beta\gamma} = \Phi_{\beta\alpha\gamma}$$

These displacements are interpreted physically as suitable averages of the 3D displacements over the thickness of the plate. The reader is referred to Sab and Lebée (2015) (Chapter 5) for corresponding details.

The Bending-Gradient generalized strains, which derive from $(W, \underline{\Phi})$, and constitute the dual of the generalized stresses $(\underline{\mathcal{M}}, \underline{\mathcal{R}})$ are :

– The curvature second-order tensor $\underline{\chi}$ defined by :

$$(1.28) \quad \underline{\chi} = \underline{\Phi} \cdot \underline{\nabla} \quad \text{or} \quad \chi_{\alpha\beta} = \Phi_{\alpha\beta\gamma,\gamma}$$

– The generalized shear strain $\underline{\Gamma}$ given by :

$$(1.29) \quad \underline{\Gamma} = \underline{\Phi} + \underline{\mathbf{i}} \cdot \underline{\nabla} W \quad \text{or} \quad \Gamma_{\alpha\beta\gamma} = \Phi_{\alpha\beta\gamma} + i_{\alpha\beta\gamma\delta} W_{,\delta}$$

$\underline{\Gamma}$ is a third-order 2D tensor which comply with the following symmetry :

$$\Gamma_{\alpha\beta\gamma} = \Gamma_{\beta\alpha\gamma}$$

Equations (1.28) and (1.29) are called the compatibility conditions on ω .

In the following section, we assume clamped boundary conditions. Nevertheless, various boundary conditions (free, simply supported..) are also considered in this paper (see Sects. 1.5 and 1.6). The clamped boundary conditions on $\partial\omega$ read :

$$(1.30) \quad \underline{\Phi} \cdot \underline{\mathbf{n}} = 0 \quad \text{and} \quad W = 0 \quad \text{on} \quad \partial\omega.$$

where $\underline{\mathbf{n}}$ is the outer normal vector to $\partial\omega$.

Note that the kinematics of the Bending-Gradient theory coincides with the Reissner-Mindlin kinematics if the deviatoric part of $\underline{\Phi}$ is set to zero. We can hence interpret the Reissner-Mindlin kinematics as the restriction of $\underline{\Phi}$ to $\underline{\mathbf{i}} \cdot \underline{\varphi}$, where $\underline{\varphi}$ designates a rotation vector.

1.3.2.3 Equilibrium equations

We start by recalling that integrating the 3D equilibrium equation (3.7a) leads to the well-known Reissner-Mindlin plate equilibrium equations :

$$(1.31) \quad \begin{cases} \underline{\underline{M}} \cdot \underline{\underline{\nabla}} = \underline{\underline{Q}} \\ \underline{\underline{Q}} \cdot \underline{\underline{\nabla}} + p = 0 \end{cases}$$

Considering that $(\underline{\underline{M}}, \underline{\underline{R}})$ are the generalized stresses of the Bending-Gradient theory instead of $(\underline{\underline{M}}, \underline{\underline{Q}})$ for the Reissner-Mindlin theory, the above equilibrium equations become :

$$(1.32a) \quad \begin{cases} \underline{\underline{R}} - \underline{\underline{M}} \otimes \underline{\underline{\nabla}} = 0, \\ \underline{\underline{i}} \vdots (\underline{\underline{R}} \otimes \underline{\underline{\nabla}}) + p = 0, \end{cases}$$

in the case when the generalized shear constitutive tensor is positive definite. Otherwise, the modified equilibrium equations are defined in Section 1.7

Note that using the first equilibrium equation to eliminate $\underline{\underline{R}}$ in the second equilibrium equation gives the equivalent form :

$$\underline{\underline{i}} \vdots (\underline{\underline{R}} \otimes \underline{\underline{\nabla}}) + p = \underline{\underline{i}} \vdots ((\underline{\underline{M}} \otimes \underline{\underline{\nabla}}) \otimes \underline{\underline{\nabla}}) + p = M_{\alpha\beta, \alpha\beta} + p = 0$$

1.3.2.4 Constitutive equations

Finally, the Bending-Gradient constitutive equations write :

$$(1.33) \quad \begin{cases} \underline{\underline{\chi}} = \underline{\underline{d}} \vdots \underline{\underline{M}}, \\ \underline{\underline{\Gamma}} = \underline{\underline{h}} \vdots \underline{\underline{R}}, \end{cases}$$

Here, $\underline{\underline{d}}$ is the classical bending compliance fourth-order tensor, inverse of the bending stiffness fourth-order tensor $\underline{\underline{D}}$. It is given by :

$$(1.34) \quad \underline{\underline{d}} = \underline{\underline{D}}^{-1} \quad \text{with} \quad \underline{\underline{D}} = \left\langle x_3^2 \underline{\underline{C}}^\sigma \right\rangle.$$

Tensors $\underline{\underline{d}}$ and $\underline{\underline{D}}$ are symmetric positive and definite. They follow both major symmetry ${}^T \underline{\underline{D}} = \underline{\underline{D}}$ and minor symmetry $D_{\alpha\beta\gamma\delta} = D_{\beta\alpha\gamma\delta}$.

The generalized shear force compliance sixth-order tensor $\underline{\underline{h}}$ is given by :

$$(1.35) \quad \underline{\underline{h}} = \left\langle \underline{\underline{T}} \underline{\underline{s}}^R \cdot \underline{\underline{S}}^\gamma \cdot \underline{\underline{s}}^R \right\rangle,$$

where the fourth order tensor $\underline{\underline{\mathbf{s}}}^R(x_3)$ is the function of x_3 defined by :

$$(1.36) \quad \underline{\underline{\mathbf{s}}}^R(x_3) = \int_{-\frac{t}{2}}^{x_3} -\underline{\underline{\mathbf{s}}}^M(y_3) dy_3 \quad \text{with} \quad \underline{\underline{\mathbf{s}}}^M(x_3) = x_3 \underline{\underline{\mathbf{C}}}^\sigma(x_3) : \underline{\underline{\mathbf{d}}}.$$

Tensor $\underline{\underline{\mathbf{h}}}$ has the major symmetry ${}^T \underline{\underline{\mathbf{h}}} = \underline{\underline{\mathbf{h}}}$ and the minor symmetries $h_{\alpha\beta\gamma\delta\epsilon\zeta} = h_{\beta\alpha\gamma\delta\epsilon\zeta}$. It is positive but not always definite. Three particular cases should be distinguished when dealing with $\underline{\underline{\mathbf{h}}}$:

- The first one is when the sixth-order tensor is positive definite. In this case, its inverse is unambiguously defined and denoted by $\underline{\underline{\mathbf{H}}} = \underline{\underline{\mathbf{h}}}^{-1}$.
- The second case is when the shear force compliance tensor can be written in the following form :

$$\underline{\underline{\mathbf{h}}} = \underline{\underline{\mathbf{i}}} \cdot \underline{\underline{\mathbf{h}}}^{\text{RM}} \cdot \underline{\underline{\mathbf{i}}}$$

where $\underline{\underline{\mathbf{h}}}^{\text{RM}}$ designates a positive definite symmetric second-order tensor called the Reissner-Mindlin shear force compliance tensor. In this case, the Bending-Gradient theory degenerates into a Reissner-Mindlin theory. The existence and uniqueness of the solution in this case is already established in the literature.

- The third case is an intermediate between the above mentioned cases. It will be studied in details in Section 1.7.

In the following (except in Section 1.7), it will be assumed that the sixth-order tensor $\underline{\underline{\mathbf{h}}}$ is positive definite. The Bending-Gradient constitutive equations can thus be inverted :

$$(1.37) \quad \begin{cases} \underline{\underline{\mathbf{M}}} = \underline{\underline{\mathbf{D}}} : \underline{\underline{\chi}}, \\ \underline{\underline{\mathbf{R}}} = \underline{\underline{\mathbf{H}}} : \underline{\underline{\Gamma}}. \end{cases}$$

1.3.2.5 Summary of the Bending-Gradient plate theory

Finally, the Bending-Gradient problem enables a good approximation of the 3D fields introduced earlier including the effects of transverse shear. It consists in finding the generalized displacement $(W, \underline{\underline{\Phi}})$ solution of the following equations :

$$\begin{aligned} (1.38a) \quad & \left\{ \begin{array}{l} \underline{\underline{\chi}} = \underline{\underline{\Phi}} \cdot \underline{\underline{\nabla}} \quad \text{and} \quad \underline{\underline{\Gamma}} = \underline{\underline{\Phi}} + \underline{\underline{\mathbf{i}}} \cdot \underline{\underline{\nabla}} W, \\ \underline{\underline{\mathbf{M}}} = \underline{\underline{\mathbf{D}}} : \underline{\underline{\chi}} \quad \text{and} \quad \underline{\underline{\mathbf{R}}} = \underline{\underline{\mathbf{H}}} : \underline{\underline{\Gamma}}, \\ \underline{\underline{\mathbf{R}}} - \underline{\underline{\mathbf{M}}} \otimes \underline{\underline{\nabla}} = 0 \quad \text{and} \quad \underline{\underline{\mathbf{i}}} \cdot (\underline{\underline{\mathbf{R}}} \otimes \underline{\underline{\nabla}}) + p = 0, \\ \underline{\underline{\Phi}} \cdot \underline{\underline{\mathbf{n}}} = 0 \quad \text{and} \quad W = 0 \quad \text{on} \quad \partial\omega. \end{array} \right. \\ (1.38b) \quad & \\ (1.38c) \quad & \\ (1.38d) \quad & \end{aligned}$$

It should be emphasized that once we find the solution of the Bending-Gradient problem, we can reconstruct the 3D stress and displacement fields (see Chapter 5 of Sab and Lebée (2015) for more details).

Now that we have presented the main features of the Bending-Gradient theory, it is useful to recall its variational approach as stated in Sab and Lebée (2015). It has to be pointed out first that generalized displacements $(W, \underline{\Phi})$ which satisfy the boundary conditions (1.38d) are called kinematically compatible fields. Besides, generalized stresses $(\underline{\mathbf{M}}, \underline{\mathbf{R}})$ that comply with equations (1.38c) are designated as statically compatible fields.

1.3.2.6 Minimum of the potential energy

The principle of the minimum of the potential energy states that the solution $(W^{\text{BG}}, \underline{\Phi}^{\text{BG}})$ of the Bending-Gradient problem (1.38) renders the potential energy functional \mathcal{E}^{BG} a minimum value on the set of kinematically compatible Bending-Gradient displacements. Here, the potential energy \mathcal{E}^{BG} is defined as :

$$(1.39) \quad \mathcal{E}^{\text{BG}} = \int_{\omega} w^{\text{BG}}(\underline{\chi}, \underline{\Gamma}) - \int_{\omega} pW,$$

where $\underline{\chi}$ and $\underline{\Gamma}$ are the generalized strains related to the generalized displacements $(W, \underline{\Phi})$ through the compatibility equations (1.38a). Furthermore, w^{BG} is the Bending-Gradient strain energy density function given by :

$$(1.40) \quad w^{\text{BG}}(\underline{\chi}, \underline{\Gamma}) = \frac{1}{2} \underline{\chi} : \underline{\mathbf{D}} : \underline{\chi} + \frac{1}{2} \underline{\Gamma} : \underline{\mathbf{H}} : \underline{\Gamma}.$$

1.3.2.7 Minimum of the complementary energy

Similarly, we introduce the complementary energy $\mathcal{E}^{*\text{BG}}$ of the Bending-Gradient problem which is defined as :

$$(1.41) \quad \mathcal{E}^{*\text{BG}} = \int_{\omega} w^{*\text{BG}}(\underline{\mathbf{M}}, \underline{\mathbf{R}}),$$

where $w^{*\text{BG}}$ represents the Bending-Gradient stress energy density function given by :

$$(1.42) \quad w^{*\text{BG}}(\underline{\mathbf{M}}, \underline{\mathbf{R}}) = \frac{1}{2} \underline{\mathbf{M}} : \underline{\mathbf{d}} : \underline{\mathbf{M}} + \frac{1}{2} \underline{\mathbf{R}} : \underline{\mathbf{h}} : \underline{\mathbf{R}}.$$

The principle of minimum complementary energy states that, among all statically compatible stress fields, the complementary energy functional $\mathcal{E}^{*\text{BG}}$ assumes a minimum value for the stress field $(\underline{\mathbf{M}}^{\text{BG}}, \underline{\mathbf{R}}^{\text{BG}})$, solution of the Bending-Gradient problem.

Having set the Bending-Gradient problem, our main concern now is to define the functional spaces in which we shall seek solutions and introduce norms in order to show that the corresponding variational problems, namely the stress and the displacement formulations, are well-posed.

1.4 Mathematical formulation of the Bending-Gradient problem for a fully clamped plate

We study in this section both stress and displacement formulations of the Bending-Gradient theory presented in the previous section and show their well-posedness.

1.4.1 Stress formulation

It is based on the principle of the minimum of the complementary energy (Section 1.3.2.7). Since the bending moment tensor $\underline{\underline{\mathbf{M}}}$ and the generalized shear force $\underline{\underline{\mathbf{R}}}$ are related by the equilibrium equation (2.8a), the complementary energy \mathcal{E}^{*BG} will be expressed solely in terms of $\underline{\underline{\mathbf{M}}}$. Therefore, it can be equivalently written in the following form :

$$(1.43) \quad \mathcal{E}^{*BG}(\underline{\underline{\mathbf{M}}}) = \int_{\omega} w^{*BG}(\underline{\underline{\mathbf{M}}}, \underline{\underline{\mathbf{M}}} \otimes \underline{\underline{\nabla}}) d\omega,$$

where w^{*BG} is defined by (1.42).

We recall that the compliance tensors $\underline{\underline{\mathbf{d}}}$ and $\underline{\underline{\mathbf{h}}}$ are positive definite in the sense that there exists two constants $c > 0$ and $c' > 0$ such that :

$$(1.44) \quad \forall \underline{\underline{\mathbf{M}}} \in \underline{\underline{\mathbb{R}}}, \quad c \underline{\underline{\mathbf{M}}} : \underline{\underline{\mathbf{M}}} \leq \underline{\underline{\mathbf{M}}} : \underline{\underline{\mathbf{d}}} : \underline{\underline{\mathbf{M}}} \leq c' \underline{\underline{\mathbf{M}}} : \underline{\underline{\mathbf{M}}},$$

$$(1.45) \quad \forall \underline{\underline{\mathbf{R}}} \in \underline{\underline{\mathbb{R}}}, \quad c^T \underline{\underline{\mathbf{R}}} : \underline{\underline{\mathbf{R}}} \leq {}^T \underline{\underline{\mathbf{R}}} : \underline{\underline{\mathbf{h}}} : \underline{\underline{\mathbf{R}}} \leq c' {}^T \underline{\underline{\mathbf{R}}} : \underline{\underline{\mathbf{R}}}.$$

Note that relations (1.44) and (1.45) also hold for the stiffness tensors $\underline{\underline{\mathbf{D}}}$ and $\underline{\underline{\mathbf{H}}}$.

Since the generalized stresses $(\underline{\underline{\mathbf{M}}}, \underline{\underline{\mathbf{R}}})$ that comply with equations (1.38c) are such that :

$$\underline{\underline{\mathbf{i}}} :: (\underline{\underline{\mathbf{R}}} \otimes \underline{\underline{\nabla}}) = \underline{\underline{\mathbf{i}}} :: ((\underline{\underline{\mathbf{M}}} \otimes \underline{\underline{\nabla}}) \otimes \underline{\underline{\nabla}}) = (\underline{\underline{\mathbf{M}}} \cdot \underline{\underline{\nabla}}) \cdot \underline{\underline{\nabla}} = M_{\alpha\beta, \alpha\beta},$$

then it is natural to define the space of statically admissible generalized stress fields as follows :

$$(1.46) \quad SC(p) = \{ \underline{\underline{\mathbf{M}}} \in \underline{\underline{\mathbf{H}}}^1(\omega), \quad M_{\alpha\beta, \alpha\beta} + p = 0 \text{ in the sense of distributions} \}.$$

The variational formulation of the Bending-Gradient problem consists in minimizing the complementary energy $\mathcal{E}^{*BG}(\underline{\underline{\mathbf{M}}})$ with respect to all $\underline{\underline{\mathbf{M}}} \in SC(p)$:

$$(1.47) \quad \min \left\{ \mathcal{E}^{*BG}(\underline{\underline{\mathbf{M}}}) = \int_{\omega} w^{*BG}(\underline{\underline{\mathbf{M}}}, \underline{\underline{\mathbf{M}}} \otimes \underline{\underline{\nabla}}), \quad \underline{\underline{\mathbf{M}}} \in SC(p) \right\}.$$

1.4.2 Well-posedness of the stress formulation

We now proceed to the study of problem (1.47). We establish the following result :

Theorem 1. *Assume that $p \in H^{-1}(\omega)$ and that assumptions (1.44) and (1.45) hold. Then, the minimization problem (1.47) admits a unique solution $\underline{\mathbf{M}}^{\text{BG}} \in \mathcal{SC}(p)$. Moreover, $\underline{\mathbf{M}}^{\text{BG}}$ is solution of the following variational problem :*

$$(1.48) \quad \begin{cases} \text{Find } \underline{\mathbf{M}}^{\text{BG}} \in \mathcal{SC}(p) \text{ such that} \\ \int_{\omega} \underline{\boldsymbol{\mu}} : \underline{\mathbf{d}} : \underline{\mathbf{M}}^{\text{BG}} + {}^T(\underline{\boldsymbol{\mu}} \otimes \underline{\nabla}) : \underline{\mathbf{h}} : (\underline{\mathbf{M}}^{\text{BG}} \otimes \underline{\nabla}) = 0, \quad \forall \underline{\boldsymbol{\mu}} \in \mathcal{SC}(0) \end{cases}$$

Démonstration. Let us first show that $\mathcal{SC}(p)$ is not empty. Indeed, let m be the unique solution in $H_0^1(\omega)$ of equation $\Delta m + p = 0$. Then, $\underline{\mathbf{P}}$ defined by $P_{\alpha\beta} = m\delta_{\alpha\beta}$ is obviously in $\mathcal{SC}(p)$. Moreover, any $\underline{\mathbf{M}} \in \mathcal{SC}(p)$ can be decomposed as the sum of $\underline{\mathbf{P}}$ and $\underline{\boldsymbol{\mu}}$ in $\mathcal{SC}(0)$. Namely :

$$(1.49) \quad \underline{\mathbf{M}} \in \mathcal{SC}(p) \iff \underline{\mathbf{M}} = \underline{\mathbf{P}} + \underline{\boldsymbol{\mu}}, \quad \underline{\boldsymbol{\mu}} \in \mathcal{SC}(0)$$

We introduce the following symmetric bilinear form on $\underline{\mathbf{H}}^1(\omega) \times \underline{\mathbf{H}}^1(\omega)$:

$$a_s(\underline{\mathbf{M}}, \underline{\mathbf{M}}') = \int_{\omega} \underline{\mathbf{M}}' : \underline{\mathbf{d}} : \underline{\mathbf{M}} + {}^T(\underline{\mathbf{M}}' \otimes \underline{\nabla}) : \underline{\mathbf{h}} : (\underline{\mathbf{M}} \otimes \underline{\nabla})$$

which enables us to write \mathcal{E}^{BG} as :

$$\mathcal{E}^{\text{BG}}(\underline{\mathbf{M}}) = \frac{1}{2} a_s(\underline{\mathbf{M}}, \underline{\mathbf{M}})$$

Using the decomposition (1.49), it can be easily seen that the following minimization problem :

$$(1.50) \quad \min \left\{ \frac{1}{2} a_s(\underline{\boldsymbol{\mu}}, \underline{\boldsymbol{\mu}}) + a_s(\underline{\mathbf{P}}, \underline{\boldsymbol{\mu}}), \quad \underline{\boldsymbol{\mu}} \in \mathcal{SC}(0) \right\}.$$

is equivalent to problem (1.47).

The space $\mathcal{SC}(0)$ equipped with the scalar product $\langle \cdot, \cdot \rangle_{\mathcal{SC}(0)}$ is actually a Hilbert space as shown in Appendix A.1.

$$\langle \underline{\boldsymbol{\mu}}, \underline{\boldsymbol{\mu}}' \rangle_{\mathcal{SC}(0)} = \int_{\omega} \underline{\boldsymbol{\mu}}' : \underline{\boldsymbol{\mu}} + {}^T(\underline{\boldsymbol{\mu}}' \otimes \underline{\nabla}) : (\underline{\boldsymbol{\mu}} \otimes \underline{\nabla}).$$

Clearly, thanks to assumptions (1.44) and (1.45), the bilinear form $a_s(\underline{\boldsymbol{\mu}}, \underline{\boldsymbol{\mu}}')$ is continuous and coercive on $\mathcal{SC}(0)$ and the linear map $\underline{\boldsymbol{\mu}} \longrightarrow a_s(\underline{\mathbf{P}}, \underline{\boldsymbol{\mu}})$ is continuous on $\mathcal{SC}(0)$. See Appendix A.2. Hence, by the application of the Lax-Milgram theorem on (1.50), we conclude that the problem (1.47) is well-posed and that its unique solution $\underline{\mathbf{M}}^{\text{BG}} \in \mathcal{SC}(p)$ satisfies

$$\forall \underline{\boldsymbol{\mu}} \in \mathcal{SC}(0), \quad a_s(\underline{\boldsymbol{\mu}}, \underline{\mathbf{M}}^{\text{BG}}) = 0,$$

This ends the proof. □

1.4.3 Well-posedness of the displacement formulation

Let $(W, \underline{\Phi})$ be a generalized displacement field defined over ω . The potential energy \mathcal{E}^{BG} expressed in terms of $(W, \underline{\Phi})$ takes the form :

$$(1.51) \quad \mathcal{E}^{\text{BG}}(W, \underline{\Phi}) = \int_{\omega} w^{\text{BG}} \left(\underline{\Phi} \cdot \underline{\nabla}, \underline{\Phi} + \underline{\mathbf{i}} \cdot \underline{\nabla} W \right) - \int_{\omega} pW$$

where w^{BG} is given by (1.40).

Assuming $p \in H^{-1}(\omega)$, \mathcal{E}^{BG} is clearly well defined for $(W, \underline{\Phi}) \in KC_0$ where the space of the generalized Bending-Gradient displacements which are kinematically compatible with clamped boundary conditions is the product of $H_0^1(\omega)$ with the space $\underline{\mathbf{H}}_0(\text{div}, \omega)$ introduced in Section 1.2.2 :

$$KC_0 = H_0^1(\omega) \times \underline{\mathbf{H}}_0(\text{div}, \omega).$$

Note that the space KC_0 is a Hilbert space as the product of two Hilbert spaces.

The Bending-Gradient problem with clamped boundary conditions consists in minimizing the potential energy $\mathcal{E}^{\text{BG}}(W, \underline{\Phi})$ over all $(W, \underline{\Phi}) \in KC_0$:

$$(1.52) \quad \min \{ \mathcal{E}^{\text{BG}}(W, \underline{\Phi}), \quad (W, \underline{\Phi}) \in KC_0 \}$$

where \mathcal{E}^{BG} is given by (1.51).

In order to show that the minimization problem (1.52) is well-posed, we introduce the bilinear form a defined on $KC_0 \times KC_0$ by

$$(1.53) \quad a((W, \underline{\Phi}), (W', \underline{\Phi}')) = \int_{\omega} (\underline{\Phi} \cdot \underline{\nabla}) : \underline{\underline{D}} : (\underline{\Phi}' \cdot \underline{\nabla}) + {}^T (\underline{\Phi} + \underline{\mathbf{i}} \cdot \underline{\nabla} W) : \underline{\underline{H}} : (\underline{\Phi}' + \underline{\mathbf{i}} \cdot \underline{\nabla} W')$$

and the linear form b defined on KC_0 by

$$(1.54) \quad b(W, \underline{\Phi}) = \int_{\omega} pW$$

Hence, $\mathcal{E}^{\text{BG}}(W, \underline{\Phi})$ can be written as :

$$\mathcal{E}^{\text{BG}}(W, \underline{\Phi}) = \frac{1}{2} a((W, \underline{\Phi}), (W, \underline{\Phi})) - b(W, \underline{\Phi}).$$

Clearly, the linear form b is continuous on KC_0 (see Appendix A.3). Furthermore, the bilinear form a is symmetric and continuous on $KC_0 \times KC_0$ (see Appendix A.4). It thus remains to prove that a is coercive on KC_0 .

1.4.3.1 Coercivity of the bilinear form a

Let us introduce a new bilinear form denoted by a_N and defined on $KC_0 \times KC_0$ by :

$$(1.55) \quad a_N((W, \underline{\Phi}), (W', \underline{\Phi}')) = \int_{\omega} (\underline{\Phi} \cdot \underline{\nabla}) : (\underline{\Phi}' \cdot \underline{\nabla}) + {}^T (\underline{\Phi} + \underline{\mathbf{i}} \cdot \underline{\nabla} W) : (\underline{\Phi}' + \underline{\mathbf{i}} \cdot \underline{\nabla} W')$$

Since $\underline{\underline{D}}$ and $\underline{\underline{H}}$ are positive definite, there exists a constant $\beta > 0$ such that, for all $\underline{\chi} \in \mathbb{R}$ and all $\underline{\Gamma} \in \mathbb{R}$, we have :

$$\beta \left(\underline{\chi} : \underline{\chi} + {}^T \underline{\Gamma} : \underline{\Gamma} \right) \leq \underline{\chi} : \underline{\underline{D}} : \underline{\chi} + {}^T \underline{\Gamma} : \underline{\underline{H}} : \underline{\Gamma}$$

Hence, the coercivity of a over $KC_0 \times KC_0$ directly follows from the below lemma :

Lemma 6. *The bilinear form a_N is a scalar product on KC_0 and the associated norm denoted by $\|\bullet\|_N$ is equivalent to the norm $\|\bullet\|_{KC_0}$.*

Démonstration. We decompose the proof into two steps.

Step 1. Since the bilinear form a_N is symmetric and positive, it only remains to prove that it is definite on KC_0 in order to show that it is a scalar product. Consider $(W, \underline{\Phi}) \in KC_0$ such that

$$a_N((W, \underline{\Phi}), (W, \underline{\Phi})) = 0.$$

Then, $\underline{\Phi} \cdot \underline{\nabla} = 0$ and $\underline{\Phi} + \underline{\mathbf{i}} \cdot \underline{\nabla} W = 0$. We therefore have that $\Delta W = 0$. This implies that $W = 0$, as $W \in H_0^1(\omega)$. Hence, $\underline{\Phi} = 0$. Thus, a_N is a scalar product on KC_0 and $\|\bullet\|_N$ defines a norm on KC_0 .

Step 2. It is important to note that there exists a constant C such that :

$$(1.56) \quad \forall (W, \underline{\Phi}) \in KC_0, \quad \|W, \underline{\Phi}\|_N^2 = \|\underline{\Phi} \cdot \underline{\nabla}\|_{\underline{\underline{L}}^2(\omega)}^2 + \|\underline{\Phi} + \underline{\mathbf{i}} \cdot \underline{\nabla} W\|_{\underline{\underline{L}}^2(\omega)}^2 \\ \leq C \|W, \underline{\Phi}\|_{KC_0}^2$$

In order to show that the norms $\|\cdot, \cdot\|_N$ and $\|\cdot, \cdot\|_{KC_0}$ are equivalent, we need to prove that there exists a constant C' such that

$$(1.57) \quad \forall (W, \underline{\Phi}) \in KC_0, \quad \|W, \underline{\Phi}\|_{KC_0} \leq C' \|W, \underline{\Phi}\|_N$$

To this aim, we proceed by contradiction. Suppose that for all $k \in \mathbb{N}$, there exists $(W_k, \underline{\Phi}_k) \in KC_0$ such that :

$$(1.58) \quad \|W_k, \underline{\Phi}_k\|_{KC_0} = 1, \quad \|W_k, \underline{\Phi}_k\|_N \leq \frac{1}{k}$$

Rather than working with the third order tensor $\underline{\Phi}$, it is more useful to work with its spherical part $\underline{\Phi}^s$ and its deviatoric part $\underline{\Phi}^d$. We define the spherical part $\underline{\Phi}^s$ by :

$$(1.59) \quad \underline{\Phi}^s = \underline{\mathbf{i}} \cdot \underline{\Phi}^s, \quad \underline{\Phi}^s = \frac{2}{3} \underline{\Phi} : \underline{\delta}$$

where $\underline{\Phi}^s$ is in $\underline{\mathbf{L}}^2(\omega)$. We can therefore write $\|W_k, \underline{\Phi}_k\|_N^2$ as follows :

$$(1.60) \quad \begin{aligned} \|W_k, \underline{\Phi}_k\|_N^2 &= \|\underline{\Phi}_k \cdot \underline{\nabla}\|_{\underline{\mathbf{L}}^2(\omega)}^2 + \|\underline{\Phi}_k^d + \underline{\Phi}_k^s + \underline{\mathbf{i}} \cdot \underline{\nabla} W_k\|_{\underline{\mathbf{L}}^2(\omega)}^2 \\ &= \|\underline{\Phi}_k \cdot \underline{\nabla}\|_{\underline{\mathbf{L}}^2(\omega)}^2 + \|\underline{\Phi}_k^d\|_{\underline{\mathbf{L}}^2(\omega)}^2 + \frac{3}{2} \|\underline{\Phi}_k^s + \underline{\nabla} W_k\|_{\underline{\mathbf{L}}^2(\omega)}^2 \end{aligned}$$

Using (1.58), we have that $\|\underline{\Phi}_k \cdot \underline{\nabla}\|_{\underline{\mathbf{L}}^2(\omega)} + \|\underline{\Phi}_k^d\|_{\underline{\mathbf{L}}^2(\omega)} \leq \frac{1}{k}$. It follows from Lemma 3 that $(\underline{\Phi}_k)$ strongly converges to zero in $\underline{\mathbf{H}}(div, \omega)$. Using (1.59), we can assure that $\underline{\Phi}_k^s$ strongly converges to zero in $\underline{\mathbf{L}}^2(\omega)$.

Hence,

$$\|\underline{\Phi}_k^s + \underline{\nabla} W_k\|_{\underline{\mathbf{L}}^2(\omega)} \leq \frac{1}{k}$$

implies that $(\underline{\nabla} W_k)$ strongly converges to zero in $\underline{\mathbf{L}}^2(\omega)$. Consequently, (W_k) strongly converges to zero in $H_0^1(\omega)$. There is hence in contradiction with $\|W_k, \underline{\Phi}_k\|_{KC_0} = 1$ \square

1.4.3.2 Existence and uniqueness of the solution to (1.52)

The existence and uniqueness of the solution to the minimization problem (1.52) is directly inferred from the Lax-Milgram theorem since its assumptions are satisfied. Namely, the symmetric bilinear form a is continuous and coercive, and the linear form b is continuous. The main result of this paper is stated in the following theorem :

Theorem 2. *Assume that $p \in H^{-1}(\omega)$ and that the stiffness tensors $\underline{\mathbf{D}}$ and $\underline{\mathbf{H}}$ are symmetric and positive definite. Then the problem (1.52) is well-posed, i.e., there exists a unique solution $(W^{\text{BG}}, \underline{\Phi}^{\text{BG}}) \in KC_0$ such that :*

$$(1.61) \quad a((W^{\text{BG}}, \underline{\Phi}^{\text{BG}}), (W, \underline{\Phi})) = b(W, \underline{\Phi})$$

for all $(W, \underline{\Phi}) \in KC_0$, where a and b are given by (1.53) and (1.54). Moreover, we have

$$(1.62) \quad \|(W^{\text{BG}}, \underline{\Phi}^{\text{BG}})\|_{KC_0} \leq c \|p\|_{H^{-1}(\omega)}$$

where c is a strictly positive constant.

1.4.4 Relation between the stress and the displacement formulations

The above-presented formulations, namely the stress formulation (1.47) and the displacement formulation (1.52), have each respectively a unique solution, as shown respectively by Theorems 1 and 2. We therefore proceed to show that we can derive the displacement solution from the stress solution, and vice-versa. We state this in the following theorem :

Theorem 3. *Under the assumptions stated in Theorem 2, let $(W^{\text{BG}}, \underline{\Phi}^{\text{BG}})$ be the unique solution to the minimization problem (1.52). Consider that the generalized strains associated to $(W^{\text{BG}}, \underline{\Phi}^{\text{BG}})$ through the compatibility conditions (1.28),(1.29) are given by*

$$(1.63) \quad \underline{\chi}^{\text{BG}} = \underline{\Phi}^{\text{BG}} \cdot \underline{\nabla}, \quad \underline{\Gamma}^{\text{BG}} = \underline{\Phi}^{\text{BG}} + \underline{\mathbf{i}} \cdot \underline{\nabla} W^{\text{BG}},$$

and that the generalized stress fields associated to $(W^{\text{BG}}, \underline{\Phi}^{\text{BG}})$ by the constitutive equations (2.7) are

$$(1.64) \quad \underline{\mathbf{M}}^{\text{BG}} = \underline{\mathbf{D}} : \underline{\chi}^{\text{BG}}, \quad \underline{\mathbf{R}}^{\text{BG}} = \underline{\mathbf{H}} : \underline{\Gamma}^{\text{BG}}.$$

Then,

$$\underline{\mathbf{M}}^{\text{BG}} \in \mathcal{SC}(p),$$

where $\mathcal{SC}(p)$ is defined by (1.46), and

$$(1.65) \quad \underline{\mathbf{R}}^{\text{BG}} = \underline{\mathbf{M}}^{\text{BG}} \otimes \underline{\nabla}.$$

Moreover, $\underline{\mathbf{M}}^{\text{BG}}$ is the unique solution to the minimization problem (1.47), where $w^{*\text{BG}}$ is defined by (1.42).

Démonstration. Since $(W^{\text{BG}}, \underline{\Phi}^{\text{BG}}) \in \mathcal{KC}_0$, relations (1.63) yield $\underline{\chi}^{\text{BG}} \in \underline{\mathbf{L}}^2(\omega)$ and $\underline{\Gamma}^{\text{BG}} \in \underline{\mathbf{L}}^2(\omega)$. Consequently, due to equations (1.64), we also have that $\underline{\mathbf{M}}^{\text{BG}} \in \underline{\mathbf{L}}^2(\omega)$ and $\underline{\mathbf{R}}^{\text{BG}} \in \underline{\mathbf{L}}^2(\omega)$. According to theorem 2, $(W^{\text{BG}}, \underline{\Phi}^{\text{BG}})$ satisfies (1.61). Therefore, we have that, for all $(W, \underline{\Phi}) \in \mathcal{KC}_0$,

$$(1.66) \quad \int_{\omega} \underline{\mathbf{M}}^{\text{BG}} : (\underline{\Phi} \cdot \underline{\nabla}) + {}^T \underline{\mathbf{R}}^{\text{BG}} : (\underline{\Phi} + \underline{\mathbf{i}} \cdot \underline{\nabla} W) = \int_{\omega} p W d\omega$$

Restricting (1.66) to $(W, \underline{\Phi}) \in D(\omega) \times \underline{\mathbf{D}}(\omega) \subset \mathcal{KC}_0$ and considering first the particular case where $W = 0$ yields after integration by parts :

$$(1.67) \quad \langle \underline{\mathbf{R}}^{\text{BG}} - \underline{\mathbf{M}}^{\text{BG}} \otimes \underline{\nabla}, \underline{\Phi} \rangle_{\underline{\mathbf{D}}'(\omega), \underline{\mathbf{D}}(\omega)} = 0$$

This proves

$$(1.68) \quad \underline{\mathbf{R}}^{\text{BG}} = \underline{\mathbf{M}}^{\text{BG}} \otimes \underline{\nabla}$$

in the sense of distributions.

Considering now the particular case where $\underline{\Phi} = 0$ yields

$$(1.69) \quad \left\langle - \left(\underset{\approx}{\mathbf{i}} : \underline{\mathbf{R}}^{\text{BG}} \right) \cdot \underline{\nabla} - p, W \right\rangle_{D'(\omega), D(\omega)} = 0$$

Hence,

$$(1.70) \quad \left(\underset{\approx}{\mathbf{i}} : \underline{\mathbf{R}}^{\text{BG}} \right) \cdot \underline{\nabla} + p = 0$$

in the sense of distributions.

Equation (1.68) shows that the bending gradient components are in $\underline{\mathbf{L}}^2(\omega)$. Hence, $\underline{\mathbf{M}}^{\text{BG}} \in \underline{\mathbf{H}}^1(\omega)$. Replacing $\underline{\mathbf{R}}^{\text{BG}}$ by $\underline{\mathbf{M}}^{\text{BG}} \otimes \underline{\nabla}$ in (1.70) yields :

$$\left(\underline{\mathbf{M}}^{\text{BG}} \cdot \underline{\nabla} \right) \cdot \underline{\nabla} + p = 0.$$

which means that $\underline{\mathbf{M}}^{\text{BG}}$ is actually in $SC(p)$. It remains to show that $\underline{\mathbf{M}}^{\text{BG}}$ is the unique solution to the problem (1.47). Consider any element $\underline{\mathbf{M}} \in SC(p)$, and set

$$\underline{\mathbf{M}}' = \underline{\mathbf{M}} - \underline{\mathbf{M}}^{\text{BG}}.$$

Clearly, $\underline{\mathbf{M}}'$ belongs to $SC(0)$ and, based on (1.63), (1.64) and (1.68), we have by simple algebra :

$$(1.71) \quad \begin{aligned} \mathcal{E}^{\text{*BG}}(\underline{\mathbf{M}}) &= \mathcal{E}^{\text{*BG}}(\underline{\mathbf{M}}') + \mathcal{E}^{\text{*BG}}(\underline{\mathbf{M}}^{\text{BG}}) + \int_{\omega} \underline{\mathbf{M}}' : \underline{\mathbf{d}} : \underline{\mathbf{M}}^{\text{BG}} + {}^T(\underline{\mathbf{M}}' \otimes \underline{\nabla}) : \underline{\mathbf{h}} : (\underline{\mathbf{M}}^{\text{BG}} \otimes \underline{\nabla}) \\ &= \mathcal{E}^{\text{*BG}}(\underline{\mathbf{M}}') + \mathcal{E}^{\text{*BG}}(\underline{\mathbf{M}}^{\text{BG}}) + \int_{\omega} \underline{\mathbf{M}}' : (\underline{\Phi}^{\text{BG}} \cdot \underline{\nabla}) + {}^T(\underline{\mathbf{M}}' \otimes \underline{\nabla}) : \left(\underline{\Phi}^{\text{BG}} + \underset{\approx}{\mathbf{i}} \cdot \underline{\nabla} W^{\text{BG}} \right) \end{aligned}$$

Recalling that the generalized displacements $(W^{\text{BG}}, \underline{\Phi}^{\text{BG}})$ belong to KC_0 and that the stress field $\underline{\mathbf{M}}'$ belongs to $SC(0)$, integrating by parts implies that the last term of the right-hand side of (1.71) vanishes. Hence, we have :

$$\mathcal{E}^{\text{*BG}}(\underline{\mathbf{M}}) = \mathcal{E}^{\text{*BG}}(\underline{\mathbf{M}}') + \mathcal{E}^{\text{*BG}}(\underline{\mathbf{M}}^{\text{BG}}).$$

We end the proof by mentioning that $\mathcal{E}^{\text{*BG}}(\underline{\mathbf{M}}')$ is positive as soon as $\underline{\mathbf{M}}'$ does not vanish. \square

Having studied the Bending-Gradient theory for clamped plates, we now introduce this theory when free boundary conditions are prescribed.

1.5 Mathematical formulation of the Bending-Gradient problem for a loaded plate with free boundary conditions

In this section, we study the problem with completely free boundary conditions. Since the shear force compliance tensor is assumed to be positive definite, these conditions write as follows when the generalized stress fields are regular enough (See Sab and Lebé (2015), chapter 6) :

$$(1.72) \quad \underline{\mathbf{M}} = 0, \quad \left(\underline{\mathbf{i}} : \underline{\mathbf{R}} \right) \cdot \underline{\mathbf{n}} = 0 \text{ on } \partial\omega$$

or in terms of components :

$$(1.73) \quad M_{\alpha\beta} = 0, \quad R_{\alpha\beta\gamma} n_\alpha = 0 \text{ on } \partial\omega$$

Here, $\underline{\mathbf{n}}$ is the outer normal vector to $\partial\omega$.

We hence have to find W , $\underline{\mathbf{\Phi}}$, $\underline{\mathbf{\chi}}$, $\underline{\mathbf{\Gamma}}$, $\underline{\mathbf{M}}$ and $\underline{\mathbf{R}}$ solution of (1.28), (1.29), (2.8), (2.7) and (1.72). This prompts us to introduce a displacement formulation (see (1.82)) then to prove that the corresponding minimization problem admits a unique solution (see Theorem 4). We finally establish the relation between this formulation and a stress formulation (Theorem 6).

1.5.1 Formulation of the problem

We introduce the set of the generalized Bending-Gradient displacements which are kinematically compatible with free boundary conditions as the quotient space :

$$KC_f = KC/\mathcal{R}$$

where

$$KC = H^1(\omega) \times \underline{\mathbf{H}}(div, \omega)$$

and \mathcal{R} is the set of the displacements $(W, \underline{\mathbf{\Phi}})$ in KC such that the generalized Bending-Gradient strains $(\underline{\mathbf{\chi}}, \underline{\mathbf{\Gamma}})$ are identically null.

Obviously, such displacements verify $\underline{\mathbf{\Phi}} = -\underline{\mathbf{i}} \cdot \underline{\nabla} W$ and $\underline{\mathbf{\Phi}} \cdot \underline{\nabla} = (-W_{,\alpha\beta}) = 0$. Therefore, W is an affine function of x_1 and x_2 and the set \mathcal{R} is defined as follows :

$$(1.74) \quad \mathcal{R} = \left\{ (W, \underline{\mathbf{\Phi}}) \in KC / W = \underline{\alpha} \cdot \underline{\mathbf{x}} + \beta, \underline{\mathbf{\Phi}} = -\underline{\mathbf{i}} \cdot \underline{\alpha}, \alpha_1, \alpha_2, \beta \in \mathbb{R} \right\}$$

In components, we have

$$W(x_1, x_2) = \alpha_1 x_1 + \alpha_2 x_2 + \beta$$

and

$$(\Phi_{111}, \Phi_{221}, \Phi_{121}, \Phi_{112}, \Phi_{222}, \Phi_{122})(x_1, x_2) = \left(-\alpha_1, 0, -\frac{1}{2}\alpha_2, 0, -\alpha_2, -\frac{1}{2}\alpha_1 \right).$$

Clearly, the space \mathcal{R} is a closed subspace of KC . We can therefore consider the orthogonal projection of KC on \mathcal{R} according to the norm $\|\bullet\|_{KC}$: For any $(W, \underline{\Phi}) \in KC$, there exists a unique $\Pi(W, \underline{\Phi})$ such that :

$$(1.75) \quad \|(W, \underline{\Phi}) - \Pi(W, \underline{\Phi})\|_{KC} = \inf_{(V, \underline{\Psi}) \in \mathcal{R}} \|(W, \underline{\Phi}) - (V, \underline{\Psi})\|_{KC}$$

Lemma 7. *The quotient space KC_f , endowed with the scalar product*

$$(1.76) \quad \left\langle \left[\check{W}, \check{\underline{\Phi}} \right], \left[\check{W}', \check{\underline{\Phi}}' \right] \right\rangle_{KC_f} = \langle (W, \underline{\Phi}) - \Pi(W, \underline{\Phi}), (W', \underline{\Phi}') - \Pi(W', \underline{\Phi}') \rangle_{KC},$$

where $(W, \underline{\Phi})$ (resp. $(W', \underline{\Phi}')$) is any element in $\left[\check{W}, \check{\underline{\Phi}} \right]$ (resp. $\left[\check{W}', \check{\underline{\Phi}}' \right]$), is a Hilbert space.

Démonstration. We start by showing that the scalar product (1.76) is well-defined. Consider $(W, \underline{\Phi})$ and $(W^*, \underline{\Phi}^*)$ two elements in $\left[\check{W}, \check{\underline{\Phi}} \right]$. Since Π is a linear operator, we can write

$$(W^*, \underline{\Phi}^*) - \Pi(W^*, \underline{\Phi}^*) = (W^*, \underline{\Phi}^*) - (W, \underline{\Phi}) - \Pi((W^*, \underline{\Phi}^*) - (W, \underline{\Phi})) + (W, \underline{\Phi}) - \Pi(W, \underline{\Phi})$$

Now, $(W^*, \underline{\Phi}^*) - (W, \underline{\Phi})$ being an element of \mathcal{R} yields

$$(W^*, \underline{\Phi}^*) - (W, \underline{\Phi}) - \Pi((W^*, \underline{\Phi}^*) - (W, \underline{\Phi})) = 0$$

We therefore have that :

$$(W^*, \underline{\Phi}^*) - \Pi(W^*, \underline{\Phi}^*) = (W, \underline{\Phi}) - \Pi(W, \underline{\Phi})$$

which means that the scalar product (1.76) is well-defined on KC_f .

We are now left to prove that KC_f is a Hilbert space. To this end, let $\left[\check{W}_n, \check{\underline{\Phi}}_n \right] \in KC_f$, $n \in \mathbb{N}$, be a Cauchy sequence in the norm $\|\bullet\|_{KC_f}$. Obviously, $(W_n, \underline{\Phi}_n) - \Pi(W_n, \underline{\Phi}_n)$ is a Cauchy sequence in KC . Hence, it converges to an element $(W_\infty, \underline{\Phi}_\infty)$ such that

$$\Pi(W_\infty, \underline{\Phi}_\infty) = 0$$

since the operator Π is continuous. We now see that

$$\left\| \left[\check{W}_n, \check{\underline{\Phi}}_n \right] - \left[\check{W}_\infty, \check{\underline{\Phi}}_\infty \right] \right\|_{KC_f}^2 = \|(W_n, \underline{\Phi}_n) - (W_\infty, \underline{\Phi}_\infty) - \Pi(W_n, \underline{\Phi}_n)\|_{KC}^2,$$

hence $\left[\check{W}_n, \check{\underline{\Phi}}_n \right]$ converges to $\left[\check{W}_\infty, \check{\underline{\Phi}}_\infty \right]$ in KC_f . This ends the proof. \square

In the absence of kinematic boundary conditions, the global equilibrium of the plate is impossible unless the applied transverse load p is self-balanced. Namely,

$$\forall (W, \underline{\Phi}) \in \mathcal{R}, \quad b(W, \underline{\Phi}) = \int_{\omega} pW = 0.$$

The above equation is equivalent to the following standard conditions stipulating that the resultant applied force and moments are null :

$$(1.77) \quad \int_{\omega} p = 0, \quad \int_{\omega} px_1 = 0 \quad \text{and} \quad \int_{\omega} px_2 = 0.$$

We are now in position to introduce a variational formulation on KC_f . We introduce the following linear form :

$$(1.78) \quad \forall [\check{W}, \check{\Phi}] \in KC_f, \quad \check{b}([\check{W}, \check{\Phi}]) = b(W, \underline{\Phi}) = \int_{\omega} pW$$

where $(W, \underline{\Phi})$ is any element in $[\check{W}, \check{\Phi}]$. This makes sense because equations (1.77) ensure that the above right-hand side does not depend on the choice of $(W, \underline{\Phi})$. Assume that p is in $L^2(\omega)$. Then, the linear form b is continuous on KC , and we have for any $[\check{W}, \check{\Phi}] \in KC_f$,

$$(1.79) \quad \begin{aligned} |\check{b}([\check{W}, \check{\Phi}])| &= |b((W, \underline{\Phi}) - \Pi(W, \underline{\Phi}))| \\ &\leq C \|(W, \underline{\Phi}) - \Pi(W, \underline{\Phi})\|_{KC} \\ &\leq C \|\check{W}, \check{\Phi}\|_{KC_f} \end{aligned}$$

We conclude that the linear form \check{b} is continuous on KC_f . Let us now introduce the following bilinear form on KC_f :

$$(1.80) \quad \begin{aligned} \check{a}([\check{W}, \check{\Phi}], [\check{W}', \check{\Phi}']) &= a((W, \underline{\Phi}), (W', \underline{\Phi}')) = \int_{\omega} (\underline{\Phi} \cdot \underline{\nabla}) : \underline{\underline{D}} : (\underline{\Phi}' \cdot \underline{\nabla}) \\ &\quad + {}^T(\underline{\Phi} + \underline{\underline{z}} \cdot \underline{\nabla} W) : \underline{\underline{H}} : (\underline{\Phi}' + \underline{\underline{z}} \cdot \underline{\nabla} W') \end{aligned}$$

where $(W, \underline{\Phi})$ (resp. $(W', \underline{\Phi}')$) is any element in $[\check{W}, \check{\Phi}]$ (resp. $[\check{W}', \check{\Phi}']$). The bilinear form \check{a} is well-defined on KC_f because, obviously, all the elements of $[\check{W}, \check{\Phi}]$ have the same generalized strains $\underline{\Phi} \cdot \underline{\nabla}$ and $\underline{\Phi} + \underline{\underline{z}} \cdot \underline{\nabla} W$. Moreover, \check{a} is continuous on KC_f .

Indeed,

$$(1.81) \quad \begin{aligned} |\check{a}([\check{W}, \check{\Phi}], [\check{W}', \check{\Phi}'])| &= |a((W, \underline{\Phi}) - \Pi(W, \underline{\Phi}), (W', \underline{\Phi}') - \Pi(W', \underline{\Phi}'))| \\ &\leq C \|(W, \underline{\Phi}) - \Pi(W, \underline{\Phi})\|_{KC} \|(W', \underline{\Phi}') - \Pi(W', \underline{\Phi}')\|_{KC} \\ &\leq C \|\check{W}, \check{\Phi}\|_{KC_f} \|\check{W}', \check{\Phi}'\|_{KC_f} \end{aligned}$$

We consider the following minimization problem :

$$(1.82) \quad \min \left\{ \check{\mathcal{P}} \left(\left[\check{W}, \check{\Phi} \right] \right), \quad \left[\check{W}, \check{\Phi} \right] \in KC_f \right\},$$

where

$$\check{\mathcal{P}} \left(\left[\check{W}, \check{\Phi} \right] \right) = \frac{1}{2} \check{a} \left(\left[\check{W}, \check{\Phi} \right], \left[\check{W}, \check{\Phi} \right] \right) - \check{b} \left(\left[\check{W}, \check{\Phi} \right] \right).$$

The well-posedness of this problem relies on the coercivity of the bilinear form \check{a} , which we will prove in the following paragraph.

1.5.2 Coercivity of the bilinear form \check{a}

In order to prove the coercivity of \check{a} , we will need the following lemma :

Lemma 8. *Let $\left[\check{W}, \check{\Phi} \right] \in KC_f$. There exist two constants $c > 0$ and $c' > 0$ such that*

$$c \left\| \check{W}, \check{\Phi} \right\|_N \leq \left\| \check{W}, \check{\Phi} \right\|_{KC_f} \leq c' \left\| \check{W}, \check{\Phi} \right\|_N$$

where $\left\| \check{W}, \check{\Phi} \right\|_N^2 = a_N \left((W, \Phi), (W, \Phi) \right)$, with a_N given by (1.55) and (W, Φ) is any element in $\left[\check{W}, \check{\Phi} \right]$, defines a norm on KC_f .

Démonstration. We decompose the proof into three steps.

Step 1. Since all the elements of $\left[\check{W}, \check{\Phi} \right]$ have the same generalized strains $\check{\Phi} \cdot \underline{\nabla}$ and $\check{\Phi} + \check{\mathbf{i}} \cdot \underline{\nabla} W$, one can define the bilinear form \check{a}_N on $KC_f \times KC_f$ as :

$$(1.83) \quad \check{a}_N \left(\left[\check{W}, \check{\Phi} \right], \left[\check{W}', \check{\Phi}' \right] \right) = a_N \left((W, \Phi), (W', \Phi') \right)$$

where (W, Φ) (resp. (W', Φ')) is any element in $\left[\check{W}, \check{\Phi} \right]$ (resp. $\left[\check{W}', \check{\Phi}' \right]$). Since the bilinear form \check{a}_N is symmetric and positive, it only remains to prove that it is definite on KC_f in order to show that it is a scalar product. Indeed, if we have $a_N \left((W, \Phi), (W, \Phi) \right) = 0$, then, $\check{\Phi} \cdot \underline{\nabla} = 0$ and $\check{\Phi} + \check{\mathbf{i}} \cdot \underline{\nabla} W = 0$. Hence, $(W, \Phi) \in \mathcal{R}$ and $\left[\check{W}, \check{\Phi} \right] = 0$. Thus, \check{a}_N is a scalar product on KC_f and $\|\cdot, \cdot\|_N$ defines a norm on KC_f .

Step 2. We first start by proving that there exists a constant $c > 0$ such that :

$$\left\| \check{W}, \check{\Phi} \right\|_{KC_f} \geq c \left\| \check{W}, \check{\Phi} \right\|_N$$

Let $(W, \underline{\Phi})$ be any element in $[\check{W}, \check{\Phi}]$. As in Section 1.4.3.1, we decompose the third-order tensor $\underline{\Phi}$ into its spherical part $\underline{\Phi}^s = \underline{\underline{i}} \cdot \underline{\Phi}^s$ and its deviatoric part $\underline{\Phi}^d$. Hence, $\|W, \underline{\Phi}\|_N$ can be written as follows :

$$(1.84) \quad \begin{aligned} \|\check{W}, \check{\Phi}\|_N^2 &= \|\underline{\Phi} \cdot \underline{\nabla}\|_{\underline{\underline{L}}^2(\omega)}^2 + \|\underline{\Phi} + \underline{\underline{i}} \cdot \underline{\nabla}W\|_{\underline{\underline{L}}^2(\omega)}^2 \\ &= \|\underline{\Phi} \cdot \underline{\nabla}\|_{\underline{\underline{L}}^2(\omega)}^2 + \|\underline{\Phi}^d\|_{\underline{\underline{L}}^2(\omega)}^2 + \frac{3}{2} \|\underline{\Phi}^s + \underline{\nabla}W\|_{\underline{\underline{L}}^2(\omega)}^2 \end{aligned}$$

Besides, we have :

$$(1.85) \quad \begin{aligned} \|\check{W}, \check{\Phi}\|_{KC_f}^2 &= \|(W - W^{\mathcal{R}}, \underline{\Phi} - \underline{\Phi}^{\mathcal{R}})\|_{KC}^2 \\ &= \|W - W^{\mathcal{R}}\|_{L^2(\omega)}^2 + \|\underline{\nabla}W - \underline{\nabla}W^{\mathcal{R}}\|_{\underline{\underline{L}}^2(\omega)}^2 \\ &\quad + \frac{3}{2} \|\underline{\Phi}^s - \underline{\Phi}^{\mathcal{R}}\|_{\underline{\underline{L}}^2(\omega)}^2 + \|\underline{\Phi}^d\|_{\underline{\underline{L}}^2(\omega)}^2 + \|\underline{\Phi} \cdot \underline{\nabla}\|_{\underline{\underline{L}}^2(\omega)}^2, \end{aligned}$$

where we denote by $(W^{\mathcal{R}}, \underline{\Phi}^{\mathcal{R}})$ the orthogonal projection of $(W, \underline{\Phi})$ on \mathcal{R} , i.e., :

$$\Pi(W, \underline{\Phi}) = (W^{\mathcal{R}}, \underline{\Phi}^{\mathcal{R}}) \in \mathcal{R}$$

We can obviously write :

$$\|\underline{\nabla}W - \underline{\nabla}W^{\mathcal{R}}\|^2 + \frac{3}{2} \|\underline{\Phi}^s - \underline{\Phi}^{\mathcal{R}}\|^2 \geq \frac{1}{2} \|\underline{\nabla}W - \underline{\nabla}W^{\mathcal{R}}\|^2 + \frac{1}{2} \|\underline{\Phi}^s - \underline{\Phi}^{\mathcal{R}}\|^2$$

By convexity of the square function, we obtain the following inequality :

$$\frac{1}{2} \|\underline{\nabla}W - \underline{\nabla}W^{\mathcal{R}}\|^2 + \frac{1}{2} \|\underline{\Phi}^s - \underline{\Phi}^{\mathcal{R}}\|^2 \geq \left\| \frac{1}{2} (\underline{\nabla}W - \underline{\nabla}W^{\mathcal{R}} + \underline{\Phi}^s - \underline{\Phi}^{\mathcal{R}}) \right\|^2$$

Noticing that $\underline{\nabla}W^{\mathcal{R}} + \underline{\Phi}^{\mathcal{R}} = 0$ by the very definition of \mathcal{R} , then equation (1.85) and the above inequalities yield :

$$(1.86) \quad \|\check{W}, \check{\Phi}\|_{KC_f}^2 \geq \frac{1}{4} \|\underline{\Phi}^s + \underline{\nabla}W\|_{\underline{\underline{L}}^2(\omega)}^2 + \|\underline{\Phi}^d\|_{\underline{\underline{L}}^2(\omega)}^2 + \|\underline{\Phi} \cdot \underline{\nabla}\|_{\underline{\underline{L}}^2(\omega)}^2 \geq \frac{1}{6} \|\check{W}, \check{\Phi}\|_N^2$$

Step 3. We are left with proving that there exists a constant $c' > 0$ such that :

$$(1.87) \quad \|\check{W}, \check{\Phi}\|_{KC_f} \leq c' \|\check{W}, \check{\Phi}\|_N$$

This is equivalent to the continuity of the injection of KC_f equipped with the norm $\|\bullet\|_N$ into KC_f equipped with the norm $\|\bullet\|_{KC_f}$. Considering a sequence $[\check{W}_k, \check{\Phi}_k] \in KC_f$, $k \in \mathbb{N}$

such that $\left\| \check{W}_k, \check{\underline{\Phi}}_k \right\|_N \rightarrow 0$ as k goes to infinity, we have to prove that $\left\| \check{W}, \check{\underline{\Phi}} \right\|_{KC_f} \rightarrow 0$ as k goes to infinity.

Using (1.84), we can see that

$$(1.88) \quad \left\| \underline{\Phi}_k^s + \underline{\nabla} W_k \right\|_{\underline{\mathbf{L}}^2(\omega)}^2 \rightarrow 0$$

and that

$$(1.89) \quad \left\| \underline{\Phi}_k \cdot \underline{\nabla} \right\|_{\underline{\mathbf{L}}^2(\omega)}^2 + \left\| \underline{\Phi}_k^d \right\|_{\underline{\mathbf{L}}^2(\omega)}^2 \rightarrow 0$$

According to Lemma 4 and the above limit, for each k , there exists a vector field $\underline{\mathbf{r}}_k$ of the form (1.10)

$$\underline{\mathbf{r}}_k(x_1, x_2) = (u_k - w_k x_2, v_k + w_k x_1)$$

such that :

$$(1.90) \quad \left\| \underline{\Phi}_k^s - \underline{\mathbf{r}}_k \right\|_{\underline{\mathbf{L}}^2(\omega)} \rightarrow 0$$

It follows from equations (1.88) and (1.90) that :

$$(1.91) \quad \left\| \underline{\mathbf{r}}_k + \underline{\nabla} W_k \right\|_{\underline{\mathbf{L}}^2(\omega)} \rightarrow 0$$

Then, according to Lemma 5, $w_k \rightarrow 0$ and there exists a sequence of real numbers denoted by z_k such that :

$$(1.92) \quad \left\| W_k + u_k x_1 + v_k x_2 + z_k \right\|_{H^1(\omega)} \rightarrow 0$$

In turn, $w_k \rightarrow 0$ and (1.90) implies that

$$(1.93) \quad \left\| \underline{\Phi}_k^s - \underline{\mathbf{r}}_k^{(u,v)} \right\|_{\underline{\mathbf{L}}^2(\omega)} \rightarrow 0$$

where $\underline{\mathbf{r}}_k^{(u,v)} = (u_k, v_k)$. Using the definition of the norm $\|\bullet\|_{KC_f}$ and $(V_k, \underline{\Psi}_k)$ in \mathcal{R} defined by :

$$(V_k, \underline{\Psi}_k) = \left(-u_k x_1 - v_k x_2 - z_k, \underline{\mathbf{i}} \cdot \underline{\mathbf{r}}_k^{(u,v)} \right)$$

we have :

$$(1.94) \quad \left\| \check{W}_k, \check{\underline{\Phi}}_k \right\|_{KC_f} \leq \left\| (W_k, \underline{\Phi}_k) - (V_k, \underline{\Psi}_k) \right\|_{KC} \rightarrow 0$$

thanks to equations (1.92) and (1.93) together with (1.89). This ends the proof. \square

1.5.3 Well-posedness of the minimization problem for free boundary conditions

We have shown in the previous sections that the bilinear form \check{a} is continuous and coercive on the Hilbert space KC_f . Moreover, we have proved that the linear form \check{b} is continuous on KC_f . As all the assumptions of the Lax-Milgram theorem are verified, we have the following result :

Theorem 4. *Assume that :*

- the transverse load $p \in L^2(\omega)$ is such that (1.77) are satisfied ;
- the symmetric stiffness tensors $\underline{\underline{D}}$ and $\underline{\underline{H}}$ are positive definite.

Then, the minimization problem (1.82) has a unique solution denoted by $[\check{W}^{\text{BG}}, \check{\Phi}^{\text{BG}}]$ which is also the unique solution of the following problem :

$$(1.95) \quad \left\{ \begin{array}{l} \text{Find } [\check{W}^{\text{BG}}, \check{\Phi}^{\text{BG}}] \in KC_f \text{ such that} \\ \check{a}([\check{W}^{\text{BG}}, \check{\Phi}^{\text{BG}}], [\check{W}, \check{\Phi}]) = \check{b}([\check{W}, \check{\Phi}]), \quad \forall [\check{W}, \check{\Phi}] \in KC_f \end{array} \right.$$

Our objective now is to build from $[\check{W}^{\text{BG}}, \check{\Phi}^{\text{BG}}]$ a solution to the problem formed by the equations (1.28), (1.29), (2.8), (2.7) and (1.72). To this end, we introduce the set $SC_0(p)$ of statically compatible moment fields which are in equilibrium (2.8) with the external load p and with free boundary conditions (1.72), in the weak sense :

$$(1.96) \quad SC_0(p) = \left\{ \underline{\underline{M}} \in \underline{\underline{H}}_0^1(\omega), \quad \int_{\omega} (\underline{\underline{M}} \cdot \underline{\underline{\nabla}}) \cdot \underline{\underline{\nabla}} W = \int_{\omega} p W \quad \forall W \in H^1(\omega) \right\}.$$

Indeed, using integration by parts, it easily seen that if $\underline{\underline{M}} \in SC_0(p)$ is regular enough, then the equations (2.8) and (1.72) will hold true in the strong sense with $\underline{\underline{R}} = \underline{\underline{M}} \otimes \underline{\underline{\nabla}}$.

Theorem 5. *Suppose that the transverse load p and the stiffness tensors $\underline{\underline{D}}$ and $\underline{\underline{H}}$ satisfy the assumptions of Theorem (4) and let $[\check{W}^{\text{BG}}, \check{\Phi}^{\text{BG}}]$ denote the unique solution to the minimization problem (1.82). Let $(W^{\text{BG}}, \Phi^{\text{BG}})$ be any element in $[\check{W}^{\text{BG}}, \check{\Phi}^{\text{BG}}]$. The generalized strains associated to $(W^{\text{BG}}, \Phi^{\text{BG}})$ through the compatibility conditions (1.28), (1.29) are given by*

$$(1.97) \quad \underline{\underline{\chi}}^{\text{BG}} = \underline{\underline{\Phi}}^{\text{BG}} \cdot \underline{\underline{\nabla}} \quad \text{and} \quad \underline{\underline{\Gamma}}^{\text{BG}} = \underline{\underline{\Phi}}^{\text{BG}} + \underline{\underline{i}} \cdot \underline{\underline{\nabla}} W^{\text{BG}},$$

and the generalized stress fields associated to $(W^{\text{BG}}, \Phi^{\text{BG}})$ by the constitutive equations (2.7) are

$$(1.98) \quad \underline{\underline{M}}^{\text{BG}} = \underline{\underline{D}} : \underline{\underline{\chi}}^{\text{BG}} \quad \text{and} \quad \underline{\underline{R}}^{\text{BG}} = \underline{\underline{H}} : \underline{\underline{\Gamma}}^{\text{BG}}.$$

Then,

$$(1.99) \quad \underline{\underline{\mathbf{M}}}^{\text{BG}} \in SC_0(p) \text{ and } \underline{\underline{\mathbf{R}}}^{\text{BG}} = \underline{\underline{\mathbf{M}}}^{\text{BG}} \otimes \underline{\underline{\nabla}}.$$

Moreover, the above fields do not depend on the choice of $(W^{\text{BG}}, \underline{\underline{\Phi}}^{\text{BG}})$ in $[\check{W}^{\text{BG}}, \check{\underline{\underline{\Phi}}}^{\text{BG}}]$.

Démonstration. The proof is similar to that of Theorem (3). Since $[\check{W}^{\text{BG}}, \check{\underline{\underline{\Phi}}}^{\text{BG}}]$ satisfies (1.95) (we refer to Theorem (4)), we have that, for all $[\check{W}^{\text{BG}}, \check{\underline{\underline{\Phi}}}^{\text{BG}}] \in KC_f$,

$$(1.100) \quad \int_{\omega} \underline{\underline{\mathbf{M}}}^{\text{BG}} : (\underline{\underline{\Phi}} \cdot \underline{\underline{\nabla}}) + {}^T \underline{\underline{\mathbf{R}}}^{\text{BG}} : (\underline{\underline{\Phi}} + \underline{\underline{\mathbf{i}}} \cdot \underline{\underline{\nabla}} W) = \int_{\omega} p W,$$

where $(W^{\text{BG}}, \underline{\underline{\Phi}}^{\text{BG}})$ is any element in $[\check{W}^{\text{BG}}, \check{\underline{\underline{\Phi}}}^{\text{BG}}]$ and $(W, \underline{\underline{\Phi}})$ is any element of KC . By arguments similar to those used in the proof of Theorem 3, we obtain (1.99). \square

1.5.4 Equivalence to a stress formulation

We have built in Theorem 5 the generalized stress fields $(\underline{\underline{\mathbf{M}}}^{\text{BG}}, \underline{\underline{\mathbf{R}}}^{\text{BG}})$ solution to the problem with free boundary conditions. Moreover, we have proved that $\underline{\underline{\mathbf{M}}}^{\text{BG}} \in SC_0(p)$ and that $\underline{\underline{\mathbf{R}}}^{\text{BG}} = \underline{\underline{\mathbf{M}}}^{\text{BG}} \otimes \underline{\underline{\nabla}}$. We have the following result :

Theorem 6.

Adopting the assumptions of Theorem 4 and the notations of Theorem 5, the stress field $\underline{\underline{\mathbf{M}}}^{\text{BG}}$ defined in Theorem 5 is the unique solution to the problem :

$$(1.101) \quad \min \left\{ \mathcal{E}^{*\text{BG}} = \int_{\omega} w^{*\text{BG}}(\underline{\underline{\mathbf{M}}}, \underline{\underline{\mathbf{M}}} \otimes \underline{\underline{\nabla}}) d\omega, \quad \underline{\underline{\mathbf{M}}} \in SC_0(p) \right\}$$

where $w^{*\text{BG}}$ is defined by (1.42).

Démonstration. For a proof, we follow in close lines the second part of that of Theorem 3, where $SC_0(p)$ is substituted to $SC(p)$. Consider any element $\underline{\underline{\mathbf{M}}} \in SC_0(p)$, and set

$$\underline{\underline{\mathbf{M}}}^{\prime} = \underline{\underline{\mathbf{M}}} - \underline{\underline{\mathbf{M}}}^{\text{BG}}.$$

Simple algebraic transformations lead to :

$$\mathcal{E}^{*\text{BG}}(\underline{\underline{\mathbf{M}}}) = \mathcal{E}^{*\text{BG}}(\underline{\underline{\mathbf{M}}}^{\prime}) + \mathcal{E}^{*\text{BG}}(\underline{\underline{\mathbf{M}}}^{\text{BG}}) + \int_{\omega} \underline{\underline{\mathbf{M}}}^{\prime} : (\underline{\underline{\Phi}}^{\text{BG}} \cdot \underline{\underline{\nabla}}) + ({}^T \underline{\underline{\mathbf{M}}}^{\prime} \otimes \underline{\underline{\nabla}}) : (\underline{\underline{\Phi}}^{\text{BG}} + \underline{\underline{\mathbf{i}}} \cdot \underline{\underline{\nabla}} W^{\text{BG}})$$

Using that $\underline{\underline{\mathbf{M}}}^{\prime} \in SC_0(0)$, integrating by parts leads to the fact that the last term in the above equation vanishes. We hence obtain that :

$$\mathcal{E}^{*\text{BG}}(\underline{\underline{\mathbf{M}}}) = \mathcal{E}^{*\text{BG}}(\underline{\underline{\mathbf{M}}}^{\prime}) + \mathcal{E}^{*\text{BG}}(\underline{\underline{\mathbf{M}}}^{\text{BG}})$$

We end the proof by mentioning that $\mathcal{E}^{*\text{BG}}(\underline{\underline{\mathbf{M}}})$ is positive as soon as $\underline{\underline{\mathbf{M}}}^{\prime}$ does not vanish. \square

1.6 Simple Support Boundary Conditions

We have already presented the Bending-Gradient theory for clamped plates (section 1.4) as well as for free plates (section 1.5) and proved its well-posedness in both cases. Nevertheless, other types of boundary conditions can also be imposed on $\partial\omega$. In this section, we discuss the simple support boundary conditions.

According to Sab and Lebée (2015), the soft simple support boundary conditions of the Bending-Gradient theory set to zero both the moment tensor $\underline{\underline{M}}$ and the transverse displacement W . Namely :

$$(1.102) \quad \underline{\underline{M}} = 0 \text{ and } W = 0 \quad \text{on} \quad \partial\omega.$$

Hence, these boundary conditions are a mixed between the clamped and the free boundary conditions. We can generalize the results established for the displacement formulation in Sect. 1.5, namely Theorems (1), (2) and (3) to the case of the mixed boundary conditions (1.102) as follows :

- The space KC_m of kinematically compatible generalized displacement fields with mixed boundary conditions is defined as :

$$KC_m = H_0^1(\omega) \times \underline{\underline{H}}(div, \omega).$$

Note that :

$$KC_0 \subset KC_m \subset KC.$$

- The transverse load p is assumed to be in $H^{-1}(\omega)$.
- The space $SC_m(p)$ of statically compatible generalized stress fields with mixed boundary conditions is defined as :

$$SC_m(p) = \{ \underline{\underline{M}} \in \underline{\underline{H}}_0^1(\omega), \quad M_{\alpha\beta, \alpha\beta} + p = 0 \text{ in the sense of distributions} \}.$$

Note that :

$$SC_0(p) \subset SC_m(p) \subset SC(p).$$

- The compliance tensors $\underline{\underline{d}}$ and $\underline{\underline{h}}$ are positive definite in the sense of (1.44) and (1.45).
- Theorem (1) holds true if $SC_m(p)$ and $SC_m(0)$ are respectively substituted for $SC(p)$ and $SC(0)$ in (1.47) and (1.48). The proof is exactly the same.
- Theorem (2) holds true if KC_m is substituted for KC_0 in problem (1.52). The proof is mainly the same but we need to prove that there exists a constant C' such that :

$$(1.103) \quad \forall (W, \underline{\underline{\Phi}}) \in KC_m, \quad \|W, \underline{\underline{\Phi}}\|_{KC_m} \leq C' \|W, \underline{\underline{\Phi}}\|_N$$

To this aim, we proceed by contradiction as usual. Suppose that for all $k \in \mathbb{N}$, there exists $(W_k, \underline{\underline{\Phi}}_k) \in KC_m$ such that :

$$(1.104) \quad \|W_k, \underline{\underline{\Phi}}_k\|_{KC_m} = 1, \quad \|W_k, \underline{\underline{\Phi}}_k\|_N \leq \frac{1}{k}.$$

The expression of $\|W_k, \underline{\Phi}_k\|_N$ is given by (1.59) and (1.60). From (1.104), we obtain (1.88) and (1.89). According to Lemma 4 and the limit (1.89), for each k , there exists a vector field $\underline{\mathbf{r}}_k$ of the form (1.10) such that (1.90). Then, (1.91) follows from equations (1.88) and (1.90) and, according to Lemma 5 with $W_k \in H_0^1(\omega)$, we obtain the convergences $\underline{\mathbf{r}}_k \rightarrow 0$ and $W_k \rightarrow 0$ in $H_0^1(\omega)$. Hence, $(W_k, \underline{\Phi}_k) \rightarrow 0$ in KC_m which is in contradiction with $\|W_k, \underline{\Phi}_k\|_{KC_m} = 1$.

- Theorem (3) which states the equivalence between the static and the kinematic approaches for clamped boundary conditions can be easily extended to prove the equivalence of these approaches for the mixed boundary conditions (1.102).

As mentioned earlier (see Sect. 1.3.2.4), the sixth order tensor $\underline{\underline{\mathbf{h}}}$ is positive but not definite on whole $\underline{\underline{\mathbb{R}}}$ in the general case. Sections 1.4-1.6 were devoted to the well-posedness of the Bending-Gradient problems when $\underline{\underline{\mathbf{h}}}$ is positive definite. It is time now to extend these results to the general case. Only clamped boundary conditions will be studied to avoid lengthening the paper.

1.7 Formulation of the Bending-Gradient theory in the general case

Since the sixth-order tensor $\underline{\underline{\mathbf{h}}}$ is not definite on whole $\underline{\underline{\mathbb{R}}}$ in the general case, Sab and Lebée Sab and Lebée (2015) orthogonally decomposed the vector space $\underline{\underline{\mathbb{R}}}$, endowed with the scalar product ${}^t\underline{\underline{\mathbf{X}}} : \underline{\underline{\mathbf{X}}}' = X_{\alpha\beta\gamma} X'_{\alpha\beta\gamma}$, into $\underline{\underline{\mathcal{S}}}$ and its orthogonal $\underline{\underline{\mathcal{K}}}$:

$$\underline{\underline{\mathbb{R}}} = \underline{\underline{\mathcal{S}}} \oplus \underline{\underline{\mathcal{K}}}$$

where $\underline{\underline{\mathcal{S}}}$ is the image of the sixth-order shear force compliance tensor $\underline{\underline{\mathbf{h}}}$:

$$\underline{\underline{\mathcal{S}}} = \{\underline{\underline{\mathbf{h}}} : \underline{\underline{\mathbf{X}}}, \quad \underline{\underline{\mathbf{X}}} \in \underline{\underline{\mathbb{R}}}\},$$

and $\underline{\underline{\mathcal{K}}}$ denotes its kernel :

$$\underline{\underline{\mathcal{K}}} = \{\underline{\underline{\mathbf{X}}} \in \underline{\underline{\mathbb{R}}} \mid \underline{\underline{\mathbf{h}}} : \underline{\underline{\mathbf{X}}} = 0\}.$$

Let $\underline{\underline{\mathbf{P}}}^S$ and $\underline{\underline{\mathbf{P}}}^K$ denote, respectively, the orthogonal projection operator onto $\underline{\underline{\mathcal{S}}}$ and $\underline{\underline{\mathcal{K}}}$. It can be easily verified that any third-order tensor $\underline{\underline{\mathbf{X}}}$ can be written as :

$$(1.105) \quad \underline{\underline{\mathbf{X}}} = \underline{\underline{\mathbf{X}}}^S + \underline{\underline{\mathbf{X}}}^K$$

with

$$\underline{\underline{\mathbf{X}}}^S = \underline{\underline{\mathbf{P}}}^S : \underline{\underline{\mathbf{X}}} \in \underline{\underline{\mathcal{S}}}, \quad \underline{\underline{\mathbf{X}}}^K = \underline{\underline{\mathbf{P}}}^K : \underline{\underline{\mathbf{X}}} \in \underline{\underline{\mathcal{K}}}, \quad {}^t\underline{\underline{\mathbf{X}}}^S : \underline{\underline{\mathbf{X}}}^K = 0.$$

It is useful to notice that we always have :

$$(1.106) \quad {}^t\underline{\underline{\mathbf{X}}} : \underline{\underline{\mathbf{h}}} : \underline{\underline{\mathbf{X}}} = {}^t\underline{\underline{\mathbf{X}}}^S : \underline{\underline{\mathbf{h}}} : \underline{\underline{\mathbf{X}}}^S.$$

In other words, the shear force compliance tensor $\underline{\underline{\mathbf{h}}}$ is definite only on the subspace $\underline{\underline{\mathcal{S}}}$.

The subspace $\underline{\mathcal{S}}$ contains all the spherical third-order tensors of the form (1.3) as shown by Sab and Lebée (2015). Hence, we have the following interesting property :

$$(1.107) \quad \underline{\underline{P}}^S : \underline{\underline{i}} = \underline{\underline{i}} : \underline{\underline{P}}^S = \underline{\underline{i}},$$

and the dimension of $\underline{\mathcal{S}}$ is at least two. Actually, it is exactly two for homogeneous plates and in this case the Bending-Gradient theory degenerates into the Reissner-Mindlin theory. When $\underline{\underline{h}}$ is definite and therefore invertible, $\underline{\mathcal{S}}$ is equal to $\underline{\mathbb{R}}$ of dimension six. In this case, $\underline{\underline{P}}^S$ is the identity operator. So, the dimension of $\underline{\mathcal{S}}$ is between two and six, depending on the elastic properties of the plate.

In order to take into account the possible non-definiteness of $\underline{\underline{h}}$, both generalized rotation tensor $\underline{\underline{\Phi}}$ and generalized shear force tensor $\underline{\underline{R}}$ are enforced to belong to $\underline{\mathcal{S}}$. The first equilibrium equation states that $\underline{\underline{R}}$ is actually the projection of the bending gradient $\underline{\underline{M}} \otimes \underline{\underline{\nabla}}$ on $\underline{\mathcal{S}}$. Moreover, using property (1.107), expressing the fact that $\underline{\mathcal{S}}$ contains all the spherical third-order of the form (1.3), shows that $\underline{\underline{i}} : (\underline{\underline{R}} \otimes \underline{\underline{\nabla}}) = M_{\alpha\beta, \alpha\beta}$ in the general case, and hence the second equilibrium equation remains the same. Finally, since $\underline{\underline{h}}$ may be not invertible, $\underline{\underline{H}}$ will denote its Moore-Penrose pseudo inverse in the general case. In summary, the Bending-Gradient problem for clamped plates is to find W and $\underline{\underline{\Phi}} \in \underline{\mathcal{S}}$ solution of the following system of equations :

$$(1.108a) \quad \begin{cases} \underline{\underline{\chi}} = \underline{\underline{\Phi}} \cdot \underline{\underline{\nabla}} & \text{and} & \underline{\underline{\Gamma}} = \underline{\underline{\Phi}} + \underline{\underline{i}} \cdot \underline{\underline{\nabla}} W, \\ (1.108b) \quad \underline{\underline{M}} = \underline{\underline{D}} : \underline{\underline{\chi}} & \text{and} & \underline{\underline{R}} = \underline{\underline{H}} : \underline{\underline{\Gamma}}, \\ (1.108c) \quad \underline{\underline{R}} - \underline{\underline{P}}^S : (\underline{\underline{M}} \otimes \underline{\underline{\nabla}}) = 0 & \text{and} & \underline{\underline{i}} : (\underline{\underline{R}} \otimes \underline{\underline{\nabla}}) + p = 0, \\ (1.108d) \quad \underline{\underline{\Phi}} \cdot \underline{\underline{n}} = 0 & \text{and} & W = 0 \quad \text{on} \quad \partial\omega. \end{cases}$$

Note that since $\underline{\underline{\Phi}}$ is in $\underline{\mathcal{S}}$ and the spherical third-order tensors of the form (1.3) are also in $\underline{\mathcal{S}}$, then $\underline{\underline{\Gamma}}$ will be also in $\underline{\mathcal{S}}$.

In general, the Bending-Gradient theory cannot be reduced to the Reissner-Mindlin theory. However, it was demonstrated that the Bending-Gradient theory coincides with the Reissner-Mindlin theory if, and only if, the shear force compliance tensor $\underline{\underline{h}}$ has the following form :

$$\underline{\underline{h}} = \underline{\underline{i}} \cdot \underline{\underline{h}}^{\text{RM}} \cdot \underline{\underline{i}}$$

where $\underline{\underline{h}}^{\text{RM}}$ denotes a positive definite second-order tensor called the Reissner-Mindlin shear force compliance tensor. This is exactly the case for homogeneous plates where $\underline{\underline{h}}$ is given by :

$$\underline{\underline{h}} = \frac{6}{5t} \underline{\underline{i}} \cdot \underline{\underline{S}}^\gamma \cdot \underline{\underline{i}}$$

and $\underline{\underline{S}}^\gamma = (4S_{\alpha 3 \beta 3})$ denotes the out-of-plane transverse shear compliance tensor.

Indeed, when $\underline{\underline{h}}$ is of the above form, then $\underline{\mathcal{S}}$ coincides with the set of spherical third-order tensors of the form (1.3). Hence, we have necessarily

$$\underline{\underline{\Phi}} = \underline{\underline{i}} \cdot \underline{\underline{\varphi}}$$

where $\underline{\varphi}$ is a 2D vector representing rotations,

$$\underline{\mathbf{R}} = \underline{\mathbf{P}}^S : (\underline{\mathbf{M}} \otimes \underline{\nabla}) = \frac{2}{3} \underline{\mathbf{i}} \cdot (\underline{\mathbf{M}} \cdot \underline{\nabla}),$$

and all the equations of the Reissner-Mindlin theory are retrieved.

We now define the proper functional spaces in which the stress formulation and the displacement formulation turn out to be well-posed in the general case where $\underline{\mathbf{h}}$ may not be definite.

1.7.1 Stress formulation

Let $(\underline{\mathbf{M}}, \underline{\mathbf{R}})$ be a generalized stress field defined over ω . We recall that the complementary energy \mathcal{E}^{*BG} and the stress energy density w^{*BG} are respectively defined by (1.41) and (1.42). Assume that the shear force compliance $\underline{\mathbf{h}}$ is positive. Let $\underline{\mathcal{S}}$ be its image and $\underline{\mathbf{P}}^S$ the orthogonal projection operator on $\underline{\mathcal{S}}$. Assume that (1.107) holds true. Then, the set of statically admissible generalized stress fields is defined as follows :

$$(1.109) \quad SC^{BG}(p) = \{(\underline{\mathbf{M}}, \underline{\mathbf{R}}) \in \underline{\mathbf{L}}^2 \times \underline{\mathbf{L}}^2 / \underline{\mathbf{R}} = \underline{\mathbf{P}}^S : (\underline{\mathbf{M}} \otimes \underline{\nabla}) \text{ and } \underline{\mathbf{i}} : (\underline{\mathbf{R}} \otimes \underline{\nabla}) + p = 0\},$$

where the equilibrium equations are in the sense of distributions, i.e., for all $(W, \underline{\Phi}) \in D(\omega) \times \underline{\mathbf{D}}(\omega)$

$$(1.110) \quad \int_{\omega} \underline{\mathbf{M}} : ((\underline{\mathbf{P}}^S : \underline{\Phi}) \cdot \underline{\nabla}) + {}^T \underline{\mathbf{R}} : (\underline{\Phi} + \underline{\mathbf{i}} \cdot \underline{\nabla} W) = \int_{\omega} p W d\omega$$

Note that the above definition of $SC^{BG}(p)$ coincides with definition (1.46) of $SC(p)$ if $\underline{\mathbf{h}}$ is definite and, hence, $\underline{\mathbf{P}}^S$ is the identity operator.

The variational formulation of the Bending-Gradient problem consists in minimizing the complementary energy $\mathcal{E}^{*BG}(\underline{\mathbf{M}}, \underline{\mathbf{R}})$ with respect to all $(\underline{\mathbf{M}}, \underline{\mathbf{R}}) \in SC^{BG}(p)$:

$$(1.111) \quad \min \left\{ \mathcal{E}^{*BG}(\underline{\mathbf{M}}, \underline{\mathbf{R}}) = \int_{\omega} w^{*BG}(\underline{\mathbf{M}}, \underline{\mathbf{R}}), \quad (\underline{\mathbf{M}}, \underline{\mathbf{R}}) \in SC^{BG}(p) \right\},$$

The following theorem states the well-posedness of the above minimization problem. Its proof is very similar to that of Theorem (1).

Theorem 7. *Assume that $p \in H^{-1}(\omega)$, the bending compliance tensor $\underline{\mathbf{d}}$ is positive definite and the shear force compliance $\underline{\mathbf{h}}$ is positive. Let $\underline{\mathcal{S}}$ be the image of $\underline{\mathbf{h}}$ and assume that (1.107) holds true where $\underline{\mathbf{P}}^S$ is the orthogonal projection operator on $\underline{\mathcal{S}}$. Then, the minimization problem (1.111) admits a unique solution $(\underline{\mathbf{M}}^{BG}, \underline{\mathbf{R}}^{BG}) \in SC^{BG}(p)$. Moreover, $(\underline{\mathbf{M}}^{BG}, \underline{\mathbf{R}}^{BG})$ satisfies the following variational formulation :*

$$(1.112) \quad \left\{ \begin{array}{l} \text{Find } (\underline{\mathbf{M}}^{BG}, \underline{\mathbf{R}}^{BG}) \in SC^{BG}(p) \text{ such that} \\ \int_{\omega} \underline{\mu} : \underline{\mathbf{d}} : \underline{\mathbf{M}}^{BG} + {}^T \underline{\rho} : \underline{\mathbf{h}} : \underline{\mathbf{R}}^{BG} = 0, \quad \forall (\underline{\mu}, \underline{\rho}) \in SC^{BG}(0) \end{array} \right.$$

1.7.2 Displacement formulation

Let $(W, \underline{\Phi})$ be a generalized displacement field defined over ω . We recall that the potential energy \mathcal{E}^{BG} and the strain energy density w^{BG} are respectively defined by (1.39) and (1.40). Because \underline{h} is definite only on $\underline{\mathcal{S}}$, the generalized rotation third-order tensor $\underline{\Phi}$ must lie in $\underline{H}_0(\text{div}, \omega)$ while satisfying $\underline{\Phi}(x_1, x_2) \in \underline{\mathcal{S}}$ almost everywhere in ω . In other words, $\underline{P}^K : \underline{\Phi} = 0$ where \underline{P}^K is the orthogonal projection operator on the kernel of \underline{h} . We hence introduce the set $\underline{\Upsilon} \subseteq \underline{H}_0(\text{div}, \omega)$ defined by :

$$\underline{\Upsilon} = \{ \underline{\Phi} \in \underline{H}_0(\text{div}, \omega) / \underline{P}^K : \underline{\Phi} = 0 \}$$

$\underline{\Upsilon}$ is obviously a closed subspace of $\underline{H}_0(\text{div}, \omega)$ equipped with the norm $\|\bullet\|_{\underline{H}(\text{div}, \omega)}$. Therefore, $\underline{\Upsilon}$ endowed with the scalar product $\langle \bullet, \bullet \rangle_{\underline{H}(\text{div}, \omega)}$ is a Hilbert space.

As in section 1.4.3, W should belong to the Hilbert space $H_0^1(\omega)$. Always assuming that $p \in H^{-1}(\omega)$, \mathcal{E}^{BG} introduced in (1.39) is well-defined for $(W, \underline{\Phi}) \in H_0^1(\omega) \times \underline{\Upsilon}$. We consider the minimization problem

$$(1.113) \quad \min \{ \mathcal{E}^{\text{BG}}(W, \underline{\Phi}), \quad (W, \underline{\Phi}) \in H_0^1(\omega) \times \underline{\Upsilon} \}$$

The following theorem states the well-posedness of the above minimization problem. Its proof is very similar to that of Theorems (2) and Theorem (3).

Theorem 8. *Under the assumptions of Theorem (7), the minimization problem (1.113) is well-posed. Its unique solution is denoted by $(W^{\text{BG}}, \underline{\Phi}^{\text{BG}})$ and satisfies*

$$(1.114) \quad \|W^{\text{BG}}, \underline{\Phi}^{\text{BG}}\|_{H_0^1(\omega) \times \underline{H}(\text{div}, \omega)} \leq c \|p\|_{H^{-1}(\omega)}$$

where c is a strictly positive constant.

Moreover, the associated generalized stresses $(\underline{M}, \underline{R})$ obtained from $(W^{\text{BG}}, \underline{\Phi}^{\text{BG}})$ via equations (1.108a,b) are the unique solutions $(\underline{M}^{\text{BG}}, \underline{R}^{\text{BG}})$ of the minimization problem (1.111).

We have seen in this section that when dealing with the Bending-Gradient problem in the general case, one has to introduce the kinematic constraint $\underline{P}^K : \underline{\Phi} = 0$ when minimizing the potential energy. Another alternative is to regularize the shear force compliance tensor by adding to it a positive multiple of the identity operator. Indeed, the regularized tensor will be always definite and its inverse will be unambiguously defined. Hence, no need to introduce the kinematic constraint. The question that arises and that will be treated in the following section is the convergence of the regularized solution to the exact solution as the regularizing parameter goes to zero.

1.8 Regularization of the shear force compliance tensor

1.8.1 The regularized problem

Since the sixth-order tensor $\underline{\underline{h}}$ is always positive, its definiteness is ensured by adding a positive multiple of the identity. The regularized tensor is denoted by $\underline{\underline{h}}_\varepsilon$ and defined by :

$$\underline{\underline{h}}_\varepsilon = \underline{\underline{h}} + \varepsilon \underline{\underline{I}}$$

where $\varepsilon > 0$. Clearly, $\underline{\underline{h}}_\varepsilon$ is always positive definite. Hence, in virtue of Section 1.4, the regularized minimization problem for clamped boundary conditions

$$(1.115) \quad \min \{ \mathcal{E}_\varepsilon^*(\underline{\underline{M}}), \quad \underline{\underline{M}} \in SC(p) \},$$

where

$$\mathcal{E}_\varepsilon^*(\underline{\underline{M}}) = \frac{1}{2} \underline{\underline{M}} : \underline{\underline{d}} : \underline{\underline{M}} + \frac{1}{2} T(\underline{\underline{M}} \otimes \underline{\underline{\nabla}}) : \underline{\underline{h}}_\varepsilon : (\underline{\underline{M}} \otimes \underline{\underline{\nabla}})$$

admits a unique solution $\underline{\underline{M}}_\varepsilon \in SC(p)$. Furthermore, we denote $\underline{\underline{R}}_\varepsilon = \underline{\underline{M}}_\varepsilon \otimes \underline{\underline{\nabla}}$. We know that there exists an unique $(W_\varepsilon, \underline{\underline{\Phi}}_\varepsilon) \in KC_0$ such that :

$$(1.116) \quad \underline{\underline{M}}_\varepsilon = \underline{\underline{D}} : \underline{\underline{\chi}}_\varepsilon, \quad \underline{\underline{R}}_\varepsilon = \underline{\underline{H}}_\varepsilon : \underline{\underline{\Gamma}}_\varepsilon, \quad \underline{\underline{\chi}}_\varepsilon = \underline{\underline{\Phi}}_\varepsilon \cdot \underline{\underline{\nabla}}, \quad \underline{\underline{\Gamma}}_\varepsilon = \underline{\underline{\Phi}}_\varepsilon + \underline{\underline{i}} \cdot \underline{\underline{\nabla}} W_\varepsilon.$$

where $\underline{\underline{H}}_\varepsilon$ is the inverse of $\underline{\underline{h}}_\varepsilon$.

1.8.2 Convergence of the regularized solution

The following theorem states the main result of this section :

Theorem 9. *Under the assumptions of Theorem (7), there exists a unique solution of the minimization problem (1.111) denoted by $(\underline{\underline{M}}^{\text{BG}}, \underline{\underline{R}}^{\text{BG}})$. Assume that $\underline{\underline{M}}^{\text{BG}}$ belongs to $\underline{\underline{H}}^1(\omega)$. Then, $\underline{\underline{M}}_\varepsilon$, the solution of the regularized problem (1.115), converges in $\underline{\underline{L}}^2(\omega)$ to $\underline{\underline{M}}^{\text{BG}}$, and $\underline{\underline{R}}_\varepsilon^S$ converges in $\underline{\underline{L}}^2(\omega)$ to $\underline{\underline{R}}^{\text{BG}}$ when ε tends to zero. Here, $\underline{\underline{R}}_\varepsilon = \underline{\underline{M}}_\varepsilon \otimes \underline{\underline{\nabla}}$ and the notation (1.105) is used. Moreover, we have the convergence of the energies :*

$$(1.117) \quad \lim_{\varepsilon \rightarrow 0} \mathcal{E}_\varepsilon^*(\underline{\underline{M}}_\varepsilon) = \mathcal{E}^{\text{BG}}(\underline{\underline{M}}^{\text{BG}}, \underline{\underline{R}}^{\text{BG}})$$

and that :

$$(1.118) \quad \limsup_{\varepsilon \rightarrow 0} \|\underline{\underline{R}}_\varepsilon^K\|_{\underline{\underline{L}}^2(\omega)} \leq \|\underline{\underline{P}}^K : (\underline{\underline{M}}^{\text{BG}} \otimes \underline{\underline{\nabla}})\|_{\underline{\underline{L}}^2(\omega)}$$

In addition, let $(W_\varepsilon, \underline{\underline{\Phi}}_\varepsilon) \in KC_0$ be associated to $\underline{\underline{M}}_\varepsilon$ through (1.116). Then, $(W_\varepsilon, \underline{\underline{\Phi}}_\varepsilon)$ converges in KC_0 to $(W^{\text{BG}}, \underline{\underline{\Phi}}^{\text{BG}})$, the solution of the minimization problem (1.113), when ε tends to zero.

Démonstration. The hypothesis $\underline{\underline{M}}^{\text{BG}} \in \underline{\underline{H}}^1(\omega)$ guarantees that $\underline{\underline{M}}^{\text{BG}}$ is in $SC(p)$, and hence $\mathcal{E}_\varepsilon^*(\underline{\underline{M}}_\varepsilon) \leq \mathcal{E}_\varepsilon^*(\underline{\underline{M}}^{\text{BG}})$ which can be written :

$$(1.119) \quad \begin{aligned} & \frac{1}{2} \int_\omega \underline{\underline{M}}_\varepsilon : \underline{\underline{d}} : \underline{\underline{M}}_\varepsilon + {}^T \underline{\underline{R}}_\varepsilon : \underline{\underline{h}} : \underline{\underline{R}}_\varepsilon + \varepsilon {}^T \underline{\underline{R}}_\varepsilon : \underline{\underline{R}}_\varepsilon \leq \\ & \frac{1}{2} \int_\omega \underline{\underline{M}}^{\text{BG}} : \underline{\underline{d}} : \underline{\underline{M}}^{\text{BG}} + {}^T(\underline{\underline{M}}^{\text{BG}} \otimes \underline{\underline{\nabla}}) : \underline{\underline{h}} : (\underline{\underline{M}}^{\text{BG}} \otimes \underline{\underline{\nabla}}) \\ & \quad + \varepsilon {}^T(\underline{\underline{M}}^{\text{BG}} \otimes \underline{\underline{\nabla}}) : (\underline{\underline{M}}^{\text{BG}} \otimes \underline{\underline{\nabla}}). \end{aligned}$$

By (1.106), we have that :

$${}^T \underline{\underline{R}}_\varepsilon : \underline{\underline{h}} : \underline{\underline{R}}_\varepsilon = {}^T \underline{\underline{R}}_\varepsilon^S : \underline{\underline{h}} : \underline{\underline{R}}_\varepsilon^S$$

and

$${}^T(\underline{\underline{M}}^{\text{BG}} \otimes \underline{\underline{\nabla}}) : \underline{\underline{h}} : (\underline{\underline{M}}^{\text{BG}} \otimes \underline{\underline{\nabla}}) = {}^T(\underline{\underline{P}}^S : (\underline{\underline{M}}^{\text{BG}} \otimes \underline{\underline{\nabla}})) : \underline{\underline{h}} : (\underline{\underline{P}}^S : (\underline{\underline{M}}^{\text{BG}} \otimes \underline{\underline{\nabla}})).$$

Recalling that

$$\underline{\underline{P}}^S : (\underline{\underline{M}}^{\text{BG}} \otimes \underline{\underline{\nabla}}) = \underline{\underline{R}}^{\text{BG}},$$

equation (1.119) can be written as :

$$(1.120) \quad \begin{aligned} & \frac{1}{2} \int_\omega \underline{\underline{M}}_\varepsilon : \underline{\underline{d}} : \underline{\underline{M}}_\varepsilon + {}^T \underline{\underline{R}}_\varepsilon^S : \underline{\underline{h}} : \underline{\underline{R}}_\varepsilon^S + \varepsilon {}^T \underline{\underline{R}}_\varepsilon : \underline{\underline{R}}_\varepsilon \leq \\ & \frac{1}{2} \int_\omega \underline{\underline{M}}^{\text{BG}} : \underline{\underline{d}} : \underline{\underline{M}}^{\text{BG}} + {}^T \underline{\underline{R}}^{\text{BG}} : \underline{\underline{h}} : \underline{\underline{R}}^{\text{BG}} \\ & \quad + \varepsilon {}^T(\underline{\underline{M}}^{\text{BG}} \otimes \underline{\underline{\nabla}}) : (\underline{\underline{M}}^{\text{BG}} \otimes \underline{\underline{\nabla}}). \end{aligned}$$

Similarly, $(\underline{\underline{M}}_\varepsilon, \underline{\underline{R}}_\varepsilon^S) \in SC^{\text{BG}}(p)$ yields :

$$(1.121) \quad \frac{1}{2} \int_\omega \underline{\underline{M}}^{\text{BG}} : \underline{\underline{d}} : \underline{\underline{M}}^{\text{BG}} + {}^T \underline{\underline{R}}^{\text{BG}} : \underline{\underline{h}} : \underline{\underline{R}}^{\text{BG}} \leq \frac{1}{2} \int_\omega \underline{\underline{M}}_\varepsilon : \underline{\underline{d}} : \underline{\underline{M}}_\varepsilon + {}^T \underline{\underline{R}}_\varepsilon^S : \underline{\underline{h}} : \underline{\underline{R}}_\varepsilon^S.$$

Comparing inequalities (1.120) and (1.121) leads to the following inequality :

$$(1.122) \quad \frac{1}{2} \int_\omega \varepsilon {}^T \underline{\underline{R}}_\varepsilon : \underline{\underline{R}}_\varepsilon \leq \frac{1}{2} \int_\omega \varepsilon {}^T(\underline{\underline{M}}^{\text{BG}} \otimes \underline{\underline{\nabla}}) : (\underline{\underline{M}}^{\text{BG}} \otimes \underline{\underline{\nabla}}).$$

Simplifying by ε , we obtain that :

$$(1.123) \quad \|\underline{\underline{R}}_\varepsilon\|_{\underline{\underline{L}}^2(\omega)} \leq \|\underline{\underline{M}}^{\text{BG}} \otimes \underline{\underline{\nabla}}\|_{\underline{\underline{L}}^2(\omega)} < C.$$

The above equation implies that :

$$(1.124) \quad \frac{1}{2} \int_\omega \varepsilon {}^T \underline{\underline{R}}_\varepsilon : \underline{\underline{R}}_\varepsilon \xrightarrow{\varepsilon \rightarrow 0} 0.$$

Then, taking the lim sup of inequality (1.120) and the lim inf of inequality (1.121), as ϵ goes to zero, results in the convergence of the energies (1.117) and in :

$$(1.125) \quad \frac{1}{2} \int_{\omega} \underline{\mathcal{M}}^{\text{BG}} : \underline{\mathcal{d}} : \underline{\mathcal{M}}^{\text{BG}} + {}^T \underline{\mathcal{R}}^{\text{BG}} : \underline{\mathcal{h}} : \underline{\mathcal{R}}^{\text{BG}} = \lim_{\epsilon \rightarrow 0} \frac{1}{2} \int_{\omega} \underline{\mathcal{M}}_{\epsilon} : \underline{\mathcal{d}} : \underline{\mathcal{M}}_{\epsilon} + {}^T \underline{\mathcal{R}}_{\epsilon}^S : \underline{\mathcal{h}} : \underline{\mathcal{R}}_{\epsilon}^S$$

Because $(\underline{\mathcal{M}}^{\text{BG}}, \underline{\mathcal{R}}^{\text{BG}})$ achieves the minimum of the complementary energy (1.111), we conclude that $\underline{\mathcal{M}}_{\epsilon}$ converges to $\underline{\mathcal{M}}^{\text{BG}}$ in $\underline{\mathcal{L}}^2(\omega)$ and that $\underline{\mathcal{R}}_{\epsilon}^S$ converges to $\underline{\mathcal{R}}^{\text{BG}}$ in $\underline{\mathcal{L}}^2(\omega)$.

Finally, using the orthogonal decomposition (1.105), equation (1.123) can be written as :

$$(1.126) \quad \|\underline{\mathcal{R}}_{\epsilon}^S\|_{\underline{\mathcal{L}}^2(\omega)}^2 + \|\underline{\mathcal{R}}_{\epsilon}^K\|_{\underline{\mathcal{L}}^2(\omega)}^2 \leq \|\underline{\mathcal{P}}^S : (\underline{\mathcal{M}}^{\text{BG}} \otimes \underline{\nabla})\|_{\underline{\mathcal{L}}^2(\omega)}^2 + \|\underline{\mathcal{P}}^K : (\underline{\mathcal{M}}^{\text{BG}} \otimes \underline{\nabla})\|_{\underline{\mathcal{L}}^2(\omega)}^2.$$

As

$$\lim_{\epsilon \rightarrow 0} \|\underline{\mathcal{R}}_{\epsilon}^S\|_{\underline{\mathcal{L}}^2(\omega)} = \|\underline{\mathcal{R}}^{\text{BG}}\|_{\underline{\mathcal{L}}^2(\omega)} = \|\underline{\mathcal{P}}^S : (\underline{\mathcal{M}}^{\text{BG}} \otimes \underline{\nabla})\|_{\underline{\mathcal{L}}^2(\omega)},$$

then, we obtain (1.118).

Now, according to Lemma 6, the convergence of $(W_{\epsilon}, \underline{\Phi}_{\epsilon})$ to $(W^{\text{BG}}, \underline{\Phi}^{\text{BG}})$ in KC_0 is equivalent to :

$$(1.127) \quad \lim_{\epsilon \rightarrow 0} \underline{\chi}_{\epsilon} = \underline{\chi}^{\text{BG}}, \quad \lim_{\epsilon \rightarrow 0} \underline{\Gamma}_{\epsilon} = \underline{\Gamma}^{\text{BG}},$$

where the limits are, respectively, in $\underline{\mathcal{L}}^2(\omega)$ and $\underline{\mathcal{L}}^2(\omega)$, and $\underline{\chi}^{\text{BG}}$ and $\underline{\Gamma}^{\text{BG}}$ are given by :

$$(1.128) \quad \underline{\chi}^{\text{BG}} = \underline{\Phi}^{\text{BG}} \cdot \underline{\nabla}, \quad \underline{\Gamma}^{\text{BG}} = \underline{\Phi}^{\text{BG}} + \underline{i} \cdot \underline{\nabla} W^{\text{BG}}.$$

The first limit in (1.127) follows from the convergence $\underline{\mathcal{M}}_{\epsilon} = \underline{\mathcal{D}} : \underline{\chi}_{\epsilon}$ to $\underline{\mathcal{M}}^{\text{BG}} = \underline{\mathcal{D}} : \underline{\chi}^{\text{BG}}$. It remains to prove the second limit. We will use the following properties of $\underline{\mathcal{H}}_{\epsilon}$ which can be easily established by performing the singular value decomposition of $\underline{\mathcal{h}}$ and $\underline{\mathcal{H}}_{\epsilon}$:

$$(1.129) \quad \lim_{\epsilon \rightarrow 0} \underline{\mathcal{h}} : \underline{\mathcal{H}}_{\epsilon} = \underline{\mathcal{P}}^S, \quad {}^T \underline{\mathcal{X}} : \underline{\mathcal{H}}_{\epsilon} : \underline{\mathcal{X}} = \epsilon^{-1} \underline{\mathcal{X}}^K : \underline{\mathcal{X}}^K, \quad \forall \underline{\mathcal{X}} \in \mathbb{R}$$

From the convergence of $\underline{\mathcal{R}}_{\epsilon}^S$ to $\underline{\mathcal{R}}^{\text{BG}}$, we have :

$$(1.130) \quad \lim_{\epsilon \rightarrow 0} \underline{\mathcal{h}} : (\underline{\mathcal{R}}_{\epsilon}^S - \underline{\mathcal{R}}^{\text{BG}}) = \lim_{\epsilon \rightarrow 0} \underline{\mathcal{h}} : \underline{\mathcal{H}}_{\epsilon} : \underline{\Gamma}_{\epsilon} - \underline{\Gamma}^{\text{BG}} = \lim_{\epsilon \rightarrow 0} \underline{\Gamma}_{\epsilon}^S - \underline{\Gamma}^{\text{BG}} = 0$$

where the limits are in $\underline{\mathcal{L}}^2(\omega)$ -norm. To end the proof, we notice that :

$$(1.131) \quad \mathcal{E}_{\epsilon}^*(\underline{\mathcal{M}}_{\epsilon}) = \frac{1}{2} \int_{\omega} \underline{\mathcal{M}}_{\epsilon} : \underline{\mathcal{d}} : \underline{\mathcal{M}}_{\epsilon} + {}^T \underline{\mathcal{R}}_{\epsilon} : \underline{\mathcal{h}} : \underline{\mathcal{R}}_{\epsilon} = \frac{1}{2} \int_{\omega} \underline{\chi}_{\epsilon} : \underline{\mathcal{D}} : \underline{\chi}_{\epsilon} + {}^T \underline{\Gamma}_{\epsilon} : \underline{\mathcal{H}}_{\epsilon} : \underline{\Gamma}_{\epsilon}$$

and hence,

$$(1.132) \quad \mathcal{E}_{\epsilon}^*(\underline{\mathcal{M}}_{\epsilon}) \geq \frac{1}{2} \int_{\omega} \epsilon^{-1T} \underline{\Gamma}_{\epsilon}^K : \underline{\Gamma}_{\epsilon}^K.$$

Then, using convergence (1.117) and the above inequality, we obtain the convergence to zero of $\underline{\Gamma}_{\epsilon}^K$ in $\underline{\mathcal{L}}^2(\omega)$, and finally the second convergence in (1.127). \square

1.9 Conclusion

In this paper, a detailed mathematical justification for the recent theory of the Bending-Gradient elasticity was provided. Using variational methods, a series of existence and uniqueness theorems were formulated and proved. Since the shear force compliance tensor is not always definite, our study was divided into two parts. In the first part, we considered the particular case where the sixth-order tensor is positive definite. In this context, we defined the functional spaces to which the variables of the Bending-Gradient theory belong. Thereafter, using results established by Sab et al. (2015), we rigorously proved that the stress and displacement minimization problems are well-posed when the plate under consideration is clamped or free. A brief discussion was then conducted concerning the simple support boundary conditions.

The second part of the paper was devoted to the extension of our findings to the general case. Some additional considerations had to be made when choosing the functional spaces. We investigated only the case of a clamped plate. The main conclusion is the existence and uniqueness of the solution to the Bending-Gradient problem.

An important point is that, in general, the Bending-Gradient theory cannot be reduced to a Reissner-Mindlin theory. However, when the plate is homogeneous, the Bending-Gradient theory corresponds to a Reissner-Mindlin theory. This case falls in the situations where the generalized shear force stiffness is not definite and was covered in Section 1.7.

It is worthwhile to point out that adding a positive multiple of the identity operator to the shear force compliance tensor renders it definite. Indeed, in this case, the regularized problem admits a unique solution. Our main concern was to prove that the regularized solution converges to the exact solution of the Bending-Gradient in the general case. We managed to establish this fundamental result by assuming that the gradient of the exact solution to the Bending-Gradient stress problem is a square integrable function.

Chapitre 2

The Bending-Gradient theory for flexural wave propagation in composite plates

*Ce chapitre est consacré à tester la validité de la théorie du Bending-Gradient pour la modélisation de la propagation d'ondes planes dans des plaques symétriques infinies, hétérogènes et anisotropes. Après un rappel des variables et des équations en statique, nous introduisons deux projections du Bending-Gradient sur un modèle de Reissner-Mindlin. Le tenseur de cisaillement généralisé du Bending-Gradient n'étant pas toujours défini, une méthode de réduction est proposée visant à calculer son inverse. Dans une deuxième partie, nous formulons les équations de mouvement du Bending-Gradient dans le cas général et suivant les projections déjà introduites. Nous expliquons ensuite comment obtenir numériquement les relations de dispersion traduisant la réponse de la plaque à la présence de perturbations. Une vérification de la méthode est effectuée par comparaison des résultats obtenus à ceux de la méthode des éléments finis. Ce chapitre a été publié dans la revue *International Journal of Solids and Structures* sous la référence *Bejjani et al. (2019)*.*

Abstract

This paper is concerned with the prediction of the propagation of flexural waves in anisotropic laminated plates with relatively high slenderness ratios by means of refined plate models. The study is conducted using the Bending-Gradient theory which is considered as an extension of the Reissner-Mindlin theory to multilayered plates. Two projections of the Bending-Gradient model on Reissner-Mindlin models are also explored. The relevance of the proposed models is tested by comparing them to well-known plate theories and to reference results obtained using the finite element method.

2.1 Introduction

Owing to their lightweight and advanced high strength, composite plates are widely used in the civil, marine, aerospace and automotive industries. Due to their anisotropic and heterogeneous nature, the accurate prediction of their structural behavior is a challenging problem that has stimulated considerable research interest. Several plate theories have been proposed in the literature. The most well-known and simplest are the Kirchhoff-Love theory (or Classical Plate Theory) for thin plates (Kirchhoff, 1850a,b; Love, 1888) and the Reissner-Mindlin theory (or First Order Shear Deformation Theory) for thin to moderately thick plates (Reissner, 1945; Mindlin, 1951). The Kirchhoff-Love and the Reissner-Mindlin models provide very satisfactory results when the constitutive material is homogeneous (Ciarlet and Destuynder, 1979; G. Ciarlet, 1990, 1997). However, the extension of these models to heterogeneous plates leads to discontinuous out of plane shear distributions and incorrect estimation of the deflection compared to exact solutions (Yang et al., 1966; M. Whitney and J. Pagano, 1970). Limitations of the Kirchhoff-Love and Reissner-Mindlin models induced the development of higher order models in order to capturing correctly the effects of out of plane shear deformations (M. Whitney, 1972; Reddy, 1989; Noor and Malik, 2000; Carrera, 2002).

In the light of the ideas presented by Reissner, Lebée and Sab (2011) have recently derived a new model, known as the Bending-Gradient theory, dedicated to thick and anisotropic plates. Here, the classical Reissner-Mindlin out-of-plane shear forces are replaced by the generalized shear force related to the first gradient of the bending moment. Furthermore, six rotations are introduced instead of two. This is why the Bending-Gradient theory is considered as an extension of the Reissner-Mindlin theory to laminated plates. The reader is referred to Sab and Lebée (2015) for thorough details. It was demonstrated that the Bending-Gradient model cannot be reduced to a Reissner-Mindlin model unless the constitutive material of the plate is homogeneous (Lebée and Sab, 2011). For this reason, these authors searched for an approximation of the Bending-Gradient model by a suitable Reissner-Mindlin model (Lebée and Sab, 2015). Several projections of the Bending-Gradient model were discussed and their relevance was tested (Sab and Lebée, 2015). Comparisons with the Reissner-Mindlin theory and the full three-dimensional exact solutions (Pagano, 1969, 1970) showed that the Bending-Gradient theory gives good prediction of deflection, shear stress distributions and in-plane displacement distributions in any material configuration. Originally designed for laminated plates, the Bending-Gradient theory was extended to in-plane periodic plates, sandwich panels (Lebée and Sab, 2012a,b), space frames (Lebée and Sab, 2013) and applied to cross laminated timber panels (Perret et al., 2016).

In recent papers, the Bending-Gradient theory was justified through asymptotic expansions (Lebée and Sab, 2013) as well as variational methods and a series of existence and uniqueness theorems were formulated and proved (Bejjani et al., 2018). Having mathematically justified this theory, the central aim of this work is to test its validity regarding plane wave propagation in symmetrical anisotropic heterogeneous plates. Since plane

waves propagate in unbounded elastic continua, the plate is considered to be infinite in the direction of wave propagation, away from boundary conditions and loadings. While the classical plate theory agrees well with the finite element solutions when the wavelength λ is very large with respect to the thickness h , our results show that it becomes invalid when the thickness-wavelength (h/λ) ratio is greater than 0.05 approximately. In this paper, we go further in the approximation and focus on wavelengths that are about two times the laminate thickness ($h/\lambda = 0.5$). It is expected that the Bending-Gradient theory will fail to give acceptable results beyond this limit. In fact, modelling a plate as a two-dimensional domain and ignoring the contributions in the transverse direction is not valid when the wavelength is about or less than the plate thickness. In what follows, we seek to relate the wave number and the angular frequency for the sake of predicting dispersion curves of flexural waves, i.e waves whose displacements are perpendicular to the direction of propagation.

Analytical solutions for the wave propagation problem in composite materials are difficult to determine. One of the most used methods to solve such problems is the Finite Element Analysis. Different methodologies have been developed over the years, the foremost being the Semi-Analytical Finite Element method (SAFE) Kausel (1986); Datta et al. (1988). Recently, Gravenkamp et al. (2012) presented a formulation of the wave propagation problem based on the Scaled Boundary Finite Element Method (SBFEM). Mention may also be made of Renno et al. (2013), who described the Wave Finite Element (WFE) approach which besides being simple in application, provides accurate results at low computational cost. In order to verify the relevance of the Bending-Gradient model and its projections on Reissner-Mindlin models, a comparative study between our results and those obtained by the finite element analysis of the three-dimensional problem detailed in Margerit (2018) is conducted.

The paper proceeds as follows. In Section 3.2, we introduce tensor notations and algebraic manipulations that are used throughout this paper. Section 2.3 concisely provides the main definitions and equations of the Bending-Gradient model for anisotropic heterogeneous plates. The particular case of homogeneous plates is also discussed and projections of the Bending-Gradient theory on a Reissner-Mindlin plate theory are presented. Section 3.3 is concerned with the derivation and the implementation of the plane waves dispersion curves either in 3D or from a plate model. Finally, in Section 3.5, we verify the accuracy of the proposed method by comparing results from the classical plate theory (CPT), the first order shear deformation theory (FOSDT), the Bending-Gradient theory (BG) and the proposed projections (SSP and SCP) to results computed using the finite element method. Conclusions are given in Section 3.6.

2.2 Notations

In this paper, we use Greek indices for 2D tensors ($\alpha, \beta, \gamma.. = 1, 2$) and Latin indices for 3D tensors ($i, j, k.. = 1, 2, 3$). For example, $(X_{\alpha\beta})$ represents the 2D tensor while (X_{ij})

denotes a 3D tensor . Index notation also provides another advantage : the number of indices indicates the order of the tensor. For example, (X_{ij}) denotes a second-rank tensor whereas (X_{ijkl}) denotes a fourth-rank tensor. To simplify expressions including tensors, we shall make use of the Einstein summation convention according to which all indices appearing twice within an expression are to be summed.

The identity for 2D vectors is $(\delta_{\alpha\beta})$ where $\delta_{\alpha\beta}$ is Kronecker symbol ($\delta_{\alpha\beta} = 1$ if $\alpha = \beta$, $\delta_{\alpha\beta} = 0$ otherwise). The identity for 2D symmetric second order tensors is $i_{\alpha\beta\gamma\delta}$ where $i_{\alpha\beta\gamma\delta} = \frac{1}{2}(\delta_{\alpha\gamma}\delta_{\beta\delta} + \delta_{\alpha\delta}\delta_{\beta\gamma})$. The reader might easily check that $i_{\alpha\beta\gamma\delta}i_{\delta\gamma\eta\theta} = i_{\alpha\beta\eta\theta}$, $i_{\alpha\beta\gamma\delta}i_{\delta\gamma\beta\theta} = 3/2\delta_{\alpha\theta}$ and $i_{\alpha\beta\gamma\delta}i_{\delta\gamma\beta\alpha} = 3$.

The gradient of a scalar field X writes $(X_{,\beta})$ while the gradient of a vector or a higher-order tensor fields writes $(X_{\alpha\beta,\gamma})$, for instance. The divergence of a vector field or a second order tensor field is noted $(X_{\alpha,\alpha})$ and $(X_{\alpha\beta,\beta})$, respectively.

Finally, the integration through the thickness is noted $\langle \bullet \rangle : \int_{-\frac{h}{2}}^{\frac{h}{2}} f(x_3)dx_3 = \langle f \rangle$.

2.3 The Bending-Gradient Model for the equilibrium of thick plates

2.3.1 The 3D plate configuration

The physical space is endowed with an orthonormal reference frame $(O, \underline{e}_1, \underline{e}_2, \underline{e}_3)$ where O is the origin and \underline{e}_i is the base vector in direction $i \in \{1, 2, 3\}$. We consider a linear elastic plate occupying the 3D domain $V = S \times]-\frac{h}{2}, \frac{h}{2}[$, where $S \subset \mathbb{R}^2$ is the middle surface of the plate and h its thickness. The boundary of the domain, denoted by ∂V , is decomposed into three parts (Figure 2.1) :

$$(2.1) \quad \begin{aligned} \partial V &= \partial V_{\text{lat}} \cup \partial V_3^+ \cup \partial V_3^-, \\ \text{with } \partial V_{\text{lat}} &= \partial S \times \left] -\frac{h}{2}, \frac{h}{2} \right[\quad \text{and} \quad \partial V_3^\pm = S \times \left\{ \pm \frac{h}{2} \right\}, \end{aligned}$$

where ∂S is the boundary of S .

Focusing only on out-of-plane loadings, the plate is subjected to forces per unit surface on ∂V_3^\pm of the form :

$$(2.2) \quad (T_1, T_2, T_3)^\pm(x_1, x_2) = \left(0, 0, \frac{1}{2}p(x_1, x_2) \right),$$

where p is a given function on S .

We suppose that the constitutive material is invariant with respect to translations in the (x_1, x_2) plane. Therefore, the fourth-rank 3D elasticity stiffness tensor (C_{ijkl}) does not

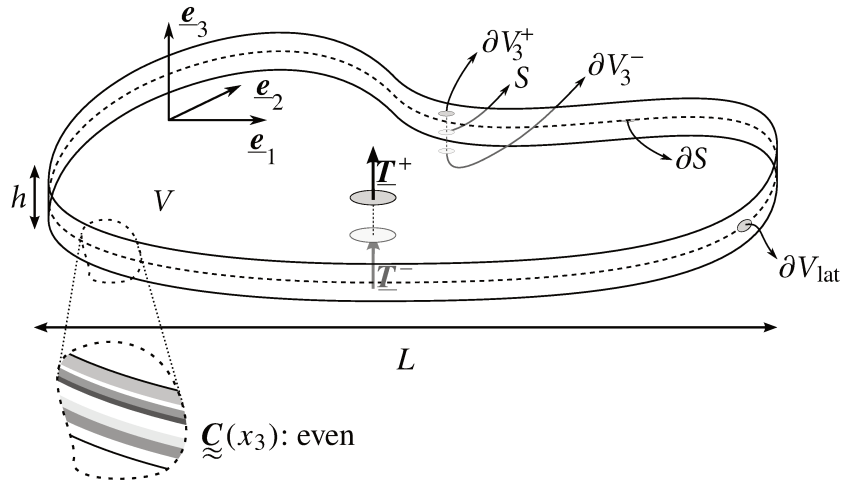


FIGURE 2.1 – The 3D configuration

depend on (x_1, x_2) . The plate is assumed to be symmetric with respect to its mid-plane S , hence C_{ijkl} is an even function of x_3 :

$$(2.3) \quad C_{ijkl}(x_3) = C_{ijkl}(-x_3).$$

This is the so-called mirror symmetry. Furthermore, we have that :

$$(2.4) \quad C_{3\alpha\beta\gamma} = C_{\alpha 333} = 0.$$

In this case, the constitutive material is said to be monoclinic.

To make the presentation self-contained, we now briefly recall the main definitions of the kinematic and static fields of the Bending-Gradient theory as well as the governing equations established by Lebée and Sab (2011). For more details concerning the Bending-Gradient theory, the reader is referred to Lebée and Sab (2011), Lebée and Sab (2011), Lebée and Sab (2015), Lebée and Sab (2015), Sab and Lebée (2015) and Bejjani et al. (2018).

2.3.2 The Bending-Gradient equations

The Bending-Gradient generalized displacements are $(U_3, \Phi_{\alpha\beta\gamma})$ where U_3 is the out-of-plane displacement of the plate (or deflection) and $(\Phi_{\alpha\beta\gamma})$ is the generalized rotation tensor with $\Phi_{\alpha\beta\gamma} = \Phi_{\beta\alpha\gamma}$.

The Bending-Gradient generalized strains, which derive from $(U_3, \Phi_{\alpha\beta\gamma})$ are $(\chi_{\alpha\beta}, \Gamma_{\alpha\beta\gamma})$. $(\chi_{\alpha\beta})$ is the curvature second-order tensor with $\chi_{\alpha\beta} = \chi_{\beta\alpha}$, and $(\Gamma_{\alpha\beta\gamma})$ is the generalized shear strain verifying $\Gamma_{\alpha\beta\gamma} = \Gamma_{\beta\alpha\gamma}$. The generalized strains are obtained through the following compatibility conditions on S :

$$(2.5a) \quad \begin{cases} \chi_{\alpha\beta} = \Phi_{\alpha\beta\gamma,\gamma}, \\ \Gamma_{\alpha\beta\gamma} = \Phi_{\alpha\beta\gamma} + i_{\alpha\beta\gamma\delta} U_{3,\delta}. \end{cases}$$

(2.5b)

The Bending-Gradient generalized strains $(\chi_{\alpha\beta}, \Gamma_{\alpha\beta\gamma})$ constitute the dual of the Bending-Gradient generalized stresses $(M_{\alpha\beta}, R_{\alpha\beta\gamma})$. The second-order tensor $(M_{\alpha\beta})$ is the conventional bending moment tensor $(M_{\alpha\beta} = M_{\beta\alpha})$ related to the 3D local stress (σ_{ij}) by :

$$(2.6) \quad M_{\alpha\beta} = \langle x_3 \sigma_{\alpha\beta} \rangle.$$

The third-order tensor $(R_{\alpha\beta\gamma})$ represents the generalized shear force which complies with the following symmetry : $R_{\alpha\beta\gamma} = R_{\beta\alpha\gamma}$. The Bending-Gradient constitutive equations write as :

$$(2.7a) \quad \begin{cases} \chi_{\alpha\beta} = d_{\alpha\beta\gamma\delta} M_{\delta\gamma}, \\ \Gamma_{\alpha\beta\gamma} = h_{\alpha\beta\gamma\delta\epsilon\zeta} R_{\zeta\epsilon\delta}, \end{cases}$$

where $(d_{\alpha\beta\gamma\delta})$ and $(h_{\alpha\beta\gamma\delta\epsilon\zeta})$ represent compliance tensors which are explicitly expressed in terms of the elastic components through the thickness of the plate (Sab and Lebée, 2015). $d_{\alpha\beta\gamma\delta}$ designates the classical bending compliance fourth-order tensor, inverse of the bending stiffness fourth-order tensor $D_{\alpha\beta\gamma\delta}$. Both tensors are positive definite and symmetric. The generalized shear compliance tensor $h_{\alpha\beta\gamma\delta\epsilon\zeta}$ is symmetric and positive but it is definite only its image $\text{Im } h$ whose dimension is between two and six, depending on the elastic properties of the plate. More details about the subspace $\text{Im } h$ are given in 3.6. The generalized shear stiffness tensor $(H_{\alpha\beta\gamma\delta\epsilon\zeta})$ is the Moore-Penrose pseudo inverse of $(h_{\alpha\beta\gamma\delta\epsilon\zeta})$. The Bending-Gradient equilibrium equations are given by :

$$(2.8a) \quad \begin{cases} R_{\alpha\beta\gamma} - P_{\alpha\beta\gamma\delta\epsilon\zeta}^S M_{\zeta\epsilon,\delta} = 0, \\ i_{\alpha\beta\gamma\delta} R_{\delta\gamma\beta,\alpha} + p = 0. \end{cases}$$

where $P_{\alpha\beta\gamma\delta\epsilon\zeta}^S$ designates the orthogonal projection operator onto $\text{Im } h$.

We note that, regardless of the positive definiteness of the shear compliance tensor $(h_{\alpha\beta\gamma\delta\epsilon\zeta})$, one can derive the conventional shear force $Q_\alpha = \langle \sigma_{\alpha 3} \rangle$ from $R_{\alpha\beta\gamma}$ by :

$$(2.9) \quad Q_\alpha = R_{\alpha\beta\beta}.$$

Hence, equation (2.8)b can be restated as :

$$(2.10) \quad Q_{\alpha,\alpha} + p = 0.$$

2.3.3 Homogeneous plates

It was shown in Lebée and Sab (2015), Lebée and Sab (2015), Sab and Lebée (2015) that the Bending-Gradient theory cannot be reduced to a Reissner-Mindlin theory in general. However, when the plate under consideration is homogeneous, the two theories coincide. In this case, the generalized shear tensor $(h_{\alpha\beta\gamma\delta\epsilon\zeta})$ can be expressed as :

$$(2.11) \quad h_{\alpha\beta\gamma\delta\epsilon\zeta} = i_{\alpha\beta\gamma\eta} f_{\eta\theta}^R i_{\theta\delta\epsilon\zeta},$$

where $(f_{\eta\theta}^R)$ is a positive definite symmetric second-order tensor called the Reissner-Mindlin shear compliance tensor. Furthermore, in this case, the generalized rotation tensor $(\Phi_{\alpha\beta\gamma})$ is of the form :

$$(2.12) \quad \Phi_{\alpha\beta\gamma} = i_{\alpha\beta\gamma\delta}\varphi_\delta,$$

where (φ_δ) is a 2D vector representing rotations. The generalized shear force $(R_{\alpha\beta\gamma})$ can be as well expressed as :

$$R_{\alpha\beta\gamma} = \frac{2}{3}i_{\alpha\beta\eta\theta}M_{\theta\gamma,\eta}.$$

It follows that equations (2.8) become :

$$(2.13a) \quad \left\{ \begin{array}{l} Q_\alpha - M_{\alpha\beta,\beta} = 0, \\ Q_{\alpha,\alpha} + p = 0, \end{array} \right.$$

which constitute the well-known Reissner-Mindlin equilibrium equations.

2.3.4 Projection of the Bending-Gradient plate model

As previously mentioned, the Bending-Gradient theory is considered as an extension of the Reissner-Mindlin theory to laminated plates. It is hence interesting to try to approximate the Bending-Gradient model through an appropriate Reissner-Mindlin's model. In this section, we present two means to project the Bending-Gradient model on a Reissner-Mindlin model : the shear compliance projection (SCP) and the shear stiffness projection (SSP). These projections are discussed in full-detail in (Sab and Lebée, 2015).

2.3.4.1 The Shear Compliance Projection (SCP)

Consider a Bending-Gradient model with shear compliance tensor $(h_{\alpha\beta\gamma\delta\epsilon\zeta})$ and let $(f_{\alpha\beta}^{\text{RM}})$ denote the corresponding Reissner-Mindlin compliance. The first approach consists in considering the following projection of $(h_{\alpha\beta\gamma\delta\epsilon\zeta})$:

$$(2.14) \quad \left\{ \begin{array}{l} f_{11}^{\text{RM}} = \frac{4}{9}(h_{111111} + h_{122221} + 2h_{111221}), \\ f_{12}^{\text{RM}} = f_{21}^{\text{RM}} = \frac{4}{9}(h_{111121} + h_{111222} + h_{121221} + h_{222221}), \\ f_{22}^{\text{RM}} = \frac{4}{9}(h_{222222} + h_{121121} + 2h_{121222}). \end{array} \right.$$

This projection is equivalent to assuming $R_{\alpha\beta\gamma} = \frac{2}{3}i_{\alpha\beta\gamma\eta}Q_\eta$ in the expression of the Bending-Gradient shear stress energy density (Sab and Lebée, 2015).

In the framework of this projection, an evaluation of the distance between the Bending-Gradient plate model and the Reissner-Mindlin model was suggested (Lebée and Sab (2011), Lebée and Sab (2011)). Indeed, when the plate is homogeneous, the distance between the two models is equal to zero.

2.3.4.2 The Shear Stiffness Projection (SSP)

We now study the Shear Stiffness Projection which consists in supposing that the Reissner-Mindlin's shear stiffness tensor ($F_{\alpha\beta}^{\text{RM}}$) associated to the Bending-Gradient shear stiffness tensor ($H_{\alpha\beta\gamma\delta\epsilon\zeta}$) is of the form :

$$(2.15) \quad \begin{cases} F_{11}^{\text{RM}} = H_{111111} + H_{122221} + 2H_{111221}, \\ F_{12}^{\text{RM}} = F_{21}^{\text{RM}} = H_{111121} + H_{111222} + H_{121221} + H_{222221}, \\ F_{22}^{\text{RM}} = H_{222222} + H_{121121} + 2H_{121222}. \end{cases}$$

Using this projection is equivalent to assuming that the generalized rotation is of the form $\Phi_{\alpha\beta\gamma} = i_{\alpha\beta\gamma\delta}\varphi_\delta$ in the expression of the Bending-Gradient shear strain energy density (Sab and Lebée, 2015), where (φ_δ) is a Reissner-Mindlin rotation vector.

It should be strongly emphasized that, unless for homogeneous plates, the shear stiffness projection and the shear compliance projection lead to different approximations. Hence, $(F_{\alpha\beta}^{\text{RM}})$ is not the inverse of $(f_{\alpha\beta}^{\text{RM}})$ in the general case (Sab and Lebée, 2015).

2.3.5 Kelvin Notations

Expressing the Bending-Gradient equations involves tensors with up to six indices which can be somehow cumbersome. This is why we introduce in this section Kelvin notation which allows us to express any order tensor in the form of a matrix. Contractions products are hence turned into conventional matrix products. In the following, brackets $[\bullet]$ are used to denote that a tensor is considered in a matrix form. Thus, $[\bullet]$ is a linear operator real-locating tensor components. For example, the bending moment ($M_{\alpha\beta}$) and the curvature tensor ($\chi_{\alpha\beta}$) can be expressed as :

$$(2.16) \quad [M] = \begin{bmatrix} M_{11} \\ M_{22} \\ \sqrt{2}M_{12} \end{bmatrix}, \quad [\chi] = \begin{bmatrix} \chi_{11} \\ \chi_{22} \\ \sqrt{2}\chi_{12} \end{bmatrix}.$$

The fourth-order tensor ($D_{\alpha\beta\gamma\delta}$) is obtained through :

$$(2.17) \quad [D] = \langle x_3^2 [C^\sigma] \rangle,$$

where $C_{\alpha\beta\gamma\delta}^\sigma = C_{\alpha\beta\gamma\delta} - \frac{C_{\alpha\beta 33}C_{\gamma\delta 33}}{C_{3333}}$ corresponds to the plane stress stiffness. $[D]$ and $[C^\sigma]$ take the following matrix form :

$$(2.18) \quad [D] = \begin{bmatrix} D_{1111} & D_{2211} & \sqrt{2}D_{1211} \\ D_{2211} & D_{2222} & \sqrt{2}D_{1222} \\ \sqrt{2}D_{1211} & \sqrt{2}D_{1222} & 2D_{1212} \end{bmatrix}.$$

The constitutive equation $M_{\alpha\beta} = D_{\alpha\beta\gamma\delta} : \chi_{\delta\gamma}$ becomes a vector-matrix product :

$$(2.19) \quad [M] = [D] \cdot [\chi].$$

Shear static unknowns are reallocated in a vector form as :

$$(2.20) \quad [R] = \begin{bmatrix} R_{111} \\ R_{221} \\ \sqrt{2}R_{121} \\ R_{112} \\ R_{222} \\ \sqrt{2}R_{122} \end{bmatrix}, \quad [\Gamma] = \begin{bmatrix} \Gamma_{111} \\ \Gamma_{221} \\ \sqrt{2}\Gamma_{121} \\ \Gamma_{112} \\ \Gamma_{222} \\ \sqrt{2}\Gamma_{122} \end{bmatrix}, \quad [\Phi] = \begin{bmatrix} \Phi_{111} \\ \Phi_{221} \\ \sqrt{2}\Phi_{121} \\ \Phi_{112} \\ \Phi_{222} \\ \sqrt{2}\Phi_{122} \end{bmatrix}.$$

The third-order tensor ($i_{\alpha\beta\gamma\delta}U_{3,\delta}$) is expressed in Kelvin notation by :

$$(2.21) \quad [i \cdot \nabla U_3] = U_{3,1} [J^1] + U_{3,2} [J^2],$$

where

$$(2.22) \quad [J^1]^T = \left[1, 0, 0, 0, 0, \frac{1}{\sqrt{2}} \right], \quad [J^2]^T = \left[0, 0, \frac{1}{\sqrt{2}}, 0, 0, 1 \right].$$

The Bending-Gradient shear compliance and stiffness tensors ($h_{\alpha\beta\gamma\delta\epsilon\zeta}$) and ($H_{\alpha\beta\gamma\delta\epsilon\zeta}$) are turned into a 6×6 -matrix :

$$(2.23) \quad [h] = \begin{bmatrix} h_{111111} & h_{111122} & \sqrt{2}h_{111121} & h_{111211} & h_{111222} & \sqrt{2}h_{111221} \\ h_{221111} & h_{221122} & \sqrt{2}h_{221121} & h_{221211} & h_{221222} & \sqrt{2}h_{221221} \\ \sqrt{2}h_{121111} & \sqrt{2}h_{121122} & 2h_{121121} & \sqrt{2}h_{121211} & \sqrt{2}h_{121222} & 2h_{121221} \\ h_{112111} & h_{112122} & \sqrt{2}h_{112121} & h_{112211} & h_{112222} & \sqrt{2}h_{112221} \\ h_{222111} & h_{222122} & \sqrt{2}h_{222121} & h_{222211} & h_{222222} & \sqrt{2}h_{222221} \\ \sqrt{2}h_{122111} & \sqrt{2}h_{122122} & 2h_{122121} & \sqrt{2}h_{122211} & \sqrt{2}h_{122222} & 2h_{122221} \end{bmatrix}.$$

Note that we use the same letter for tensor and matrix components. However, two indices represent matrix components whereas six indices designate tensor components. For instance, h_{221121} is the tensor component of ($h_{\alpha\beta\gamma\delta\epsilon\zeta}$) whereas $h_{23} = \sqrt{2}h_{221121}$ is the matrix component of $[h]$.

As already indicated, the shear compliance tensor $h_{\alpha\beta\gamma\delta\epsilon\zeta}$ is not always invertible. A new feature of our work is the reduction method, presented and detailed thereafter, in order to calculate the shear stiffness tensor.

2.3.6 The reduction method

The reduction method consists in introducing the constraint $(\Phi_{\alpha\beta\gamma}) \in \text{Im } h$ when the dimension of $\text{Im } h$ is strictly lower than six (see 3.6). The first step consists in computing the pseudo inverse $(H_{\alpha\beta\gamma\delta\epsilon\zeta})$ through the Singular Value decomposition (SVD). Accordingly, the real-valued compliance matrix $[h]$ is factored into :

$$(2.24) \quad [h] = [N] \cdot [a] \cdot [N]^T,$$

where $[a]$ is a 6×6 diagonal matrix :

$$(2.25) \quad [a] = \begin{bmatrix} a_1 & 0 & 0 & 0 & 0 & 0 \\ 0 & a_2 & 0 & 0 & 0 & 0 \\ 0 & 0 & a_3 & 0 & 0 & 0 \\ 0 & 0 & 0 & a_4 & 0 & 0 \\ 0 & 0 & 0 & 0 & a_5 & 0 \\ 0 & 0 & 0 & 0 & 0 & a_6 \end{bmatrix},$$

and $[N]$ is an orthogonal 6×6 matrix with $[N]^T = [N]^{-1}$, where $[N]^T$ denotes the transpose of $[N]$.

The Moore-Penrose pseudo inverse $(H_{\alpha\beta\gamma\delta\epsilon\zeta})$ is hence obtained through :

$$(2.26) \quad [H] = [N] \cdot [A] \cdot [N]^T = [N] \cdot \begin{bmatrix} A_1 & 0 & 0 & 0 & 0 & 0 \\ 0 & A_2 & 0 & 0 & 0 & 0 \\ 0 & 0 & A_3 & 0 & 0 & 0 \\ 0 & 0 & 0 & A_4 & 0 & 0 \\ 0 & 0 & 0 & 0 & A_5 & 0 \\ 0 & 0 & 0 & 0 & 0 & A_6 \end{bmatrix} \cdot [N]^T,$$

with $A_k = 0$ if $a_k = 0$ and $A_k = \frac{1}{a_k}$ if $a_k \neq 0$.

Sab and Lebée (2015) demonstrated that the projection operator $(P_{\alpha\beta\gamma\delta\epsilon\zeta}^S)$ can be expressed in the form of a matrix as :

$$(2.27) \quad [P^S] = [H] \cdot [h] = [h] \cdot [H].$$

Substituting $[h]$ and $[H]$ by their expressions (2.24) and (2.26), we obtain that :

$$(2.28) \quad [P^S] = [N] \cdot [\alpha] \cdot [N]^T = [N] \cdot \begin{bmatrix} \alpha_1 & 0 & 0 & 0 & 0 & 0 \\ 0 & \alpha_2 & 0 & 0 & 0 & 0 \\ 0 & 0 & \alpha_3 & 0 & 0 & 0 \\ 0 & 0 & 0 & \alpha_4 & 0 & 0 \\ 0 & 0 & 0 & 0 & \alpha_5 & 0 \\ 0 & 0 & 0 & 0 & 0 & \alpha_6 \end{bmatrix} \cdot [N]^T,$$

where $\alpha_k = 0$ if $a_k = 0$ and $\alpha_k = 1$ if $a_k \neq 0$. In practice, assuming α_k are sorted in decreasing order, if $\alpha_k \leq 10^{-3}\alpha_1$, then $\alpha_k = 0$.

Let $(P_{\alpha\beta\gamma\delta\epsilon\zeta}^K)$ denote the projection operator onto $\text{Ker } h$ (see 3.6). $(P_{\alpha\beta\gamma\delta\epsilon\zeta}^K)$ has the following form :

$$(2.29) \quad [P^K] = [N] \cdot [\beta] \cdot [N]^T = [N] \cdot \begin{bmatrix} \beta_1 & 0 & 0 & 0 & 0 & 0 \\ 0 & \beta_2 & 0 & 0 & 0 & 0 \\ 0 & 0 & \beta_3 & 0 & 0 & 0 \\ 0 & 0 & 0 & \beta_4 & 0 & 0 \\ 0 & 0 & 0 & 0 & \beta_5 & 0 \\ 0 & 0 & 0 & 0 & 0 & \beta_6 \end{bmatrix} \cdot [N]^T,$$

where $\beta_k = 1$ if $a_k = 0$ and $\beta_k = 0$ if $a_k \neq 0$.

As stated earlier, the condition $\Gamma_{\alpha\beta\gamma} \in \text{Im } h$ is equivalent to $\Phi_{\alpha\beta\gamma} \in \text{Im } h$ since $i_{\alpha\beta\gamma\delta}U_{3,\delta}$ always belongs to $\text{Im } h$. This implies that

$$(2.30) \quad [P^K] \cdot [\Phi] = [P^K] \cdot [\Gamma],$$

and

$$(2.31) \quad [P^K] \cdot [i \cdot \nabla U_3] = 0.$$

Combining equations (2.7)b, (2.29) and (2.30) yields :

$$(2.32) \quad [P^K] \cdot [\Phi] = [P^K] \cdot [\Gamma] = [N] \cdot [\beta] \cdot [N]^T \cdot [N] \cdot [\alpha] \cdot [N]^T \cdot [R] = 0$$

since we have that :

$$(2.33) \quad [N] \cdot [N]^T = [I] \quad \text{and} \quad [\beta] \cdot [\alpha] = 0.$$

Introducing the change of variable $[\Phi] = [N] \cdot [\Phi^*]$ in equation (2.32) grants :

$$(2.34) \quad [P^K] \cdot [\Phi] = [N] \cdot [\beta] \cdot [N]^T \cdot [\Phi] = [N] \cdot [\beta] \cdot [\Phi^*] = 0 \iff [\beta] \cdot [\Phi^*] = 0,$$

which means that $(\Phi_{\alpha\beta\gamma}) \in \text{Im } h$ if, and only if, $\Phi_i^* = 0$ for all i such that $a_i = 0$.

In brief, the reduction method consists in making the change of variable

$$(2.35) \quad [\Phi] = [N] \cdot [\Phi^*]$$

in the Bending-Gradient equations (2.5), (2.7) and (2.8), and imposing $\Phi_i^* = 0$ for all i such that $a_i = 0$. This allows us to write the reciprocal relationship of equation (2.7)b :

$$(2.36) \quad R_{\alpha\beta\gamma} = H_{\alpha\beta\gamma\delta\epsilon\zeta} \Gamma_{\zeta\epsilon\delta}, \quad \Gamma_{\alpha\beta\gamma} \in \text{Im } h.$$

2.4 Propagation of plane waves in an anisotropic plate

In this section, we first study the propagation of waves in anisotropic plates in the framework of the three-dimensional elasticity theory. Our main purpose is to accurately predict the dispersion curve associated to long flexural waves, which is conventionally approximated by the finite element method.

Good approximations of the static 3D solutions can be obtained from the Bending-Gradient plate model (Sab and Lebée, 2015). It is hence worth to also estimate the dispersion relation through the Bending-Gradient equations of motion. We also suggest using the Reissner-Mindlin models obtained by projections of the Bending-Gradient model as explained in Section 2.3.4.

In this part, we consider a symmetrical plate with the same configuration as Section 2.3. Assuming the plate is infinite in directions 1 and 2, no boundary conditions need to be applied on ∂V_{lat} . We particularly focus attention on waves propagating in direction 1.

2.4.1 Exact dispersion curves for guided waves

2.4.1.1 Three-dimensional equations of motion

For plane waves propagating in direction 1, the displacement vector u_i is a function of the coordinates (x_1, x_3) and of the time t :

$$u_i = u_i(x_1, x_3, t), \quad i = 1, 2, 3.$$

The basic equation of motion is obtained by relating the stress σ_{ij} to the motion of the particles in the plate using Newton's second law. Let ρ denote the density (mass per unit volume). In the absence of body forces, the Momentum equation writes :

$$(2.37) \quad \sigma_{ij,j} - \rho \ddot{u}_i = 0,$$

where the double dot indicates a second derivative with respect to time $\left(\ddot{x} = \frac{dx^2}{dt^2}\right)$.

Wave propagation in infinite anisotropic elastic plate is governed by the full set of equations of the three-dimensional theory of elasticity, namely :

$$\begin{aligned}
 (2.38a) \quad & \sigma_{ij,j} - \rho \ddot{u}_i = 0, \\
 (2.38b) \quad & \sigma_{ij} - C_{ijkl}(x_3) : \varepsilon_{lk} = 0, \\
 (2.38c) \quad & \varepsilon_{ij} - \frac{1}{2}(u_{i,j} + u_{j,i}) = 0, \\
 (2.38d) \quad & \sigma_{i3} = 0 \text{ at } x_3 = \pm \frac{h}{2}.
 \end{aligned}$$

Additionally, the stresses σ_{i3} and the displacements u_i must be continuous at the interfaces between the different layers of the plate.

For harmonic waves propagating in direction 1 at time t , the displacements u_i , solution to (2.38), can be described using :

$$(2.39) \quad u_i(x_1, x_3, t) = \Re(\hat{u}_i(x_3) e^{j(\omega t - kx_1)}), \quad i = 1, 2, 3,$$

where $(\hat{u}_i)_{i=1,2,3}$ are amplitudes of the displacement components, ω is the angular frequency, $k \neq 0$ is the wave number and j the imaginary unit. The symbol $\Re(z)$ is used to designate the real part of the complex number z . We denote by λ the wavelength and c the wave velocity. We recall that the wave number is related to the wavelength through :

$$(2.40) \quad k = \frac{2\pi}{\lambda},$$

and that the phase velocity c is expressed as :

$$(2.41) \quad c = \frac{\omega}{k}.$$

The problem is to find a relation between the angular frequency ω and the wave number k which ensures the existence of a non-zero vector $(\hat{u}_i)_{i=1,2,3}$, satisfying the three-dimensional equations of motion (2.38).

Reference solutions of the 3D problem (2.38) can be computed via the finite element method whose procedure is presented next.

2.4.1.2 Resolution by means of Finite Element Analysis

Injecting the plane wave displacement (3.8) in the local equations (2.38) leads to the formulation of a quadratic eigenvalue problem in both wavenumber k and frequency ω that has to be solved. In the case of homogeneous isotropic plates, it can be reduced to the well known Lamb modes transcendental equation (Lamb, 1917). The case of laminated plates has been first investigated by T. Thomson (1950), who expressed the inter-lamina continuity conditions with the help of *transfer matrices*. As a consequence of the numerical

instability of the method (Haskell, 1953), several reformulations has been proposed in the following decades (Schmidt and Tango, 2007; Nayfeh, 1991; Rokhlin and Wang, 2002).

Alternatively, the variationnal formulation of the problem (integral equations) can be used (Dong and B. Nelson, 1972; Datta et al., 1988; Xi et al., 2000). The finite element approach then leads to the following eigenvalue problem :

$$(2.42) \quad \left(k^2 [K_2] + jk [K_1] + [K_0] - \omega^2 [\mathbb{M}] \right) [\mathbf{U}] = \mathbf{0},$$

where $[K_i]$, $i = 1, 2, 3$ and $[\mathbb{M}]$ are symmetric hermitian matrices and $[\mathbf{U}]$ is the vector of nodal displacements. This formulation is usually referred as the Spectral Finite Element Method (J. Shorter, 2004; Barbieri et al., 2009) (SFEM) or Semi-Analytical Finite Element method (Bartoli et al., 2006) (SAFE). The preceding eigenvalue problem is solved more easily by searching the eigenfrequencies related to a given wavenumber. However, it is often more convenient to search for the wavenumber solutions corresponding to a fixed frequency ; this can be performed by the resolution of the associated quadratic eigenvalue problem, giving both real and imaginary solutions (resp. denoting propagating and evanescent waves).

This method has been implemented here to compute reference solutions to the problem of wave propagation in anisotropic plates. Linear elements were used since the problem is one-dimensional in x_3 . We used three degrees of freedom per node to take account of the three components of the displacement field. In the wavelength range of interest, it has been observed that 10 elements by layer was sufficient to avoid convergence issues.

2.4.2 Plate models dispersion curves

2.4.2.1 Bending-Gradient equations of motion

In this section, we study wave propagation in anisotropic media using the Bending-Gradient model. We first provide the formulation of the Bending-Gradient equations of motion for heterogeneous plates. Then, we explain how to find numerically the corresponding dispersion curves. Finally, the classical dispersion relation for the Reissner-Mindlin and the Kirchhoff-Love model are retrieved.

The formulation of the wave propagation problem is based on Mindlin's paper (Mindlin, 1951), in which a comparison was made between the exact solution of the three-dimensional equations and the solution obtained using the CPT. It was shown that the CPT deviates significantly from the three-dimensional theory whether the rotatory inertia correction is added or not. However, when taking into consideration the effects of transverse shear deformation solely, the obtained solution is very close to the three-dimensional solution. Thereby, the Bending-Gradient equations of motion are formulated by considering that the only inertia forces are those due to the transverse translation of the plate elements, and hence neglecting rotatory effects. In this case, the transverse load p given

by :

$$(2.43) \quad p = -\ddot{U}_3 \bar{\rho},$$

where $\bar{\rho} = \langle \rho \rangle$. In the following, we assume that the shear compliance tensor $h_{\alpha\beta\gamma\delta\epsilon\zeta}$ is definite. In this case, $P_{\alpha\beta\gamma\delta\epsilon\zeta}^S$ is the identity operator. Hence, the generalized shear force $R_{\alpha\beta\gamma}$ is the gradient of the bending moment $M_{\alpha\beta}$.

Wave propagation in anisotropic plates in the absence of body forces is thus modelled by :

$$(2.44) \quad \begin{cases} R_{\alpha\beta\gamma} - M_{\alpha\beta,\gamma} = 0, \\ Q_\alpha = R_{\alpha\beta\beta}, \\ Q_{\alpha,\alpha} = \ddot{U}_3 \bar{\rho}. \end{cases}$$

Using constitutive equations (2.7) and compatibility conditions (2.5), equations (2.44) are restated in terms of the generalized displacements $(U_3, \Phi_{\alpha\beta\gamma})(x_1, t)$ as :

$$(2.45a) \quad \begin{cases} H_{\alpha\beta\gamma\delta\epsilon\zeta} (\Phi_{\zeta\epsilon\delta} + i_{\zeta\epsilon\delta\eta} U_{3,\eta}) - D_{\alpha\beta\theta\epsilon} \Phi_{\epsilon\theta\xi,\xi\gamma} = 0, \\ H_{\alpha\beta\beta\delta\epsilon\zeta} (\Phi_{\zeta\epsilon\delta,\alpha} + i_{\zeta\epsilon\delta\eta} U_{3,\eta\alpha}) = \ddot{U}_3 \bar{\rho}. \end{cases}$$

We point out that when the sixth-order tensor $h_{\alpha\beta\gamma\delta\epsilon\zeta}$ is not definite, it suffices to make the change of variables (2.35) in equations (2.45) as detailed in Sect. 2.3.6.

For waves propagating in direction 1, the generalized displacements $(U_3, \Phi_{\alpha\beta\gamma})(x_1, t)$, solution to (2.45), can be described using :

$$(2.46a) \quad \begin{cases} U_3(x_1, t) = \Re \left(\hat{U}_3 e^{j(\omega t - kx_1)} \right), \\ \Phi_{\alpha\beta\gamma}(x_1, t) = \Re \left(\hat{\Phi}_{\alpha\beta\gamma} e^{j(\omega t - kx_1)} \right), \end{cases}$$

where \hat{U}_3 and $\hat{\Phi}_{\alpha\beta\gamma}$ are arbitrary constants. Indeed, all derivatives with respect to x_2 are equal to zero, since the displacements U_3 and $\Phi_{\alpha\beta\gamma}$ are functions of x_1 . Thus, substituting (2.46) into (2.45) yields :

$$(2.47a) \quad \begin{cases} H_{\alpha\beta\gamma\delta\epsilon\zeta} \left(\hat{\Phi}_{\zeta\epsilon\delta} - jk i_{\zeta\epsilon\delta 1} \hat{U}_3 \right) + k^2 D_{\alpha\beta\theta\epsilon} \hat{\Phi}_{\epsilon\theta 1} \delta_{1\gamma} = 0, \\ H_{1\beta\beta\delta\epsilon\zeta} \left(-jk \hat{\Phi}_{\zeta\epsilon\delta} - k^2 i_{\zeta\epsilon\delta 1} \hat{U}_3 \right) + \omega^2 \hat{U}_3 \bar{\rho} = 0. \end{cases}$$

Finding the dispersion relation associated to flexural waves requires using a mathematical computing software such as Matlab. The implementation of equations (2.47) is presented in the following section.

2.4.2.2 Implementation of plate dispersion equations

Suppose that the shear compliance tensor $h_{\alpha\beta\gamma\delta\epsilon\zeta}$ is definite. Using Kelvin notation introduced in Section 2.3.5, equation (2.44)a writes :

$$(2.48) \quad [R] - [M \otimes \nabla] = 0,$$

where $[M \otimes \nabla]$ represents the gradient of the bending moment expressed by :

$$(2.49) \quad [M \otimes \nabla] = \begin{bmatrix} M_{11,1} \\ M_{22,1} \\ \sqrt{2}M_{12,1} \\ 0 \\ 0 \\ 0 \end{bmatrix}.$$

Using compatibility conditions (2.5)b, $[R]$ is defined by :

$$(2.50) \quad [R] = [H] \cdot ([\Phi] + [i \cdot \nabla U_3]).$$

The third-order tensor $[i \cdot \nabla U_3]$ is expressed in Kelvin notation by :

$$(2.51) \quad [i \cdot \nabla U_3] = U_{3,1} [J^1] = -jk\hat{U}_3 [J^1].$$

Using compatibility conditions (2.5)a, we have :

$$(2.52) \quad \begin{bmatrix} M_{11,1} \\ M_{22,1} \\ \sqrt{2}M_{12,1} \end{bmatrix} = [D] \cdot \begin{bmatrix} \Phi_{111,11} \\ \Phi_{221,11} \\ \sqrt{2}\Phi_{121,11} \end{bmatrix} = -k^2 [D] \cdot \begin{bmatrix} \hat{\Phi}_{111} \\ \hat{\Phi}_{221} \\ \sqrt{2}\hat{\Phi}_{121} \end{bmatrix}.$$

Making use of the notations described above, wave propagation equations (2.47) can be written as a matrix-vector product :

$$(2.53) \quad [\mathcal{A}] \cdot [\delta] = 0,$$

where $[\delta]$ is a vector representing the generalized displacements $(\hat{U}_3, \hat{\Phi}_{\alpha\beta\gamma})$:

$$(2.54) \quad [\delta]^T = [\hat{U}_3, \hat{\Phi}_{111}, \hat{\Phi}_{221}, \sqrt{2}\hat{\Phi}_{121}, \hat{\Phi}_{112}, \hat{\Phi}_{222}, \sqrt{2}\hat{\Phi}_{122}],$$

and $[\mathcal{A}]$ is a symmetric 7×7 matrix given by :

$$(2.55) \quad [\mathcal{A}] = \begin{bmatrix} \mathcal{A}_{11} & \mathcal{A}_{12} & \mathcal{A}_{13} & \mathcal{A}_{14} & \mathcal{A}_{15} & \mathcal{A}_{16} & \mathcal{A}_{17} \\ \mathcal{A}_{12} & H_{11} + k^2 D_{11} & H_{12} + k^2 D_{12} & H_{13} + k^2 D_{13} & H_{14} & H_{15} & H_{16} \\ \mathcal{A}_{13} & H_{21} + k^2 D_{21} & H_{22} + k^2 D_{22} & H_{23} + k^2 D_{23} & H_{24} & H_{25} & H_{26} \\ \mathcal{A}_{14} & H_{31} + k^2 D_{31} & H_{32} + k^2 D_{32} & H_{33} + k^2 D_{33} & H_{34} & H_{35} & H_{36} \\ \mathcal{A}_{15} & H_{41} & H_{42} & H_{43} & H_{44} & H_{45} & H_{46} \\ \mathcal{A}_{16} & H_{51} & H_{52} & H_{53} & H_{54} & H_{55} & H_{56} \\ \mathcal{A}_{17} & H_{61} & H_{62} & H_{63} & H_{64} & H_{65} & H_{66} \end{bmatrix},$$

with

$$(2.56) \quad \left\{ \begin{array}{l} \mathcal{A}_{11} = \omega^2 \bar{\rho} - k^2 \left(H_{11} + \sqrt{2} H_{61} + \frac{1}{2} H_{66} \right), \\ \mathcal{A}_{12} = -jk \left(H_{11} + \frac{\sqrt{2}}{2} H_{16} \right), \\ \mathcal{A}_{13} = -jk \left(H_{12} + \frac{\sqrt{2}}{2} H_{26} \right), \\ \mathcal{A}_{14} = -jk \left(H_{13} + \frac{\sqrt{2}}{2} H_{36} \right), \\ \mathcal{A}_{15} = -jk \left(H_{14} + \frac{\sqrt{2}}{2} H_{46} \right), \\ \mathcal{A}_{16} = -jk \left(H_{15} + \frac{\sqrt{2}}{2} H_{56} \right), \\ \mathcal{A}_{17} = -jk \left(H_{16} + \frac{\sqrt{2}}{2} H_{66} \right). \end{array} \right.$$

The problem (2.53) can either be seen as a linear eigenvalue problem in ω^2 , for a given wave number k , or as a quadratic eigenvalue problem in k , for a given ω . The focus of the present work being on propagating waves travelling in elastic plates, the first formulation is used, with real wave numbers k as input. As a consequence, evanescent waves (i.e with an imaginary wave number) are discarded from the results.

The existence of non-trivial solutions to equation (2.53) implies the vanishing of the determinant of the square matrix $[\mathcal{A}]$:

$$(2.57) \quad \det[\mathcal{A}] = 0.$$

The analytical expression of the determinant of $[\mathcal{A}]$, being very lengthy, is omitted here. Nevertheless, it can be noticed that $\det[\mathcal{A}]$ is a second degree polynomial in ω of the form $a\omega^2 + b$, where a and b are functions of the wave number k . Therefore, equation (2.57) admits only two roots whose nature is determined by the sign of the quantity $-\frac{b}{a}$.

It appears through numerical calculations using Matlab that the quantity $-\frac{b}{a}$ is always positive, and that the two roots of equation (2.57) are purely real and correspond to the forward and backward flexural waves.

We shall not go into details concerning the case when $h_{\alpha\beta\gamma\delta\epsilon\zeta}$ is not definite, but we note that the dispersion relation is obtained by setting to zero the determinant of a $(m+1) \times (m+1)$ matrix, where m denotes the dimension of $\text{Im } h$, with $2 < m < 6$. For

calculation and implementation details in the case of a single layer of anisotropic material, the reader is referred to 3.6.

For ease of computing the Bending-Gradient flexural dispersion curves, a code was created using the Matlab programming language. Kindly refer to Bejjani (2019) for further details. The code is simple to use in the sense that it provides the desired results just by inputting the constitutive material properties.

2.4.2.3 Reissner-Mindlin and Kirchhoff-Love plate models

Let us recall that when the Bending-Gradient shear compliance tensor $h_{\alpha\beta\gamma\delta\epsilon\zeta}$ is of the form (2.11), the Bending-Gradient model is turned into the Reissner-Mindlin model with $f_{\alpha\beta}^R$ as shear forces compliance. In this case the flexural branches of the dispersion curve may be written as (see 3.6) :

$$(2.58) \quad \omega = \pm k \sqrt{\frac{k^4 F_{11}^R (D_{1111} D_{2121} - D_{1121}^2) + k^2 D_{1111} (F_{11}^R F_{22}^R - (F_{12}^R)^2)}{\bar{\rho} ((F_{11}^R + k^2 D_{1111}) (F_{22}^R + k^2 D_{2121}) - (F_{12}^R + k^2 D_{2111})^2)}}.$$

where $F_{\alpha\beta}^R$ is the shear stiffness tensor, inverse of the shear compliance tensor $f_{\alpha\beta}^R$.

Finally, the Kirchhoff-Love theory is obtained setting $h_{\alpha\beta\gamma\delta\epsilon\zeta} = 0$. This leads to the classical result :

$$(2.59) \quad \omega = \pm \sqrt{\frac{D_{1111}}{\bar{\rho}}} k^2.$$

2.5 Numerical Results and Verification

Having presented the wave propagation problem and the derivation of its solution, we are now in position to evaluate the effectiveness of the Bending-Gradient theory and of the shear compliance and shear stiffness projections. Generally, this evaluation is performed by comparing obtained results to reference results. The natural reference for such an assessment is the solution of the three-dimensional dynamic problem, which can be computed using the finite element method (FEM) as detailed in Section 3.3.1.2. In the following, reference results are compared to those obtained using the Classical Plate Theory (CPT), the Bending-Gradient theory (BG) as well as the Shear Compliance (SCP), the Shear Stiffness (SSP) projections and the first order shear deformation theory ($\frac{\pi^2}{12}$ -FOSDT).

Simulations reported in the present paper were performed using the calculation software Matlab. The proposed numerical method applies to any stack of layers whether the shear compliance tensor is definite or not. If the latter is the case, the reduction method presented in Section 2.3.6 is used in the calculations.

TABLE 2.1 – Elastic properties of the laminate, E and G in Pa , ρ in kg/m^3

E_L	$E_N = E_T$	$G_{LN} = G_{LT}$	G_{TN}	$\nu_{LN} = \nu_{LT} = \nu_{TN}$	ρ
1.72e+11	6.89e+09	3.45e+09	2.75e+09	0.25	2260

The analytical models presented throughout this work were applied to various laminate configurations. Below we present numerical simulations realized for a laminate whose material properties are listed in table 3.1 (Lebée and Sab, 2015; Pagano, 1969) :

The symbols E , G , ν and ρ respectively denote the Young's modulus, the shear modulus, Poisson's ratio and the density of the material. The indices L , T and N correspond respectively to the longitudinal, transversal and normal directions. Each ply of the laminate is made of unidirectional fiber-reinforced material oriented at θ relative to the bending direction x_1 . All plies have the same thickness $h = 0.01$ mm and are perfectly bounded. In the following, symmetric laminates are designated by the sequence of fiber orientations, from the outermost ply till the midplane, enclosed by brackets subscripted with an s . For instance $[0^\circ, 90^\circ]_s$ denotes a 4-ply laminate with $[0^\circ, 90^\circ, 90^\circ, 0^\circ]$.

In the figures below, the x -axis indicates the thickness-wavelength ratio (h/λ). The y -axis corresponds to the ratio (c/c_S), where c is the wave velocity and c_S denotes a normalization factor defined by Mindlin (1951) :

$$c_S = \sqrt{\frac{G_{LN}}{\rho}}.$$

In Figs. 2.2, 2.3 and 2.4 are illustrated the dispersion curves for a $[0^\circ, 90^\circ]_s$ ply, a $[-30^\circ, 30^\circ]_s$ ply and a $[0^\circ, -45^\circ, 90^\circ, 45^\circ]_s$ ply respectively. We mention that the shear compliance tensor $h_{\alpha\beta\gamma\delta\epsilon\zeta}$ of both 4-layer laminates is not definite and that the dimension of $\text{Im } h$ is equal to 4. However, when considering the 8-layer laminate, the sixth-order tensor $h_{\alpha\beta\gamma\delta\epsilon\zeta}$ is definite and therefore $\dim \text{Im } h = 6$.

The relative error is computed as follows :

$$(2.60) \quad \mathcal{E}_r = \frac{c_{\text{app}} - c_{\text{fem}}}{c_{\text{fem}}},$$

where c_{app} and c_{fem} respectively denote the approximate value and the reference value of the the wave velocity. The relative errors with respect to reference solutions computed with the finite element method (FEM) are shown in Table 2.2 for a thickness-wavelength ratio $h/\lambda = 0.3$.

It is worth noting that dispersion relations generally depend on the angle of wave propagation ψ . Taking into account ψ in the computations consists in rotating the entire

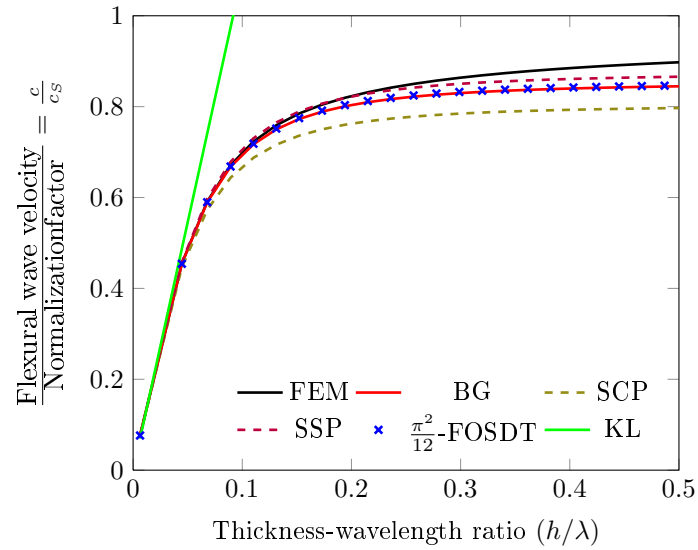


FIGURE 2.2 – Comparison of the dispersion curves for a $[0^\circ, 90^\circ]_s$ ply

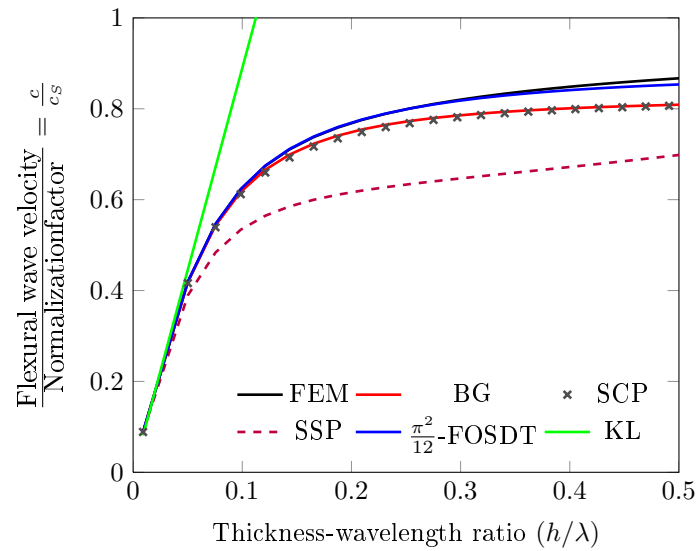
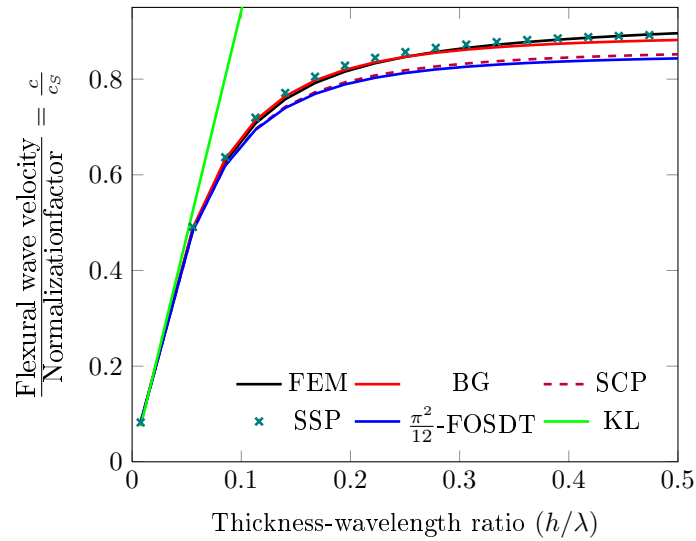


FIGURE 2.3 – Comparison of the dispersion curves for a $[-30^\circ, 30^\circ]_s$ ply

FIGURE 2.4 – Comparison of the dispersion curves for a $[0^\circ, -45^\circ, 90^\circ, 45^\circ]_s$ ply

laminate by $-\psi$. In the following, calculations on the $[0^\circ, -45^\circ, 90^\circ, 45^\circ]_s$ ply are performed for several values of ψ ($+15^\circ$, $+22^\circ$ and $+45^\circ$) and the related relative errors are set out in Table 2.3.

TABLE 2.2 – Relative error of plate models compared to finite element results with $h/\lambda = 0.3$

Laminate	KL	$\frac{\pi^2}{12}$ FOSDT	BG	SCP	SSP
$[0^\circ, 90^\circ]_s$	1.044	-0.035	-0.038	-0.091	-0.015
$[-30^\circ, 30^\circ]_s$	0.896	-0.002	-0.041	-0.046	-0.211
$[0^\circ, -45^\circ, 90^\circ, 45^\circ]_s$	0.917	-0.045	-0.006	-0.037	0.008

As is seen from Figs. 2.2, 2.3 and 2.4, when the wavelength becomes less than 10 times the plate thickness, the Kirchhoff-Love theory (KL) fails to correctly predict the dispersion curve of the flexural mode. In fact, relative errors noticed for $h/\lambda = 0.3$ are greater than 80%. This is expected since the rotatory inertia and the transverse shear deformations are supposed to be negligible (Love, 1888).

In the case of a $[0^\circ, 90^\circ]_s$ ply, one can observe on Fig. 2.2 that the results obtained with the shear stiffness projection (SSP) agree well with the reference results (FEM). Indeed, the SSP wave velocity is lower than the reference value by 1.5% approximately. The Shear stiffness projection (SSP) is clearly more efficient than the shear compliance projection (SCP), which nevertheless gives a satisfactory approximation of the solution with an error $|\mathcal{E}_r|$ that does not exceed 9.1%.

TABLE 2.3 – Relative error of plate models compared to finite element results for a $[0^\circ, -45^\circ, 90^\circ, 45^\circ]_s$ ply with $h/\lambda = 0.3$

ψ	KL	$\frac{\pi^2}{12}$ FOSDT	BG	SCP	SSP
+15°	0.935	-0.046	-0.005	-0.037	0.0029
+22°	0.960	-0.042	0.024	-0.036	0.005
+45°	1.064	0.0006	-0.024	-0.014	0.054

When considering a $[-30^\circ, 30^\circ]_s$ ply, Fig. 2.3 shows a very good accordance between the shear compliance projection (SCP) and the finite element method (FEM). In this case, the shear stiffness projection (SSP) underestimates the dispersion curve of the flexural mode by 21.1%.

For the $[0^\circ, -45^\circ, 90^\circ, 45^\circ]_s$ ply, it is evidently seen on Fig. 2.4 that the curve obtained by the shear compliance (SCP) and the shear stiffness projections (SSP) match very well the solution computed with the finite element method (FEM). The relative error $|\mathcal{E}_r|$ has a minimum value of 0.5% and a maximum value of 5% for both projections in case of all measurements (see Tables 2.2 and 2.3).

The conformity between the $\frac{\pi^2}{12}$ -FOSDT and the reference results is very good according to Figs. 2.2, 2.3 and 2.4 with a relative error that reaches a maximum of about 4.6% in absolute value for the considered examples.

Tables 2.2 and 2.3 show that the the relative error $|\mathcal{E}_r|$ of the Bending-Gradient model ranges from 0.5% to 4.1%. Such small errors result in precise approximation of the wave dispersion relation, which is illustrated in Figs. 2.2, 2.3 and 2.4.

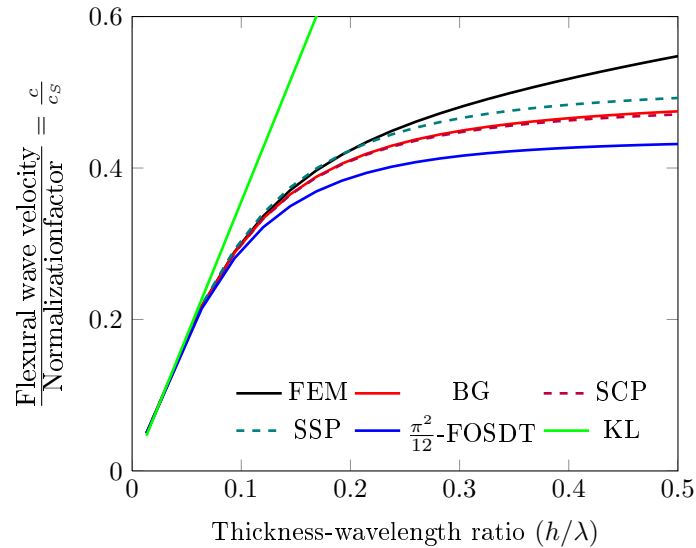
More numerical simulations were carried out to assess the validity range of the Bending-Gradient model and the Reissner-Mindlin models suggested in Section 2.3.4. For instance, we considered a multilayered plate consisting of alternate layers of the same thickness $h = 1$ mm of epoxy-glass woven composite and aluminium whose elastic properties are respectively set down in Tables 3.2 and 3.3. The sequence is $[\text{GFRP}, \text{Al}, \text{GFRP}, \text{Al}]_s$ and the GFRP material directions L, N are aligned with Directions 1 and 2.

TABLE 2.4 – Elastic properties of epoxy-glass fiber composite material Renno et al. (2013), E and G in Pa , ρ in kg/m^3

$E_L = E_T$	E_N	G_{LT}	$G_{LN} = G_{TN}$	ν_{LT}	$\nu_{LN} = \nu_{TN}$	ρ
5.40e+10	4.80e+09	3.16e+09	1.78e+09	0.06	0.31	2000

TABLE 2.5 – Elastic properties of aluminium material Liu et al. (2016), E and G in Pa , ρ in kg/m^3

E	G	ν	ρ
7.20e+10	2.67e+10	0.35	2700


 FIGURE 2.5 – Comparison of the dispersion curves for a $[GFRP, Al, GFRP, Al]_s$ ply

The obtained dispersion curves are depicted in Fig. 2.5. The relative errors with respect to finite element (FEM) solutions are given in Table 2.6 for a thickness-wavelength ratio $h/\lambda = 0.3$.

 TABLE 2.6 – Relative error of plate models compared to finite element results with $h/\lambda = 0.3$ for a $[0^\circ, 0^\circ, 90^\circ, 0^\circ]_s$ ply

Laminate	$\frac{\pi^2}{12}$ FOSDT	BG	SCP	SSP
$[0^\circ, 0^\circ, 90^\circ, 0^\circ]_s$	-0.134	-0.065	-0.069	-0.031

According to Fig. 2.5, the agreement between the $\frac{\pi^2}{12}$ -FOSDT and the reference results is poor. For a thickness-wavelength ratio $h/\lambda = 0.3$, the relative error $|\mathcal{E}_r|$ is around 13%.

It can be seen that the Bending-Gradient model (BG) and the shear compliance projection (SCP) provide good approximations of the flexural dispersion curves. The relative error $|\mathcal{E}_r|$ is lower than 7% as stated in Table 2.6.

The computed results reveal the better approximation from the shear stiffness projection (SSP) in this case. The relative error $|\mathcal{E}_r|$ is equal to 3.1% for $h/\lambda = 0.3$.

Whereas Reissner-Mindlin approximations (SCP, SSP, $\frac{\pi^2}{12}$ -FOSDT) may give very accurate estimates of the dispersion curve in some specific cases, it appears that the Bending-Gradient approximation is the most robust one. Indeed, in all cases, reasonable estimates of the wave velocity is provided.

2.6 Conclusion

In this paper, we addressed the problem of flexural wave propagation in anisotropic laminated plates by using the Bending-Gradient theory. The Bending-Gradient problem was briefly recalled and two projections on a simplified Reissner-Mindlin model were introduced : the shear compliance projection and the shear stiffness projection. The particular case of homogeneous plates, in which the Bending-Gradient model is turned into a Reissner-Mindlin model, was also discussed.

Inspired by Mindlin's paper, the dynamic problem was formulated by taking into account transverse shear deformations and neglecting rotatory inertia effects. The solution of these equations enabled the derivation of the dispersion relation connecting the angular frequency and the wave number. The analytical models were verified by comparing them to finite element solutions considered as reference solutions. Numerical simulations were conducted and it was shown that the Reissner-Mindlin models obtained by projections may yield accurate estimations of the solution in some cases. Nevertheless, it was clear that the numerical results obtained by the Bending-Gradient theory are more robust and less sensitive to the ply configuration. Though the Bending-Gradient theory seems more complicated than the Reissner-Mindlin theory, a practical, easy-to-use and publicly accessible Matlab code was created for obtaining the Bending-Gradient flexural dispersion curves.

Chapitre 3

On asymptotic expansions for modelling wave propagation in composite plates

Ce chapitre traite de la propagation des ondes dans les plaques composites infinies par le moyen de la méthode des développements asymptotiques. Cette méthode fait appel à l'utilisation d'un petit paramètre associant l'épaisseur de la plaque à la longueur d'onde. Les équations tridimensionnelles sont en premier adimensionnalisées. La solution du problème est ensuite recherchée sous forme d'un développement asymptotique en puissance croissante du petit paramètre. On présente en détails la démarche utilisée pour la résolution du problème et l'obtention des relations de dispersion des trois modes de Kirchhoff-Love. En vue de vérifier la pertinence de la méthode des développements asymptotiques, nos résultats sont enfin comparés à ceux des théories de Kirchhoff-Love, de Reissner-Mindlin, du Bending-Gradient et de la méthode des éléments finis. Ce chapitre a été soumis dans la revue Journal of Elasticity.

Abstract

This paper addresses the problem of plane wave propagation in composite plates. It explores the asymptotic expansion method and assesses its suitability and functionality. The 3D problem is first recalled and scaled by using a parameter defined as the ratio of the plate's thickness to the wave length. Assuming that the mechanical fields can be written as expansions in power of this parameter, a series of problems which can be solved recursively is obtained. Numerical results are computed and compared to those of classical and refined plate models as well as reference results obtained using the finite element method. It is found that the asymptotic expansion method can accurately predict the flexural, compressional and in-plane shear wave modes, even for large thickness-wavelength ratio, when higher orders in the expansion are used.

3.1 Introduction

Owing to their lightweight and high-performance, composite plates are being increasingly used in many engineering applications. Understanding the dynamic characteristics of such structures have hence aroused the interest of researchers over the last decade. Important investigations have been conducted by many authors such as Green (1839), B. Christoffel (1970), Rayleigh (1888), Lamb (1917) and many others.

An important tool for the analysis of wave propagation are the dispersion curves. For isotropic structures, these curves are accessible through the literature (see, e.g., Lamb (1917); Lowe (1993); Graff (1991); Miklowitz (1978); Chimenti (1997); D. D. Achenbach (1974); Mindlin (1960)). However, for composite plates, anisotropy makes the calculations more difficult and time-consuming. The simplest approaches for estimating dispersion curves of three-dimensional waves are the classical plate theory (CPT) and the first order shear deformation theory (FOSDT) which both assume that the laminate is in a state of plane stress.

The classical plate theory (CPT) is based on Kirchhoff's proposition whereby straight lines normal to the mid-plane of the plate remain straight and normal after deformation (Kirchhoff, 1850a,b; Love, 1888). The classical plate theory gives reasonably accurate results in the low frequency range, when the wavelength λ is much larger than the plate thickness h . However, enormous discrepancies with the three-dimensional solution were reported in the higher frequency range due to neglecting rotatory inertia and transverse shear effects (N. Reddy (1984), Turvey and Osman (1989, 1990, 1991)).

Reissner (1945) and Mindlin (1960) were the two pioneers to improve the estimation of transverse shear stresses by dropping Kirchhoff normality assumption. The Reissner-Mindlin theory, referred to as the first order shear deformation theory (FOSDT), assumes that the displacement field is linear within the domain and leads to a constant distribution of the transverse shear stresses across the thickness. This is inexact since the transverse shear stress function is known to be at least quadratic through the thickness. Improving the accuracy of shear stress prediction thus requires the use of a shear correction factor, which is usually set to $\frac{5}{6}$ or $\frac{\pi^2}{12}$ as proposed by Reissner and Mindlin respectively; the first being derived from static considerations, and the second being related to the out-of-plane shear wave mode cutoff frequency. For highly anisotropic plates, the shear correction factor is not always simply determined since it depends on the loadings and the stacking of the laminate (Whitney, 1991).

A vast amount of literature exists on the analysis of wave propagation in composite plates. Aiming to improve the Reissner-Mindlin model predictions, higher-order shear deformation theories were proposed by many researchers such as M. Whitney and J. Pagano (1970); Whitney and Sun (1973, 1974), Gautham and Ganesan (1992) and others Ambartsumyan (1970); Nelson and Lorch (1974); Lo et al. (1977a,b); N. Reddy (1984). The dynamic behavior of laminated plates was studied by N. Reddy (1987); Reddy (1989); N. Reddy (1997), Liu et al. (1990). In 1991, Nayfeh (1991) obtained dispersion relation curves of elastic waves propagating in anisotropic media by developing a transfer matrix

technique. Detailed review on the propagation of waves in anisotropic laminates was later given by Liu et al. (2002). In a recent work (Bejjani et al., 2019), the propagation of flexural waves in composite plates was studied using a new model, known as the Bending-Gradient theory, which is considered as an extension of the Reissner-Mindlin theory to laminated plates (Lebée and Sab, 2011). The equations of motion of the Bending-Gradient theory were formulated and dispersion relations connecting the angular frequency and the wave number were derived. Numerical results were obtained and compared to finite element results. It was shown that the Bending-Gradient theory gives a robust estimate of the dispersion curve regardless of the type of stacking and material of the laminate.

Obtaining exact analytical solutions of differential equations is often very challenging and impracticable. A common mathematical tool to solve such problems in plate-like structures is the asymptotic expansion method. This technique consists in constructing approximations to the solutions of equations through the successive terms of a power series with respect to a small parameter. Asymptotic expansions date back to the time of Poincaré (1886) and have since then received significant attention, as exemplified by the papers and books of Friedrichs and Dressler (1961), Goldenveizer (1962, 1966), Reissner and Synge (1963), G. Ciarlet (1990, 1997), Le Dret (1991) and many others. The asymptotic expansion method can be applied to both static and dynamic problems in the framework of linear and non linear elasticity aiming to find solutions for plate structures, derive 2D plate models or justify classical and refined plate theories (Arnold and Falk, 1996; G. Ciarlet, 1997; Arnold et al., 2002; Lebée and Sab, 2013).

In this paper, we use the formal asymptotic expansion method to approximate dispersion relations waves propagating in symmetrical composite plates with relatively high slenderness ratios. It is well known that the first terms in the expansions lead to the Kirchhoff-Love theory (G. Ciarlet, 1997; Dauge et al., 2017) which does not incorporate the effect of shear forces. Thus, seeking higher orders is necessary to improve the estimation of the three modes of propagation predicted by the Kirchhoff-Love theory, which are called the compressional, the in-plane shear and the flexural modes (Graff, 1991). The wavelength being much greater than the thickness of the plate, a small parameter associating both quantities is introduced. The asymptotic expansion method is based on scaling the three-dimensional problem so as to be defined on a fixed domain. The solution is then written as a series of powers of the small parameter and inserted in the general equilibrium equations. This yields a cascade of problems at different orders whose solving determines the successive approximations of the solution. The validity of the present approach is assessed by comparing the numerical results to reference results obtained by the finite element method (Margerit, 2018).

The paper begins with the notations adopted in this study (Section 3.2). In Section 3.3 are recalled the three-dimensional equations of motion for a composite plate and is presented the finite element analysis of the problem. The derivation of the plane waves dispersion curves through the asymptotic expansion method is detailed in Section 3.4. Numerical results are exploited in Section 3.5 and compared to those from the Kirchhoff-Love theory (KL), the first order shear deformation theory (FOSDT), the Bending-Gradient theory

(BG) and the finite element method (FEM). Finally, the conclusion is given in Section 3.6.

3.2 Notations

We respectively denote by $\underline{\mathbf{X}}$, $\underline{\underline{\mathbf{X}}}$, $\underline{\mathbf{X}}$, $\underline{\underline{\mathbf{X}}}$, $\underline{\underline{\underline{\mathbf{X}}}}$ first, second, third, fourth and sixth rank real tensors. Indicical notation allows us to differentiate between 2D and 3D tensors. We use Greek indices for 2D tensors ($\alpha, \beta, \gamma, \dots = 1, 2$) and Latin indices for 3D tensors ($i, j, k, \dots = 1, 2, 3$). For example, $(X_{\alpha\beta})$ represents the 2D tensor $\underline{\underline{\mathbf{X}}}$ while (X_{ij}) denotes the 3D tensor $\underline{\underline{\underline{\mathbf{X}}}}$. Index notation also provides another advantage : the number of indices indicates the order of the tensor. For example, (X_{ij}) denotes the second-rank tensor $\underline{\underline{\mathbf{X}}}$ whereas (X_{ijkl}) denotes the fourth-rank tensor $\underline{\underline{\underline{\mathbf{X}}}}$. To simplify expressions including tensors, we shall make use of the Einstein summation convention according to which all indices appearing twice within an expression are to be summed.

The transpose operation T is applied to any order tensors as follows : $({}^T X)_{\alpha\beta\dots\psi\omega} = X_{\omega\psi\dots\beta\alpha}$. Four symbols are defined : (\cdot) , $(:)$, $(\dot{:})$ and $(\ddot{:})$ for contraction on, respectively, one, two, three and four indices. By convention, the closest indices are successively summed together in contraction products. Thus, $\underline{\underline{\mathbf{X}}} : \underline{\underline{\mathbf{Y}}} = (X_{\alpha\beta\gamma\delta\lambda\mu} Y_{\mu\lambda\delta})$ and $\underline{\underline{\mathbf{X}}} \cdot \underline{\underline{\mathbf{Y}}} = (X_{\alpha\beta\gamma} Y_{\gamma})$ is different from $\underline{\underline{\mathbf{Y}}} \cdot \underline{\underline{\mathbf{X}}} = (Y_{\alpha} X_{\alpha\beta\gamma})$.

The identity for 2D vectors is $\underline{\underline{\delta}} = (\delta_{\alpha\beta})$ where $\delta_{\alpha\beta}$ is Kronecker symbol ($\delta_{\alpha\beta} = 1$ if $\alpha = \beta$, $\delta_{\alpha\beta} = 0$ otherwise). The identity for 2D symmetric second order tensors is $\underline{\underline{\mathbf{i}}}$ where $\underline{\underline{\mathbf{i}}}_{\alpha\beta\gamma\delta} = \frac{1}{2} (\delta_{\alpha\gamma}\delta_{\beta\delta} + \delta_{\alpha\delta}\delta_{\beta\gamma})$. The reader might easily check that $\underline{\underline{\mathbf{i}}} : \underline{\underline{\mathbf{i}}} = \underline{\underline{\mathbf{i}}}$, $\underline{\underline{\mathbf{i}}} : \underline{\underline{\mathbf{i}}} = 3/2 \underline{\underline{\delta}}$ and $\underline{\underline{\mathbf{i}}} \dot{:} \underline{\underline{\mathbf{i}}} = 3$.

The gradient of a scalar field X writes $\underline{\underline{\nabla}} X = (X_{,\beta})$ while the gradient of a vector or a higher-order tensor fields writes $\underline{\underline{\mathbf{X}}} \otimes \underline{\underline{\nabla}} = (X_{\alpha\beta,\gamma})$, for instance, where \otimes is the dyadic product. The divergence of a vector field or a second order tensor field is noted $\underline{\underline{\mathbf{X}}} \cdot \underline{\underline{\nabla}} = (X_{\alpha,\alpha})$ and $\underline{\underline{\mathbf{X}}} \cdot \underline{\underline{\nabla}} = (X_{\alpha\beta,\beta})$, respectively.

3.3 Propagation of plane waves in composite plates

3.3.1 Exact dispersion curves for guided waves

3.3.1.1 Three-dimensional equations of motion

The physical space is endowed with an orthonormal reference frame $(O, \underline{\mathbf{e}}_1, \underline{\mathbf{e}}_2, \underline{\mathbf{e}}_3)$ where O is the origin and $\underline{\mathbf{e}}_i$ is the base vector in direction $i \in \{1, 2, 3\}$. We consider an unbounded composite elastic plate occupying the 3D domain $V = \mathbb{R}^2 \times]-\frac{h}{2}, \frac{h}{2}[$, where h is the

thickness of the plate. The composite plate is assumed to be symmetrical with respect to the midplane.

In this work, we consider the propagation of waves in direction 1. The displacement vector, denoted by $\underline{\mathbf{u}}$, is thus a function of the coordinates (x_1, x_3) and of the time t :

$$(3.1) \quad \underline{\mathbf{u}} = (u_i)_{i=1,2,3} = \underline{\mathbf{u}}(x_1, x_3, t).$$

The displacement vector $\underline{\mathbf{u}}$ satisfies the basic equation of motion in the absence of body forces, which writes :

$$(3.2) \quad \underline{\boldsymbol{\sigma}} \cdot \underline{\nabla} - \rho(x_3) \underline{\ddot{\mathbf{u}}} = 0 \quad \text{or} \quad \sigma_{ij,j} - \rho(x_3) \ddot{u}_i = 0,$$

where $\underline{\boldsymbol{\sigma}}$ designates the stress tensor and ρ the density (mass per unit volume). The two dots above a variable are used to denote the second derivative with respect to time ($\ddot{x} = \frac{d^2x}{dt^2}$).

We denote by $\underline{\underline{\mathbf{C}}}$ the stiffness tensor which describes the properties of the constitutive material at every point $\underline{\mathbf{x}} = (x_1, x_2, x_3)$. In the following, each layer of the composite plate is considered to be monoclinic. Namely,

$$C_{3\alpha\beta\gamma} = C_{\alpha 333} = 0.$$

Due to plane symmetry, the fourth order tensor $\underline{\underline{\mathbf{C}}}$ and the density ρ are even functions of x_3 :

$$(3.3) \quad \underline{\underline{\mathbf{C}}}(-x_3) = \underline{\underline{\mathbf{C}}}(x_3) \quad \text{and} \quad \rho(-x_3) = \rho(x_3).$$

We recall that the tensor $\underline{\underline{\mathbf{C}}}$ obeys minor ($C_{ijkl} = C_{jikl} = C_{ijlk}$) and major ($C_{ijkl} = C_{klij}$) symmetries. The elasticity tensor is positive definite and its inverse, denoted by $\underline{\underline{\mathbf{S}}}$, is called the compliance tensor. $\underline{\underline{\mathbf{S}}}$ follows the same classical symmetries as $\underline{\underline{\mathbf{C}}}$.

The constitutive equation which connects the stress $\underline{\boldsymbol{\sigma}}$ to the strain $\underline{\boldsymbol{\varepsilon}}$ may be written as :

$$(3.4) \quad \underline{\boldsymbol{\sigma}} - \underline{\underline{\mathbf{C}}}(x_3) : \underline{\boldsymbol{\varepsilon}} = 0.$$

The strain-displacement relations read :

$$(3.5) \quad \underline{\boldsymbol{\varepsilon}} - \frac{1}{2}(\underline{\mathbf{u}} \otimes \underline{\nabla} + \underline{\nabla} \otimes \underline{\mathbf{u}}) = 0.$$

To complete the description, we must associate boundary conditions on the top and bottom boundaries of the plate :

$$(3.6) \quad \underline{\boldsymbol{\sigma}} \cdot \underline{\mathbf{e}}_3 = 0 \quad \text{at} \quad x_3 = \pm \frac{h}{2}$$

In addition, the stress vector $\underline{\sigma} \cdot \underline{e}_3$ and the displacement vector \underline{u} must be continuous at the interfaces between the different layers of the plate.

In summary, the three-dimensional equations of motion for an infinite composite elastic plate are :

$$\begin{aligned}
 (3.7a) \quad & \underline{\sigma} \cdot \underline{\nabla} - \rho(x_3) \underline{\ddot{u}} = 0, \\
 (3.7b) \quad & \underline{\sigma} - \underline{\underline{C}}(x_3) : \underline{\underline{\varepsilon}} = 0, \\
 (3.7c) \quad & \underline{\underline{\varepsilon}} - \frac{1}{2}(\underline{u} \otimes \underline{\nabla} + \underline{\nabla} \otimes \underline{u}) = 0, \\
 (3.7d) \quad & \underline{\sigma} \cdot \underline{e}_3 = 0 \text{ at } x_3 = \pm \frac{h}{2}.
 \end{aligned}$$

Particular solutions to the above equations are plane waves, which are of peculiar importance since it can be shown that any other solution to (3.7) can be described as a superposition of plane waves. The displacement \underline{u} at a time t and a distance x_1 due to a plane wave can be mathematically described in exponential form as :

$$(3.8) \quad \underline{u} = (u_i)_{i=1,2,3} = \underline{u}(x_1, x_3, t) = \Re(\hat{\underline{u}}(x_3) e^{j(\omega t - kx_1)}),$$

where $\hat{\underline{u}} = (\hat{u}_i)_{i=1,2,3}$ is a vector associated to the amplitudes of displacement, ω is the angular frequency, $k \neq 0$ is the wave number and j the imaginary unit. The symbol $\Re(z)$ is used to designate the real part of the complex number z . We denote by λ the wavelength and c the wave velocity. We recall that the wave number is related to the wavelength through :

$$(3.9) \quad k = \frac{2\pi}{\lambda},$$

and that the phase velocity c is expressed as :

$$(3.10) \quad c = \frac{\omega}{k}.$$

Our main purpose is to relate the angular frequency ω to the wave number k such that there exists a non-zero vector $\hat{\underline{u}}$ satisfying the three-dimensional equations of motion (3.7). This relationship between ω and k is commonly displayed in graphs called dispersion curves. These curves supply key information on the propagation characteristics of wave modes.

One of the most popular tools for modelling wave propagation in elastic media is the finite element method (FEM) whose procedure is detailed below. The corresponding numerical results are considered as reference solutions of the 3D problem (3.7).

3.3.1.2 Resolution by means of Finite Element Analysis

Injecting the plane wave displacement (3.8) in the local equations (3.7) leads to the formulation of a quadratic eigenvalue problem in both wavenumber k and frequency ω that has to be solved. In the case of homogeneous isotropic plates, it can be reduced to the well known Lamb modes transcendental equation (Lamb, 1917). The case of laminated plates has been first investigated by T. Thomson (1950), who expressed the inter-lamina continuity conditions with the help of *transfer matrices*. As a consequence of the numerical instability of the method (Haskell, 1953), several reformulations has been proposed in the following decades (Schmidt and Tango, 2007; Nayfeh, 1991; Rokhlin and Wang, 2002).

Alternatively, the variationnal formulation of the problem (integral equations) can be used (Dong and B. Nelson, 1972; Datta et al., 1988; Xi et al., 2000). The finite element approach then leads to the following eigenvalue problem :

$$(3.11) \quad \left(k^2 [K_2] + jk [K_1] + [K_0] - \omega^2 [\mathbb{M}] \right) [\mathbb{U}] = \underline{\mathbf{0}},$$

where $[K_i]$, $i = 1, 2, 3$ and $[\mathbb{M}]$ are symmetric hermitian matrices and $[\mathbb{U}]$ is the vector of nodal displacements. This formulation is usually referred as the Spectral Finite Element Method (J. Shorter, 2004; Barbieri et al., 2009) (SFEM) or Semi-Analytical Finite Element method (Bartoli et al., 2006) (SAFE). The preceding eigenvalue problem is solved more easily by searching the eigenfrequencies related to a given wavenumber. However, it is often more convenient to search for the wavenumber solutions corresponding to a fixed frequency; this can be performed by the resolution of the associated quadratic eigenvalue problem, giving both real and imaginary solutions (resp. denoting propagating and evanescent waves).

This method has been implemented here to compute reference solutions to the problem of wave propagation in composite plates. Linear elements were used. In the wavelength range of interest, it has been observed that 10 elements by layer was sufficient to avoid convergence issues.

3.4 The asymptotic expansion method

3.4.1 The asymptotic expansion framework

In this section, we perform the asymptotic analysis (Sanchez-Palencia, 1980) of the dynamic problem (3.7). Simplifications due to material and geometrical symmetries of the plate are first investigated. The three-dimensional equations (3.7) are then scaled and the properties of the new dimensionless fields are presented. We thereafter develop asymptotic expansions of the fields in powers of a small parameter introduced in the following.

3.4.1.1 Scaling

In order to apply the asymptotic expansion method, we need first to scale system (3.7) so that all computed quantities are of relatively similar magnitudes. It is hence convenient to make the following change of variables

$$(3.12) \quad z = \frac{x_3}{h}, \quad z \in \left[-\frac{1}{2}, \frac{1}{2}\right].$$

According to this change of variables, the stiffness tensor can be rewritten as :

$$\underset{\approx}{\mathbf{C}}(x_3) = \underset{\approx}{\mathbf{C}}(h^{-1}x_3) = \underset{\approx}{\mathbf{C}}(z),$$

where $\underset{\approx}{\mathbf{C}}$ is a function of z .

Furthermore, from the field $\hat{\mathbf{u}} = (\hat{u}_i)_{i=1,2,3}$, we define the non-dimensional field $\underline{\mathbf{v}} = (v_i)_{i=1,2,3}$ as follows :

$$(3.13) \quad \hat{\mathbf{u}} = k^{-1}\underline{\mathbf{v}}\left(\frac{x_3}{h}\right) = k^{-1}\underline{\mathbf{v}}(z).$$

The following non-dimensional parameter is naturally introduced :

$$(3.14) \quad k^* = hk = \frac{2\pi h}{\lambda}.$$

Using (3.13) and injecting (3.8) into equation (3.7)c, simple algebraic manipulations yield :

$$(3.15) \quad \underline{\boldsymbol{\varepsilon}} = \Re\left(\hat{\underline{\boldsymbol{\varepsilon}}}(z)e^{i(\omega t - kx_1)}\right),$$

where $\hat{\underline{\boldsymbol{\varepsilon}}}$ is expressed in terms of the non-dimensional field $\underline{\mathbf{v}}$ and the parameter k^* through :

$$(3.16) \quad \hat{\underline{\boldsymbol{\varepsilon}}}(z) = \begin{pmatrix} -iv_1(z) & -\frac{1}{2}iv_2(z) & -\frac{1}{2}iv_3(z) + \frac{1}{2}k^{*-1}v'_1(z) \\ -\frac{1}{2}iv_2(z) & 0 & \frac{1}{2}k^{*-1}v'_2(z) \\ -\frac{1}{2}iv_3(z) + \frac{1}{2}k^{*-1}v'_1(z) & \frac{1}{2}k^{*-1}v'_2(z) & k^{*-1}v'_3(z) \end{pmatrix}.$$

Here, f' designates the derivative of the function f with respect to z ($f' = \frac{df}{dz}$).

Similarly, we obtain through equation (3.7)b that the stress tensor $\boldsymbol{\sigma}$ can be written as :

$$(3.17) \quad \boldsymbol{\sigma} = \Re\left(\hat{\boldsymbol{\sigma}}(z)e^{i(\omega t - kx_1)}\right),$$

where $\hat{\boldsymbol{\sigma}}$ is given by :

$$(3.18) \quad \hat{\boldsymbol{\sigma}}(z) = \underset{\approx}{\mathbf{C}}(z) : \hat{\underline{\boldsymbol{\varepsilon}}}(z).$$

Finally, the equations of motion (3.7) can be restated in terms of the parameter k^* and the fields v_i , $\hat{\varepsilon}_{ij}$ and $\hat{\sigma}_{ij}$ as follows :

$$\begin{aligned}
 (3.19a) & \quad -i\hat{\sigma}_{11}(z) + k^{*-1}\hat{\sigma}'_{13}(z) + \rho c^2 v_1(z) = 0, \\
 (3.19b) & \quad -i\hat{\sigma}_{12}(z) + k^{*-1}\hat{\sigma}'_{23}(z) + \rho c^2 v_2(z) = 0, \\
 (3.19c) & \quad -i\hat{\sigma}_{13}(z) + k^{*-1}\hat{\sigma}'_{33}(z) + \rho c^2 v_3(z) = 0, \\
 (3.19d) & \quad \hat{\boldsymbol{\sigma}}(z) = \underset{\sim}{\mathbb{C}}(z) : \underset{\sim}{\boldsymbol{\varepsilon}}(z), \\
 (3.19e) & \quad \hat{\varepsilon}_{11}(z) = -iv_1(z), \\
 (3.19f) & \quad \hat{\varepsilon}_{12}(z) = -\frac{1}{2}iv_2(z), \\
 (3.19g) & \quad \hat{\varepsilon}_{13}(z) = -\frac{1}{2}iv_3(z) + \frac{1}{2}k^{*-1}v'_1(z), \\
 (3.19h) & \quad \hat{\varepsilon}_{22}(z) = 0, \\
 (3.19i) & \quad \hat{\varepsilon}_{23}(z) = \frac{1}{2}k^{*-1}v'_2(z), \\
 (3.19j) & \quad \hat{\varepsilon}_{33}(z) = k^{*-1}v'_3(z), \\
 (3.19k) & \quad \hat{\sigma}_{13} = \hat{\sigma}_{23} = \hat{\sigma}_{33} = 0 \text{ at } z = \pm\frac{1}{2}.
 \end{aligned}$$

It is crucial to note that $\hat{\sigma}_{i3}$ and v_i , $i = 1, 2, 3$, must be continuous at the interfaces between the different layers of the plate.

The fields \mathbb{C} and ρ being given, the problem consists in expressing the phase velocity squared c^2 in terms of the normalized wave number k^* in order to approximate the solution of the problem (3.19).

3.4.1.2 Expansion

We now proceed to perform an asymptotic analysis (Sanchez-Palencia, 1980; Sanchez-Hubert and Sanchez-Palencia, 1992) of the scaled problem (3.19). To this aim, the displacement $\underline{\mathbf{v}}$, the strain $\underset{\sim}{\boldsymbol{\varepsilon}}$ and the stress $\hat{\boldsymbol{\sigma}}$ are expanded in terms of the parameter k^* as follows :

$$(3.20a) \quad \begin{cases} \underline{\mathbf{v}} = k^{*-1}\underline{\mathbf{v}}^{-1} + k^{*0}\underline{\mathbf{v}}^0 + k^{*1}\underline{\mathbf{v}}^1 + \dots \\ \underset{\sim}{\boldsymbol{\varepsilon}} = k^{*0}\underset{\sim}{\boldsymbol{\varepsilon}}^0 + k^{*1}\underset{\sim}{\boldsymbol{\varepsilon}}^1 + \dots \\ \hat{\boldsymbol{\sigma}} = k^{*0}\hat{\boldsymbol{\sigma}}^0 + k^{*1}\hat{\boldsymbol{\sigma}}^1 + \dots \end{cases}$$

where $\underline{\mathbf{v}}^p$, $\underset{\sim}{\boldsymbol{\varepsilon}}^p$ and $\hat{\boldsymbol{\sigma}}^p$, $p = -1, 0, 1, 2, \dots$ are functions of z which have the following properties :

- v_3^p , $\hat{\sigma}_{\alpha 3}^p$ and $\hat{\varepsilon}_{\alpha 3}^p$ are null for even p and even in z for odd p .
- v_α^p , $\hat{\sigma}_{\alpha\beta}^p$, $\hat{\sigma}_{33}^p$, $\hat{\varepsilon}_{\alpha\beta}^p$ and $\hat{\varepsilon}_{33}^p$ are null for odd p and odd in z for even p .

The series are started from the order k^{*-1} for $\underline{\mathbf{v}}$ and from the order k^{*0} for $\hat{\underline{\boldsymbol{\varepsilon}}}$ and $\hat{\underline{\boldsymbol{\sigma}}}$. We note that the choice of the value of the starting order has no influence on the final results.

With that said, it is interesting to highlight that by making the change of variables $k^* \rightarrow -k^*$, $v_3 \rightarrow -v_3$, $(v_1, v_2) \rightarrow (v_1, v_2)$, equations (3.19) still hold true with the same value of the phase velocity c . This means that c , v_1 and v_2 are even functions of k^* , and v_3 is an odd function of k^* .

Consequently, the in-plane strain $\hat{\varepsilon}_{\alpha\beta}$ and stress $\hat{\sigma}_{\alpha\beta}$, the normal strain $\hat{\varepsilon}_{33}$ and stress $\hat{\sigma}_{33}$ are even in k^* , whereas the transverse shear strain $\hat{\varepsilon}_{\alpha 3}$ and stress $\hat{\sigma}_{\alpha 3}$ are odd in k^* .

Using the above properties, we can express the phase velocity squared c^2 , the out-of-plane displacement v_3 and the in-plane displacements v_α in terms of k^* respectively as :

$$(3.21) \quad c^2 = \alpha_0 + \alpha_2 k^{*2} + \alpha_4 k^{*4} + \dots,$$

$$(3.22) \quad v_3 = v_3^{-1} k^{*-1} + v_3^1 k^* + v_3^3 k^{*3} + \dots,$$

and

$$(3.23) \quad v_\alpha = v_\alpha^0 k^{*0} + v_\alpha^2 k^{*2} + v_\alpha^4 k^{*4} + \dots$$

In the above equations, α_{2p} , v_3^{2p-1} , v_α^{2p} , $p = 0, 1, 2, \dots$, designate unknown constants to be determined in the following.

It obviously follows from equations (3.22) and (3.23) that for any $p \geq 0$, the displacement fields $\underline{\mathbf{v}}^{2p-1}$ and $\underline{\mathbf{v}}^{2p}$ can be expressed as :

$$(3.24) \quad \underline{\mathbf{v}}^{2p-1} = \begin{pmatrix} 0 \\ 0 \\ v_3^{2p-1} \end{pmatrix}, \quad \underline{\mathbf{v}}^{2p} = \begin{pmatrix} v_1^{2p} \\ v_2^{2p} \\ 0 \end{pmatrix}.$$

3.4.2 Cascade resolution

The asymptotic expansion method leads to a sequence of differential problems which we are about to solve order by order (Caillerie and Nedelec, 1984; Lewinski, 1991).

Since the series are started from the order k^{*0} for $\hat{\underline{\boldsymbol{\varepsilon}}}$, we indeed have :

$$(3.25) \quad \hat{\underline{\boldsymbol{\varepsilon}}}^{-2} = 0 \quad \text{and} \quad \hat{\underline{\boldsymbol{\varepsilon}}}^{-1} = 0.$$

Equation (3.25) implies that :

$$(3.26) \quad \hat{\varepsilon}_{33}^{-2} = (v_3^{-1})' = 0,$$

and

$$(3.27a) \quad \begin{cases} \hat{\varepsilon}_{13}^{-1} = -\frac{1}{2}iv_3^{-1} + \frac{1}{2}v_1^{0'} = 0, \end{cases}$$

$$(3.27b) \quad \begin{cases} \hat{\varepsilon}_{23}^{-1} = \frac{1}{2}v_2^{0'} = 0. \end{cases}$$

From (3.26), it is deduced that v_3^{-1} is a uniform function of z . We write :

$$v_3^{-1} = V_3^{-1}.$$

Here and in the following, capital letters are used to indicate uniform functions of z . Equations (3.27)a and (3.27)b respectively imply :

$$(3.28) \quad v_1^0 = V_1^0 + iV_3^{-1}z,$$

and

$$(3.29) \quad v_2^0 = V_2^0.$$

Hence, \underline{v}^{-1} and \underline{v}^0 can be written as :

$$(3.30) \quad \underline{v}^{-1} = \begin{pmatrix} 0 \\ 0 \\ V_3^{-1} \end{pmatrix}, \quad \underline{v}^0 = \begin{pmatrix} V_1^0 + iV_3^{-1}z \\ V_2^0 \\ 0 \end{pmatrix}.$$

In order to study the dynamic equations (3.19)a, (3.19)b and (3.19)c, we start by expanding the expressions of c^2v_α and c^2v_3 using (3.21), (3.22) and (3.23) :

$$(3.31) \quad \begin{cases} c^2v_\alpha = k^{*0}(\alpha_0v_\alpha^0) + k^{*2}(\alpha_2v_\alpha^0 + \alpha_0v_\alpha^2) + k^{*4}(\alpha_4v_\alpha^0 + \alpha_2v_\alpha^2 + \alpha_0v_\alpha^4) + \dots \\ c^2v_3 = k^{*-1}(\alpha_0v_3^{-1}) + k^{*1}(\alpha_2v_3^{-1} + \alpha_0v_3^1) + k^{*3}(\alpha_4v_3^{-1} + \alpha_2v_3^1 + \alpha_0v_3^3) + \dots \end{cases}$$

Injecting the above expressions in equations (3.19)a, (3.19)b and (3.19)c leads for $p = 0, 1, 2, \dots$ to :

$$(3.32a) \quad \begin{cases} -i\hat{\sigma}_{11}^{2p} + (\hat{\sigma}_{13}^{2p+1})' + \rho(\alpha_{2p}v_1^0 + \alpha_{2p-2}v_1^2 + \dots + \alpha_0v_1^{2p}) = 0, \\ -i\hat{\sigma}_{12}^{2p} + (\hat{\sigma}_{23}^{2p+1})' + \rho(\alpha_{2p}v_2^0 + \alpha_{2p-2}v_2^2 + \dots + \alpha_0v_2^{2p}) = 0, \\ -i\hat{\sigma}_{13}^{2p-1} + (\hat{\sigma}_{33}^{2p})' + \rho(\alpha_{2p}v_3^{-1} + \alpha_{2p-2}v_3^1 + \dots + \alpha_0v_3^{2p-1}) = 0. \end{cases}$$

We also have that :

$$(3.33a) \quad \begin{cases} \hat{\varepsilon}_{11}^{2p} = -iv_1^{2p}, \\ \hat{\varepsilon}_{12}^{2p} = -iv_2^{2p}, \\ \hat{\varepsilon}_{13}^{2p-1} = -iv_3^{2p-1} + (v_1^{2p})', \\ \hat{\varepsilon}_{22}^{2p} = 0, \\ \hat{\varepsilon}_{23}^{2p-1} = (v_2^{2p})', \\ \hat{\varepsilon}_{33}^{2p} = (v_3^{2p+1})', \\ \hat{\varepsilon}_{\alpha 3}^{2p} = 0, \\ \hat{\varepsilon}_{\alpha\beta}^{2p-1} = \hat{\varepsilon}_{33}^{2p-1} = 0. \end{cases}$$

Integrating equations (3.32) with respect to z and using boundary conditions (3.19)k, we obtain :

$$\begin{aligned} (3.34a) \quad & -iN_{11}^{2p} + \alpha_{2p} \langle \rho v_1^0 \rangle + \dots + \alpha_0 \langle \rho v_1^{2p} \rangle = 0, \\ (3.34b) \quad & -iN_{12}^{2p} + \alpha_{2p} \langle \rho v_2^0 \rangle + \dots + \alpha_0 \langle \rho v_2^{2p} \rangle = 0, \\ (3.34c) \quad & -iQ_1^{2p-1} + \alpha_{2p} \langle \rho v_3^{-1} \rangle + \dots + \alpha_0 \langle \rho v_3^{2p-1} \rangle = 0, \end{aligned}$$

where $\langle \bullet \rangle$ is used to denote the integration with respect to z : $\langle f \rangle = \int_{-\frac{1}{2}}^{\frac{1}{2}} f(z) dz$, $N_{\alpha\beta}^{2p}$ is the normalized membrane stress defined as :

$$N_{\alpha\beta}^{2p} = \langle \hat{\sigma}_{\alpha\beta}^{2p} \rangle,$$

and Q_α^{2p-1} is the normalized shear force given by :

$$Q_\alpha^{2p-1} = \langle \hat{\sigma}_{\alpha 3}^{2p} \rangle.$$

Multiplying equation (3.32)a by z and integrating with respect to z yield :

$$(3.35) \quad -iM_{11}^{2p} - Q_1^{2p+1} + \alpha_{2p} \langle \rho z v_1^0 \rangle + \dots + \alpha_0 \langle \rho z v_1^{2p} \rangle = 0,$$

where $M_{\alpha\beta}^{2p}$ represents the normalized bending moment defined as :

$$M_{\alpha\beta}^{2p} = \langle z \hat{\sigma}_{\alpha\beta}^{2p} \rangle.$$

Substituting p for $p + 1$ in equation (3.34)c yields :

$$(3.36) \quad -iQ_1^{2p+1} + \alpha_{2p+2} \langle \rho v_3^{-1} \rangle + \dots + \alpha_0 \langle \rho v_3^{2p+1} \rangle = 0.$$

By multiplying equation (3.35) by the imaginary unit i and equation (3.36) by -1 , then we obtain after summation :

$$(3.37) \quad M_{11}^{2p} + i\alpha_{2p} \langle \rho z v_1^0 \rangle + \dots + i\alpha_0 \langle \rho z v_1^{2p} \rangle - \alpha_{2p+2} \langle \rho v_3^{-1} \rangle - \dots - \alpha_0 \langle \rho v_3^{2p+1} \rangle = 0.$$

Gathering equations (3.34)a, (3.34)b and (3.37), integrability conditions write :

$$\begin{aligned} (3.38a) \quad & -iN_{11}^{2p} + \alpha_{2p} \langle \rho v_1^0 \rangle + \dots + \alpha_0 \langle \rho v_1^{2p} \rangle = 0, \\ (3.38b) \quad & -iN_{12}^{2p} + \alpha_{2p} \langle \rho v_2^0 \rangle + \dots + \alpha_0 \langle \rho v_2^{2p} \rangle = 0, \\ (3.38c) \quad & M_{11}^{2p} + i\alpha_{2p} \langle \rho z v_1^0 \rangle + \dots + i\alpha_0 \langle \rho z v_1^{2p} \rangle - \alpha_{2p+2} \langle \rho v_3^{-1} \rangle - \dots - \alpha_0 \langle \rho v_3^{2p+1} \rangle = 0. \end{aligned}$$

It is important to note that for $p = 0$, equation (3.34)c implies that

$$(3.39) \quad \alpha_0 V_3^{-1} = 0.$$

Therefore, it can be easily seen through (3.32)c that

$$(\hat{\sigma}_{33}^0)' = 0.$$

Using boundary conditions (3.19)k, we deduce that :

$$\hat{\sigma}_{33}^0 = 0.$$

Since $\hat{\sigma}_{\alpha 3}^0 = \hat{\sigma}_{33}^0 = 0$, the plate is in plane stress at the order 0. In this case, the constitutive law at this order writes :

$$\hat{\sigma}_{\alpha\beta}^0 = \mathcal{C}_{\alpha\beta\gamma\delta}^\sigma \hat{\varepsilon}_{\gamma\delta}^0,$$

where $\mathcal{C}_{\alpha\beta\gamma\delta}^\sigma = \mathcal{C}_{\alpha\beta\gamma\delta} - \frac{\mathcal{C}_{\alpha\beta 33} \mathcal{C}_{33\gamma\delta}}{\mathcal{C}_{3333}}$ denotes the plane-stress elasticity tensor.

Moreover, we have that :

$$(3.40) \quad \hat{\varepsilon}_{\alpha\beta}^0 = \begin{pmatrix} -i(V_1^0 + iV_3^{-1}z) & -\frac{1}{2}iV_2^0 \\ -\frac{1}{2}iV_2^0 & 0 \end{pmatrix} = \tilde{\mathbf{E}}^0 + z\tilde{\boldsymbol{\chi}}^0.$$

Here, $\tilde{\mathbf{E}}^0$ represents the plate in-plane strain field given by :

$$(3.41) \quad \tilde{\mathbf{E}}^0 = \begin{pmatrix} -iV_1^0 & -\frac{1}{2}iV_2^0 \\ -\frac{1}{2}iV_2^0 & 0 \end{pmatrix},$$

and $\tilde{\boldsymbol{\chi}}^0$ designates the curvature strain field given by :

$$(3.42) \quad \tilde{\boldsymbol{\chi}}^0 = \begin{pmatrix} V_3^{-1} & 0 \\ 0 & 0 \end{pmatrix}.$$

In terms of components, the plate constitutive law has the following form :

$$(3.43) \quad \begin{pmatrix} N_{11}^0 \\ N_{12}^0 \\ M_{11}^0 \end{pmatrix} = \begin{pmatrix} A_{11} & A_{13} & 0 \\ A_{13} & A_{33} & 0 \\ 0 & 0 & D_{11} \end{pmatrix} \cdot \begin{pmatrix} E_{11}^0 \\ 2E_{12}^0 \\ \chi_{11}^0 \end{pmatrix},$$

where

$$\begin{pmatrix} A_{11} & A_{13} \\ A_{13} & A_{33} \end{pmatrix} = \begin{pmatrix} \langle \mathcal{C}_{1111}^\sigma \rangle & \langle \mathcal{C}_{1112}^\sigma \rangle \\ \langle \mathcal{C}_{1112}^\sigma \rangle & \langle \mathcal{C}_{1212}^\sigma \rangle \end{pmatrix},$$

and

$$D_{11} = \langle z^2 \mathcal{C}_{1111}^\sigma \rangle.$$

In view of equation (3.39), one can deduce that either $\alpha_0 \neq 0$ and $V_3^{-1} = 0$ or $\alpha_0 = 0$ and $V_3^{-1} \neq 0$. Both cases are treated in the sequel.

3.4.2.1 The case of in-plane membranal waves : $\alpha_0 \neq 0$ and $V_3^{-1} = 0$

Zeroth-order problem ($p = 0$).

For $p = 0$, system (3.38) writes :

$$\begin{aligned} (3.44a) \quad & -iN_{11}^0 + \alpha_0 \langle \rho v_1^0 \rangle = 0, \\ (3.44b) \quad & -iN_{12}^0 + \alpha_0 \langle \rho v_2^0 \rangle = 0, \\ (3.44c) \quad & M_{11}^0 + i\alpha_0 \langle \rho z v_1^0 \rangle - \alpha_0 \langle \rho v_3^1 \rangle = 0. \end{aligned}$$

Equations (3.44)a and (3.44)b can be written as an eigenvalue problem :

$$(3.45) \quad \begin{pmatrix} A_{11} & A_{13} \\ A_{13} & A_{33} \end{pmatrix} \cdot \begin{pmatrix} V_1^0 \\ V_2^0 \end{pmatrix} = \alpha_0 \langle \rho \rangle \begin{pmatrix} V_1^0 \\ V_2^0 \end{pmatrix}.$$

Being symmetric and positive definite, the matrix A has two eigenvalues A_1 and A_2 which are real and strictly positive. Moreover, there exists two associated eigenvectors $\underline{\mathbf{X}}_1$ and $\underline{\mathbf{X}}_2$ forming an orthonormal basis in \mathbb{R}^2 . Two cases arise from (3.45) :

$$(3.46) \quad \alpha_0 = \frac{A_1}{\langle \rho \rangle} \text{ or } \alpha_0 = \frac{A_2}{\langle \rho \rangle}.$$

In the remainder of the paper, we shall assume that $\alpha_0 = \frac{A_1}{\langle \rho \rangle}$, the other case follows analogously. As a consequence, the vector $\underline{\mathbf{V}}^0 = \begin{pmatrix} V_1^0 \\ V_2^0 \end{pmatrix}$ is collinear to the eigenvector $\underline{\mathbf{X}}_1$.

Recalling that $\hat{\sigma}_{33}^0 = 0$, the constitutive law implies :

$$(3.47) \quad \hat{\varepsilon}_{33}^0 = -\frac{C_{1133}}{C_{3333}} \hat{\varepsilon}_{11}^0 - 2\frac{C_{1233}}{C_{3333}} \hat{\varepsilon}_{12}^0$$

Using equation (3.33)f, it can be found that the displacement field v_3^1 has the following form :

$$(3.48) \quad v_3^1 = \bar{v}_3^1 + V_3^1,$$

where \bar{v}_3^1 is given by :

$$(3.49) \quad \bar{v}_3^1 = \mathbb{P}(\hat{\varepsilon}_{33}^0).$$

Here, $\mathbb{P}(f)$ designates the unique primitive of the function f such that $\langle \mathbb{P}(f) \rangle = 0$ (see Appendix 3.6 for computational details). As for V_3^1 , it can be determined through equation (3.44)c :

$$(3.50) \quad V_3^1 = \frac{M_{11}^0 + i\alpha_0 \langle \rho z v_1^0 \rangle - \alpha_0 \langle \rho \bar{v}_3^1 \rangle}{\alpha_0 \langle \rho \rangle}.$$

The density ρ being even in z implies that

$$\langle \rho z v_1^0 \rangle = 0,$$

as we have that $v_\alpha^0 = V_\alpha^0$. Hence,

$$(3.51) \quad V_3^1 = -\frac{\langle \rho \bar{v}_3^1 \rangle}{\langle \rho \rangle}.$$

Equations (3.32)a and (3.32)b allow us to write :

$$(3.52) \quad (\hat{\sigma}_{\alpha 3}^1)' = i\hat{\sigma}_{1\alpha}^0 - \rho\alpha_0 v_\alpha^0.$$

Thus, using the boundary conditions $\hat{\sigma}_{\alpha 3}^1(\pm\frac{1}{2}) = 0$, the transverse shear stresses $\hat{\sigma}_{\alpha 3}^1$ are given by :

$$(3.53) \quad \hat{\sigma}_{\alpha 3}^1 = \mathbb{Q}(i\hat{\sigma}_{1\alpha}^0 - \rho\alpha_0 v_\alpha^0),$$

where $\mathbb{Q}(f) = \int_{-\frac{1}{2}}^z f(y)dy$ (see Appendix 3.6 for computational details).

The constitutive law and equation (3.33)c yield :

$$(3.54) \quad \begin{aligned} 2\hat{\varepsilon}_{13}^1 &= 4\mathcal{S}_{3131}\hat{\sigma}_{31}^1 + 4\mathcal{S}_{2331}\hat{\sigma}_{23}^1 \\ &= -iv_3^1 + (v_1^2)', \end{aligned}$$

which implies that :

$$(3.55) \quad \begin{aligned} v_1^2 &= \mathbb{P}(2\hat{\varepsilon}_{13}^1 + iv_3^1) + V_1^2 + izV_3^1 \\ &= \bar{v}_1^2 + V_1^2 + izV_3^1. \end{aligned}$$

Likewise, we write :

$$(3.56) \quad \begin{aligned} 2\hat{\varepsilon}_{23}^1 &= 4\mathcal{S}_{2331}\hat{\sigma}_{31}^1 + 4\mathcal{S}_{2323}\hat{\sigma}_{23}^1 \\ &= (v_2^2)'. \end{aligned}$$

Therefore,

$$(3.57) \quad \begin{aligned} v_2^2 &= \mathbb{P}(2\hat{\varepsilon}_{23}^1) + V_2^2 \\ &= \bar{v}_2^2 + V_2^2. \end{aligned}$$

Determining the unknown constants V_α^2 requires solving the first-order problem ($p = 1$).

First-order problem ($p = 1$).

It is easy to check that through boundary conditions $\hat{\sigma}_{33}^2(\pm\frac{1}{2}) = 0$, equation (3.32)c reduces to :

$$(3.58) \quad \hat{\sigma}_{33}^2 = \mathbb{Q} (i\hat{\sigma}_{13}^1 - \rho\alpha_0 v_3^1).$$

For $p = 1$, system (3.38) writes :

$$(3.59a) \quad \begin{cases} -iN_{11}^2 + \alpha_2 \langle \rho v_1^0 \rangle + \alpha_0 \langle \rho v_1^2 \rangle = 0, \\ -iN_{12}^2 + \alpha_2 \langle \rho v_2^0 \rangle + \alpha_0 \langle \rho v_2^2 \rangle = 0, \\ M_{11}^2 + i\alpha_2 \langle \rho z v_1^0 \rangle + i\alpha_0 \langle \rho z v_1^2 \rangle - \alpha_2 \langle \rho v_3^1 \rangle - \alpha_0 \langle \rho v_3^3 \rangle = 0. \end{cases}$$

To make notations clear, we write :

$$(3.60a) \quad \begin{cases} \hat{\varepsilon}_{11}^2 = -iv_1^2 = -i\bar{v}_1^2 - iV_1^2 + zV_3^1 = \bar{\varepsilon}_{11}^2 + E_{11}^2 + z\chi_{11}^2, \\ 2\hat{\varepsilon}_{12}^2 = -iv_2^2 = -i\bar{v}_2^2 - iV_2^2 = 2\bar{\varepsilon}_{12}^2 + E_{12}^2. \end{cases}$$

Hence, $\hat{\sigma}_{1\alpha}^2$ are expressed as :

$$(3.61) \quad \begin{aligned} \hat{\sigma}_{1\alpha}^2 &= \mathcal{C}_{111\alpha}^\sigma \hat{\varepsilon}_{11}^2 + 2\mathcal{C}_{1\alpha 12}^\sigma \hat{\varepsilon}_{12}^2 + \frac{\mathcal{C}_{1\alpha 33}}{\mathcal{C}_{3333}} \hat{\sigma}_{33}^2 \\ &= \mathcal{C}_{111\alpha}^\sigma (E_{11}^2 + z\chi_{11}^2) + \mathcal{C}_{1\alpha 12}^\sigma E_{12}^2 + \bar{\sigma}_{1\alpha}^2, \end{aligned}$$

with

$$(3.62) \quad \bar{\sigma}_{1\alpha}^2 = \mathcal{C}_{111\alpha}^\sigma \bar{\varepsilon}_{11}^2 + 2\mathcal{C}_{1\alpha 12}^\sigma \bar{\varepsilon}_{12}^2 + \frac{\mathcal{C}_{1\alpha 33}}{\mathcal{C}_{3333}} \hat{\sigma}_{33}^2.$$

Therefore,

$$(3.63) \quad \begin{pmatrix} N_{11}^2 \\ N_{12}^2 \end{pmatrix} = \begin{pmatrix} A_{11} & A_{13} \\ A_{13} & A_{33} \end{pmatrix} \cdot \begin{pmatrix} -iV_1^2 \\ -iV_2^2 \end{pmatrix} + \begin{pmatrix} \bar{N}_{11}^2 \\ \bar{N}_{12}^2 \end{pmatrix},$$

where

$$(3.64) \quad \bar{N}_{1\alpha}^2 = \langle \bar{\sigma}_{1\alpha}^2 \rangle.$$

Using short notation, equations (3.59)a and (3.59)b can be rewritten as :

$$(3.65) \quad \underline{\mathbf{A}} \cdot \underline{\mathbf{V}}^2 - \alpha_0 \langle \rho \rangle \underline{\mathbf{V}}^2 = \alpha_2 \langle \rho \rangle \underline{\mathbf{V}}^0 + \underline{\mathbf{U}}^2,$$

where $\underline{\mathbf{U}}_\alpha^2$ are given by :

$$(3.66) \quad \underline{\mathbf{U}}_\alpha^2 = -i\bar{N}_{1\alpha}^2 + \alpha_0 \langle \rho \bar{v}_\alpha^2 \rangle.$$

Recalling that $(\underline{\mathbf{X}}_1, \underline{\mathbf{X}}_2)$ forms an orthonormal basis in \mathbb{R}^2 , the vector $\underline{\mathbf{V}}^2$ can be expressed as a linear combination of $\underline{\mathbf{X}}_1$ and $\underline{\mathbf{X}}_2$:

$$\underline{\mathbf{V}}^2 = a_1 \underline{\mathbf{X}}_1 + a_2 \underline{\mathbf{X}}_2, \quad a_1, a_2 \in \mathbb{R}.$$

Injecting the above expression in equation (3.65) yields :

$$a_2 (A_2 - A_1) \underline{\mathbf{X}}_2 = \alpha_2 \langle \rho \rangle \underline{\mathbf{V}}^0 + \underline{\mathbf{U}}^2.$$

It follows that the right side term of equation (3.65) and $\underline{\mathbf{V}}^2$ are collinear to $\underline{\mathbf{X}}_2$. Consequently, α_2 is given by :

$$(3.67) \quad \alpha_2 = - \frac{(\underline{\mathbf{U}}^2, \underline{\mathbf{X}}_1)}{\langle \rho \rangle (\underline{\mathbf{V}}^0, \underline{\mathbf{X}}_1)},$$

and $\underline{\mathbf{V}}^2$ is expressed as :

$$(3.68) \quad \underline{\mathbf{V}}^2 = \frac{1}{A_2 - A_1} (\alpha_2 \langle \rho \rangle \underline{\mathbf{V}}^0 + \underline{\mathbf{U}}^2) = \frac{1}{A_2 - A_1} \left(\underline{\mathbf{U}}^2 - \frac{(\underline{\mathbf{U}}^2, \underline{\mathbf{X}}_1)}{(\underline{\mathbf{V}}^0, \underline{\mathbf{X}}_1)} \underline{\mathbf{V}}^0 \right),$$

where (\cdot, \cdot) denotes the usual scalar product of \mathbb{R}^2 .

Since $\|\underline{\mathbf{X}}_1\| = 1$, we clearly have that :

$$(3.69) \quad \frac{\underline{\mathbf{V}}^0}{(\underline{\mathbf{V}}^0, \underline{\mathbf{X}}_1)} = \underline{\mathbf{X}}_1.$$

Thus, $\underline{\mathbf{V}}^2$ writes :

$$(3.70) \quad \underline{\mathbf{V}}^2 = \frac{1}{A_2 - A_1} [\underline{\mathbf{U}}^2 - (\underline{\mathbf{U}}^2, \underline{\mathbf{X}}_1) \underline{\mathbf{X}}_1].$$

Normal strains $\hat{\varepsilon}_{33}^2$ are obtained through the constitutive law and equation (3.33)f :

$$(3.71) \quad \begin{aligned} \hat{\varepsilon}_{33}^2 &= \frac{\hat{\sigma}_{33}^2}{\mathcal{C}_{3333}} - \frac{\mathcal{C}_{3311}}{\mathcal{C}_{3333}} \hat{\varepsilon}_{11}^2 - 2 \frac{\mathcal{C}_{3312}}{\mathcal{C}_{3333}} \hat{\varepsilon}_{12}^2 \\ &= (v_3^3)'. \end{aligned}$$

Consequently, the displacement field v_3^3 writes as :

$$(3.72) \quad v_3^3 = \mathbb{P}(\hat{\varepsilon}_{33}^2) + V_3^3 = \bar{v}_3^3 + V_3^3,$$

where the constant V_3^3 is determined from equation (3.59)c :

$$(3.73) \quad V_3^3 = \frac{M_{11}^2 + i\alpha_0 \langle \rho z v_1^2 \rangle - \alpha_2 \langle \rho v_3^1 \rangle - \alpha_0 \langle \rho \bar{v}_3^3 \rangle}{\alpha_0 \langle \rho \rangle}.$$

From equations (3.32)a and (3.32)b and the boundary conditions $\hat{\sigma}_{\alpha 3}^3(\pm\frac{1}{2}) = 0$, it follows that :

$$(3.74) \quad \hat{\sigma}_{\alpha 3}^3 = \mathbb{Q}(i\hat{\sigma}_{1\alpha}^2 - \rho(\alpha_2 v_\alpha^0 + \alpha_0 v_\alpha^2)).$$

Since $\hat{\varepsilon}_{\alpha 3}^3$ are expressed in terms of $\hat{\sigma}_{\alpha 3}^3$ as :

$$(3.75) \quad 2\hat{\varepsilon}_{\alpha 3}^3 = 4\mathcal{S}_{\alpha 3\beta 3}\hat{\sigma}_{\beta 3}^3,$$

equations (3.33)c and (3.33)f yield :

$$(3.76a) \quad \begin{cases} v_1^4 = \bar{v}_1^4 + V_1^4 + izV_3^3, \\ v_2^4 = \bar{v}_2^4 + V_2^4, \end{cases}$$

where \bar{v}_α^4 are given by :

$$(3.77a) \quad \begin{cases} \bar{v}_1^4 = \mathbb{P}(2\hat{\varepsilon}_{13}^3 + i\bar{v}_3^3), \\ \bar{v}_2^4 = \mathbb{P}(2\hat{\varepsilon}_{13}^3), \end{cases}$$

and V_α^4 are obtained by going one order higher in the expansion ($p = 2$).

Higher-order problems ($p \geq 2$).

It is clearly possible to carry out a recursive approximation of the solution to higher orders. This section is dedicated to suggest a computational algorithm for evaluating the unknown fields v_α^{2p} , v_3^{2p-1} , α_{2+} and $\hat{\sigma}_{33}^{2p}$ for any order $p \geq 2$.

Using (3.32)c and boundary conditions $\hat{\sigma}_{33}^{2p}(\pm\frac{1}{2}) = 0$ yields :

$$(3.78) \quad \hat{\sigma}_{33}^{2p} = \mathbb{Q}(i\hat{\sigma}_{13}^{2p-1} - \rho(\alpha_{2p-2}v_3^1 + \dots + \alpha_0v_3^{2p-1})).$$

Equations (3.38)a and (3.38)b write :

$$(3.79) \quad \underline{\mathbf{A}} \cdot \underline{\mathbf{V}}^{2p} - \alpha_0 \langle \rho \rangle \underline{\mathbf{V}}^{2p} = \alpha_{2p} \langle \rho \rangle \underline{\mathbf{V}}^0 + \underline{\mathbf{U}}^{2p},$$

where $\underline{\mathbf{U}}_\alpha^{2p}$ is given by :

$$(3.80) \quad \underline{\mathbf{U}}_\alpha^{2p} = -i\bar{N}_{1\alpha}^{2p} + \alpha_{2p-2} \langle \rho v_\alpha^2 \rangle + \dots + \alpha_0 \langle \rho \bar{v}_\alpha^{2p} \rangle.$$

Following the same procedure as the previous section, α_{2p} and $\underline{\mathbf{V}}^{2p}$ are respectively given by :

$$(3.81) \quad \alpha_{2p} = -\frac{(\underline{\mathbf{U}}^{2p}, \underline{\mathbf{X}}_1)}{\langle \rho \rangle (\underline{\mathbf{V}}^0, \underline{\mathbf{X}}_1)},$$

and

$$(3.82) \quad \underline{V}^{2p} = \frac{1}{A_2 - A_1} [\underline{U}^{2p} - (\underline{U}^{2p} \underline{X}_1, \underline{X}_1)].$$

Equation (3.33)f together with the constitutive law imply :

$$(3.83) \quad \begin{aligned} \hat{\varepsilon}_{33}^{2p} &= \frac{1}{C_{3333}} \hat{\sigma}_{33}^{2p} - \frac{C_{1133}}{C_{3333}} \hat{\varepsilon}_{11}^{2p} - 2 \frac{C_{1233}}{C_{3333}} \hat{\varepsilon}_{12}^{2p} \\ &= (v_3^{2p+1})'. \end{aligned}$$

Consequently, the displacement field v_3^{2p+1} writes as :

$$(3.84) \quad v_3^{2p+1} = \mathbb{P}(\hat{\varepsilon}_{33}^{2p}) + V_3^{2p+1} = \bar{v}_3^{2p+1} + V_3^{2p+1}.$$

V_3^{2p+1} is determined through equation (3.38)c by :

$$(3.85) \quad V_3^{2p+1} = \frac{M_{11}^{2p} + i\alpha_{2p-2} \langle \rho z v_1^2 \rangle + \dots + i\alpha_0 \langle \rho z v_1^{2p} \rangle - \alpha_{2p} \langle \rho v_3^1 \rangle - \dots - \alpha_0 \langle \rho \bar{v}_3^{2p+1} \rangle}{\alpha_0 \langle \rho \rangle}.$$

Let us now determine $\hat{\sigma}_{\alpha 3}^{2p+1}$. Using (3.32)a and (3.32)b and the boundary conditions $\hat{\sigma}_{\alpha 3}^{2p+1}(\pm \frac{1}{2}) = 0$, we obtain :

$$(3.86) \quad \hat{\sigma}_{\alpha 3}^{2p+1} = \mathbb{Q}(i\hat{\sigma}_{1\alpha}^{2p} - \rho(\alpha_{2p} v_\alpha^0 + \dots + \alpha_0 v_\alpha^{2p})).$$

Through the constitutive law, the transverse shear strains $\hat{\varepsilon}_{\alpha 3}^{2p+1}$ write :

$$(3.87) \quad 2\hat{\varepsilon}_{\alpha 3}^{2p+1} = 4\mathcal{S}_{\alpha 3\beta 3} \hat{\sigma}_{\alpha 3}^{2p+1}.$$

Thus, we have that :

$$(3.88a) \quad \begin{cases} v_1^{2(p+1)} = \bar{v}_1^{2(p+1)} + V_1^{2(p+1)} + izV_3^{2p+1}, \\ v_2^{2(p+1)} = \bar{v}_2^{2(p+1)} + V_2^{2(p+1)}, \end{cases}$$

$$(3.88b)$$

where $\bar{v}_\alpha^{2(p+1)}$ are known and given by :

$$(3.89a) \quad \begin{cases} \bar{v}_1^{2(p+1)} = \mathbb{P}(2\hat{\varepsilon}_{13}^{2p+1} + i\bar{v}_3^{2p+1}), \\ \bar{v}_2^{2(p+1)} = \mathbb{P}(2\hat{\varepsilon}_{23}^{2p+1}). \end{cases}$$

$$(3.89b)$$

In order to determine $V_\alpha^{2(p+1)}$, we need to go further in the expansion.

3.4.2.2 The case of flexural (or bending) waves : $\alpha_0 = 0$ and $V_3^{-1} \neq 0$

Zeroth-order problem ($p = 0$).

For $p = 0$, equations (3.38) become :

$$\begin{aligned} (3.90\text{a}) & & & \begin{cases} -iN_{11}^0 = 0, \\ -iN_{12}^0 = 0, \\ M_{11}^0 - \alpha_2 V_3^{-1} \langle \rho \rangle = 0. \end{cases} \\ (3.90\text{b}) & & & \\ (3.90\text{c}) & & & \end{aligned}$$

Equations (3.90)a and (3.90)b can be rewritten as :

$$(3.91) \quad \begin{pmatrix} A_{11} & A_{13} \\ A_{13} & A_{33} \end{pmatrix} \cdot \begin{pmatrix} V_1^0 \\ V_2^0 \end{pmatrix} = 0.$$

Since $\underline{\mathbf{A}}$ is positive definite, we obtain that :

$$(3.92) \quad \begin{pmatrix} V_1^0 \\ V_2^0 \end{pmatrix} = \begin{pmatrix} 0 \\ 0 \end{pmatrix}.$$

Equation (3.90)c can be written as :

$$(3.93) \quad (D_{11} - \alpha_2 \langle \rho \rangle) V_3^{-1} = 0$$

for any $V_3^{-1} \neq 0$. We hence have that :

$$(3.94) \quad \alpha_2 = \frac{D_{11}}{\langle \rho \rangle}.$$

In view of equation (3.33) and the constitutive law, the normal strain $\hat{\varepsilon}_{33}^0$ is expressed as :

$$(3.95) \quad \begin{aligned} \hat{\varepsilon}_{33}^0 &= (v_3^1)' \\ &= -\frac{\mathcal{C}_{3311}}{\mathcal{C}_{3333}} \hat{\varepsilon}_{11}^0. \end{aligned}$$

It is therefore deduced that :

$$(3.96) \quad v_3^1 = \bar{v}_3^1 + V_3^1,$$

where $\bar{v}_3^1 = \mathbb{P}(\hat{\varepsilon}_{33}^0)$ and V_3^1 is a constant to be determined in the following.

According to equations (3.32)a and (3.32)b for $p = 0$, transverse shear stresses $\hat{\sigma}_{\alpha 3}^1$ are given by :

$$(3.97) \quad \hat{\sigma}_{\alpha 3}^1 = \mathbb{Q}(i\hat{\sigma}_{1\alpha}^0).$$

Transverse shear strains $\hat{\varepsilon}_{\alpha 3}^1$ are then obtained through :

$$(3.98) \quad 2\hat{\varepsilon}_{\alpha 3}^1 = 4\mathcal{S}_{\alpha 3\beta 3} \hat{\sigma}_{\beta 3}^1.$$

By identification with (3.33)c and (3.33)e, we get :

$$(3.99a) \quad \begin{cases} v_1^2 = \bar{v}_1^2 + V_1^2 + izV_3^1, \\ (3.99b) \quad v_2^2 = \bar{v}_2^2 + V_2^2, \end{cases}$$

where \bar{v}_α^2 are given by :

$$(3.100a) \quad \begin{cases} \bar{v}_1^2 = \mathbb{P}(2\hat{\varepsilon}_{13}^1 + i\bar{v}_3^1), \\ (3.100b) \quad \bar{v}_2^2 = \mathbb{P}(2\hat{\varepsilon}_{23}^1), \end{cases}$$

and V_α^2 are constants identified afterwards.

First-order problem ($p = 1$).

The stress field $\hat{\sigma}_{33}^2$ is obtained through equation (3.32)c :

$$(3.101) \quad \hat{\sigma}_{33}^2 = \mathbb{Q}(i\hat{\sigma}_{13}^1 - \alpha_2 V_3^{-1} \rho).$$

Equations (3.38)a and (3.38)b write as :

$$(3.102) \quad \begin{pmatrix} A_{11} & A_{13} \\ A_{13} & A_{33} \end{pmatrix} \cdot \begin{pmatrix} V_1^2 \\ V_2^2 \end{pmatrix} = \begin{pmatrix} -i\bar{N}_{11}^2 \\ -i\bar{N}_{12}^2 \end{pmatrix}.$$

The constants V_α^2 are easily obtained through equations (3.102).

α_4 is derived using equation (3.38)c :

$$(3.103) \quad \alpha_4 = \frac{\bar{M}_{11}^2 + i\alpha_2 \langle \rho z v_1^0 \rangle - \alpha_2 V_3^{-1} \langle \rho \bar{v}_3^1 \rangle}{V_3^{-1} \langle \rho \rangle}.$$

Due to (3.94), α_4 can be clearly computed regardless of the value taken by V_3^1 . This also applies to the rest of the cascade, which means that we can calculate α_{2p} whatever the value taken by V_3^{2p-1} for any order p . In fact, taking arbitrary values of V_3^{2p-1} , $p \geq 1$ in our Matlab code Bejjani (2019) does not affect the final results. For this reason, we shall assume hereafter that V_3^{2p-1} is equal to zero for all $p \geq 1$.

Likewise the previous section, the field v_3^3 writes :

$$(3.104) \quad v_3^3 = \bar{v}_3^3 = \mathbb{P}(\hat{\varepsilon}_{33}^2).$$

Equations (3.32)a and (3.32)b imply that :

$$(3.105) \quad \hat{\sigma}_{\alpha 3}^3 = \mathbb{Q}(i\hat{\sigma}_{1\alpha}^2 - \rho\alpha_2 v_\alpha^0).$$

The fields $\hat{\sigma}_{\alpha 3}^3$ fully identified, the strains $\hat{\varepsilon}_{\alpha 3}^3$ write :

$$(3.106) \quad 2\hat{\varepsilon}_{\alpha 3}^3 = 4\mathcal{S}_{\alpha 3\beta 3}\hat{\sigma}_{\beta 3}^3.$$

By identification with (3.33)c and (3.33)e, we obtain the expression of v_α^4 :

$$(3.107) \quad v_\alpha^4 = \bar{v}_\alpha^4 + V_\alpha^4,$$

where \bar{v}_α^4 are given by :

$$(3.108a) \quad \begin{cases} \bar{v}_1^4 = \mathbb{P}(2\hat{\varepsilon}_{13}^3 + iv_3^3), \\ \bar{v}_2^4 = \mathbb{P}(2\hat{\varepsilon}_{23}^3), \end{cases}$$

and V_α^4 are determined by solving the second-order problem ($p = 2$).

Higher-order problems ($p \geq 2$).

One of the advantages of the asymptotic expansion method is that it allows to obtain the expressions of $\hat{\sigma}_{33}^{2p}$, V_α^{2p} , α_{2p+2} , v_3^{2p+1} and v_α^{2p+2} for any order p from computed fields for orders q ranging from 0 to $p - 1$.

Equation (3.32)c enables the derivation of the stress fields $\hat{\sigma}_{33}^{2p}$:

$$(3.109) \quad \hat{\sigma}_{33}^{2p} = \mathbb{Q}(i\hat{\sigma}_{13}^{2p-1} - \rho(\alpha_{2p}V_3^{-1} + \dots + \alpha_2v_3^{2p-3})).$$

Exactly as for the zeroth and first-order problems, the expressions of V_α^{2p} follow from using equations (3.38)a and (3.38)b and thus solving :

$$(3.110) \quad \begin{pmatrix} A_{11} & A_{13} \\ A_{13} & A_{33} \end{pmatrix} \cdot \begin{pmatrix} V_1^{2p} \\ V_2^{2p} \end{pmatrix} = \begin{pmatrix} -i\bar{N}_{11}^{2p} + \alpha_{2p}\langle\rho v_1^0\rangle + \dots + \alpha_2\langle\rho v_1^{2p-2}\rangle \\ -i\bar{N}_{12}^{2p} + \alpha_{2p}\langle\rho v_2^0\rangle + \dots + \alpha_2\langle\rho v_2^{2p-2}\rangle \end{pmatrix}.$$

Making use of equation (3.38)c gives :

$$(3.111) \quad \alpha_{2p+2} = \frac{M_{11}^{2p} + i\alpha_{2p}\langle\rho z v_1^0\rangle + \dots + i\alpha_2\langle\rho z v_1^{2p-2}\rangle - \alpha_{2p}\langle\rho v_3^1\rangle - \dots - \alpha_2\langle\rho v_3^{2p-1}\rangle}{V_3^{-1}\langle\rho\rangle}.$$

We now proceed to obtain the expression of v_3^{2p+1} using equation (3.33)f which writes :

$$(3.112) \quad \hat{\varepsilon}_{33}^{2p} = (v_3^{2p+1})'$$

, and the constitutive law :

$$(3.113) \quad \hat{\varepsilon}_{33}^{2p} = \frac{1}{\mathcal{C}_{3333}}\hat{\sigma}_{33}^{2p} - \frac{\mathcal{C}_{3311}}{\mathcal{C}_{3333}}\hat{\varepsilon}_{11}^{2p} - 2\frac{\mathcal{C}_{3312}}{\mathcal{C}_{3333}}\hat{\varepsilon}_{12}^{2p}.$$

It follows that :

$$(3.114) \quad v_3^{2p+1} = \bar{v}_3^{2p+1} = \mathbb{P}(\hat{\varepsilon}_{33}^{2p}).$$

Finally, we aim to determine v_α^{2p+2} . By equations (3.32)a and (3.32)b ,we can write :

$$(3.115) \quad \hat{\sigma}_{\alpha 3}^{2p+1} = \mathbb{Q} (i\hat{\sigma}_{1\alpha}^{2p} - \rho (\alpha_{2p} v_\alpha^0 + \alpha_{2p-2} v_1^2 + \dots + \alpha_2 v_\alpha^{2p-2})).$$

Using the constitutive law, the strain fields $\hat{\varepsilon}_{\alpha 3}^{2p+1}$ are given by :

$$(3.116) \quad 2\hat{\varepsilon}_{\alpha 3}^{2p+1} = 4\mathcal{S}_{\alpha 3\beta 3}\hat{\sigma}_{\beta 3}^{2p+1}.$$

Hence, we have :

$$(3.117) \quad v_\alpha^{2p+2} = \bar{v}_\alpha^{2p+2} + V_\alpha^{2p+2},$$

where \bar{v}_α^{2p+2} write :

$$(3.118a) \quad \left\{ \begin{array}{l} \bar{v}_1^{2p+2} = \mathbb{P} (2\hat{\varepsilon}_{13}^{2p+1} + i v_3^{2p+1}), \\ \bar{v}_2^{2p+2} = \mathbb{P} (2\hat{\varepsilon}_{23}^{2p+1}), \end{array} \right.$$

$$(3.118b)$$

and V_α^{2p+2} are obtained sequentially.

We draw the reader's attention that a code allowing the computation of the dispersion curves, corresponding to the three wave modes, through Matlab is available at Bejjani (2019).

3.5 Numerical results

We now turn to explore the capability of the constructed expansion in providing good approximations of dispersion relations of the longitudinal, in-plane shear and flexural wave modes propagating in composite plates. To this aim, comparisons between the asymptotic expansion method, the Kirchhoff-Love theory and the finite element method are established with the help of the mathematical calculation software MATLAB. Flexural dispersion curves are particularly compared to the Bending-Gradient theory (Appendix 3.6) and the First Order Shear Deformation theory corrected by the factor $\frac{\pi^2}{12}$.

Numerical simulations presented hereafter are realized for a $[0^\circ, 90^\circ]_s$ ply, a $[-30^\circ, 30^\circ]_s$ ply and a $[0^\circ, -45^\circ, 90^\circ, 45^\circ]_s$ ply. The index S , for symmetric, means that the angles between square brackets correspond to half of the stack, the other half being symmetrical with respect to the midplane of the plate. All plies have the same thickness and they are perfectly bounded. The constitutive material of the laminates is characterized by :

The symbols E , G , ν and ρ respectively denote the Young's modulus, the shear modulus, Poisson's ratio and the density of the material. The indices L , T and N correspond respectively to the longitudinal, transversal and normal directions. Each ply of the laminate is made of unidirectional fiber-reinforced material oriented at θ relative to the bending direction x_1 .

TABLE 3.1 – Elastic properties of the laminate, E and G in Pa , ρ in kg/m^3 (Lebée and Sab, 2015; Pagano, 1969)

E_L	$E_N = E_T$	$G_{LN} = G_{LT}$	G_{TN}	$\nu_{LN} = \nu_{LT} = \nu_{TN}$	ρ
1.72e+11	6.89e+09	3.45e+09	2.75e+09	0.25	2260

TABLE 3.2 – Elastic properties of epoxy-glass fiber composite material, E and G in Pa , ρ in kg/m^3 (Renno et al., 2013)

$E_L = E_T$	E_N	G_{LT}	$G_{LN} = G_{TN}$	ν_{LT}	$\nu_{LN} = \nu_{TN}$	ρ
5.40e+10	4.80e+09	3.16e+09	1.78e+09	0.06	0.31	2000

Further simulations are performed for a multilayered plate consisting of alternate layers having the same thickness of epoxy-glass woven composite and aluminium whose elastic properties are respectively set down in Tables 3.2 and 3.3. The sequence is [GFRP, Al, GFRP, Al]_s and the GFRP material directions L, N are aligned with directions 1 and 2.

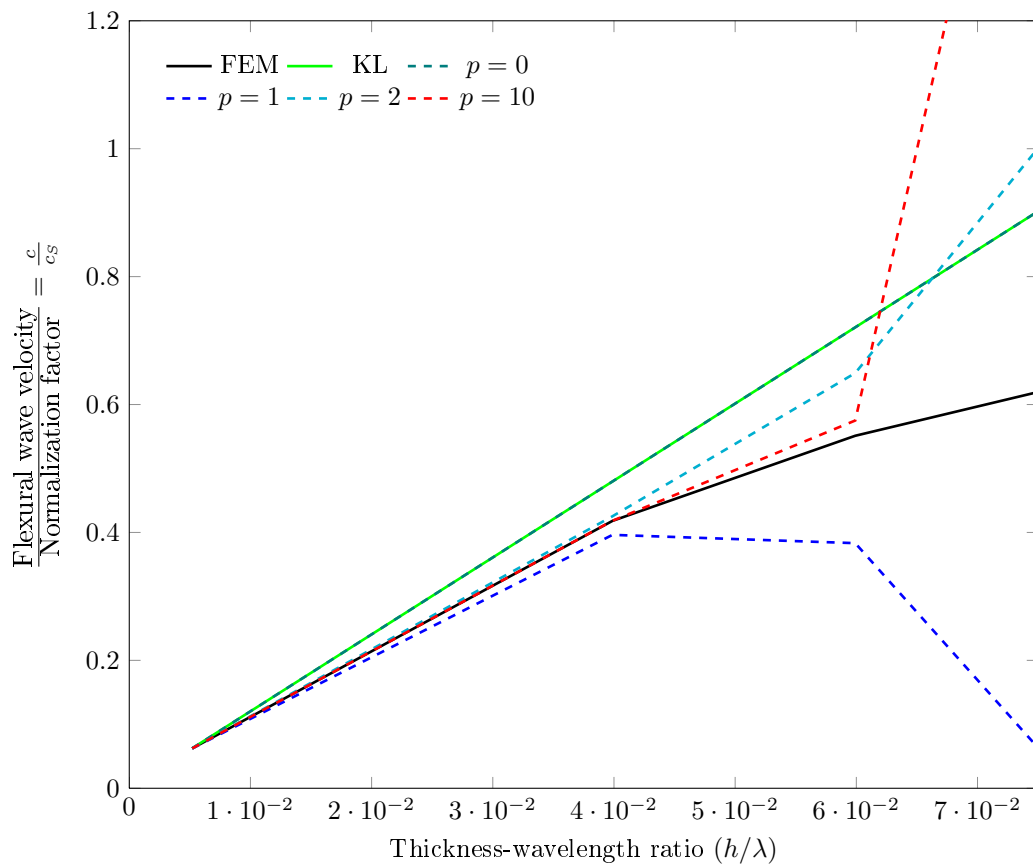
In the figures below, the x -axis indicates the thickness-wavelength ratio (h/λ). The y -axis corresponds to the ratio (c/c_S), where c is the wave velocity and c_S denotes a normalization factor defined by Mindlin (1951) :

$$c_S = \sqrt{\frac{G_{LN}}{\rho}}.$$

The Kirchhoff-Love, the Bending-Gradient and the finite element curves are plotted as solid lines. The blue "x" markers are used to show the first-order shear deformation theory ($\frac{\pi^2}{12}$ -FOSDT) results. The asymptotic approximations are described by dashed lines.

3.5.1 Flexural waves

Flexural dispersion curves are obtained by solving the sequence of problems for $\alpha_0 = 0$. A comparison between calculated values and reference values showed that the convergence radius of the asymptotic expansion (3.21) is small enough. It can be clearly seen on figure 3.1 for example that the asymptotic series clearly diverges for $h/\lambda > 0.06$. Interestingly, this problem was solved as follows. Using Lagrange (1770) inversion theorem (see Appendix 3.6 for more details), we expressed the Taylor expansion of k^{*2} in terms of c^2 from the knowledge of the Taylor expansion of c^2 in terms of k^{*2} which is given through the asymptotic expansion method. Then we checked the convergence of the Taylor expansion of k^{*2} in terms of c^2 for all our numerical applications. Finally, we took the inverse functions of the truncated series as approximations of the flexural dispersion curves and we plotted them in figures 3.2, 3.3, 3.4 and 3.5.

FIGURE 3.1 – Comparison of the flexural dispersion curves for a $[0^\circ, 90^\circ]_s$ ply

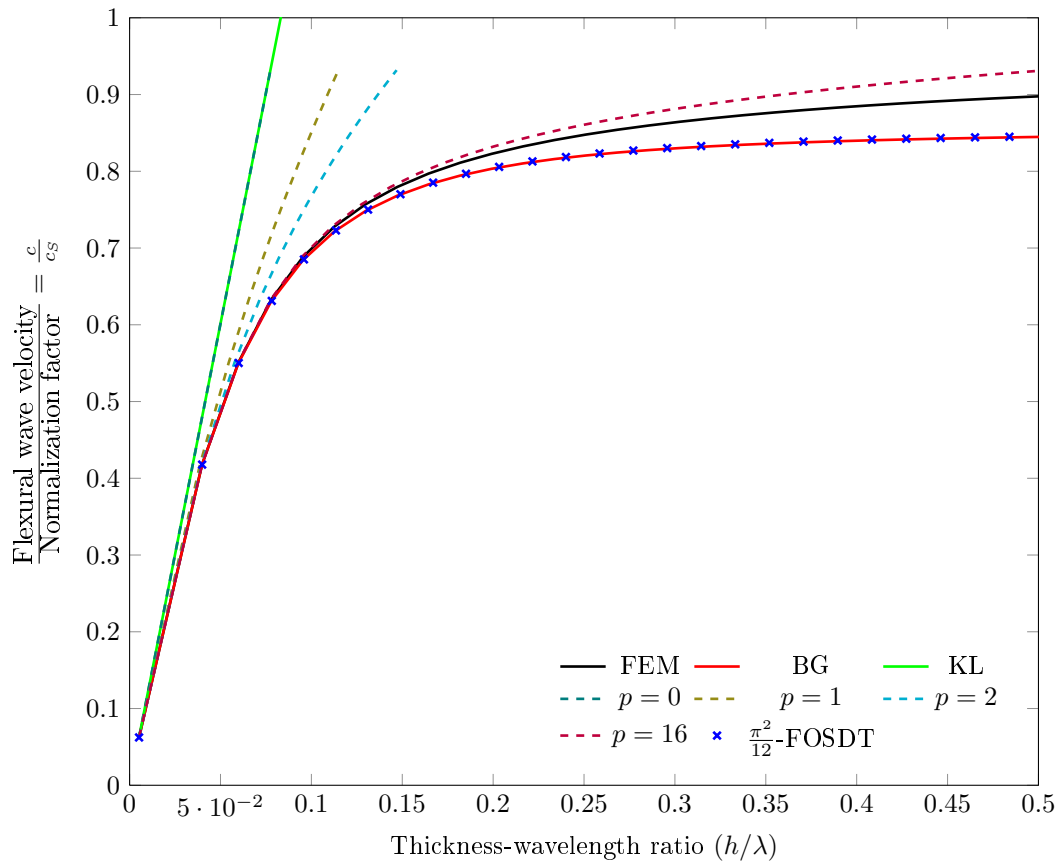


FIGURE 3.2 – Comparison of the flexural dispersion curves for a $[0^\circ, 90^\circ]_s$ ply

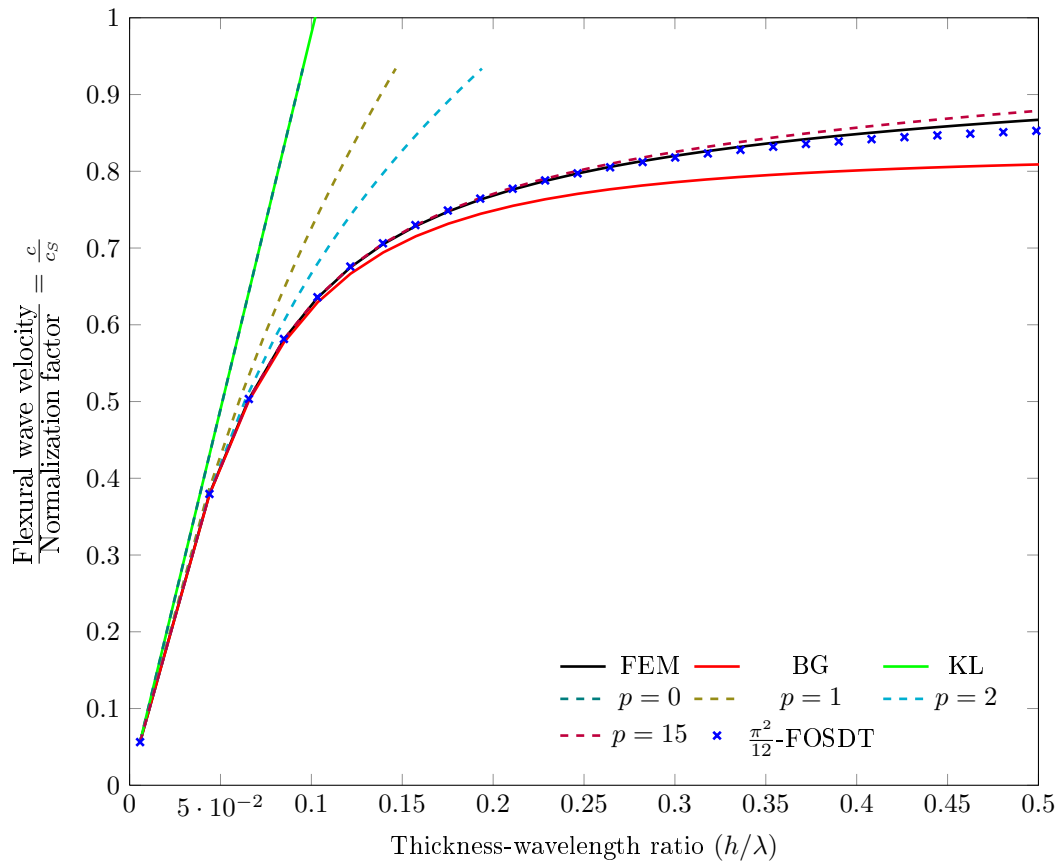


FIGURE 3.3 – Comparison of the flexural dispersion curves for a $[-30^\circ, 30^\circ]_s$ ply

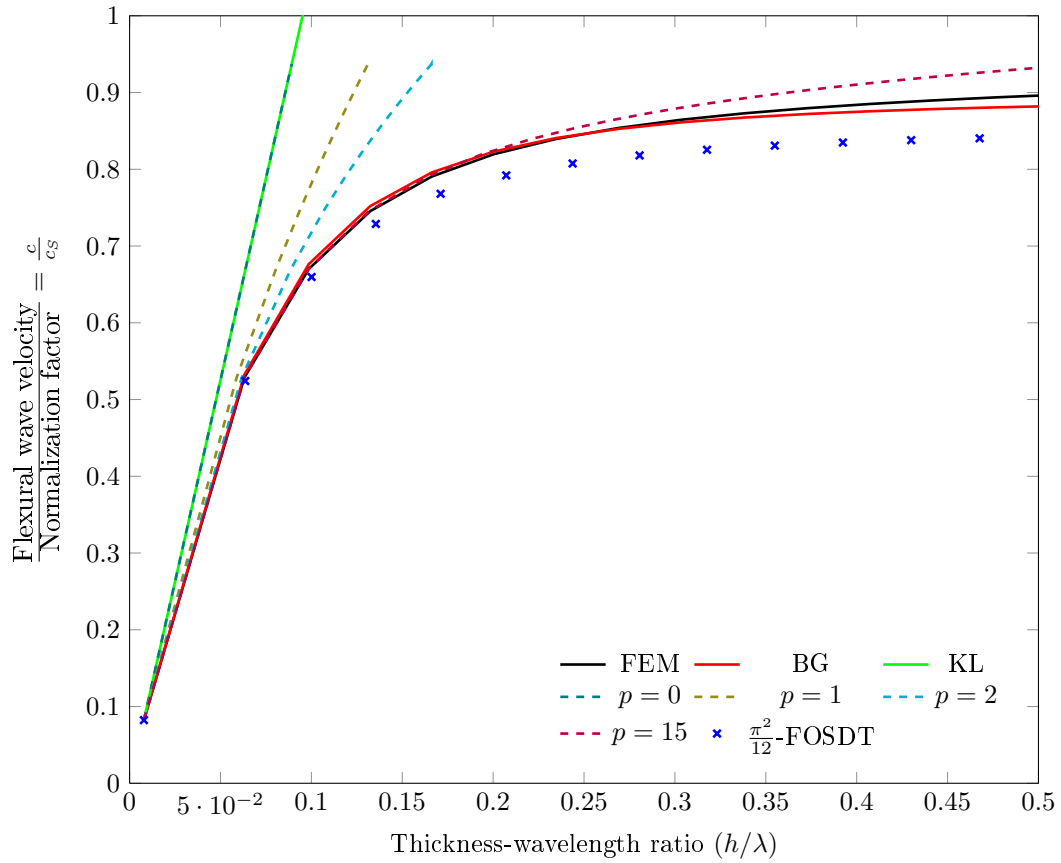


FIGURE 3.4 – Comparison of the flexural dispersion curves for a $[0^\circ, -45^\circ, 90^\circ, 45^\circ]_s$ ply

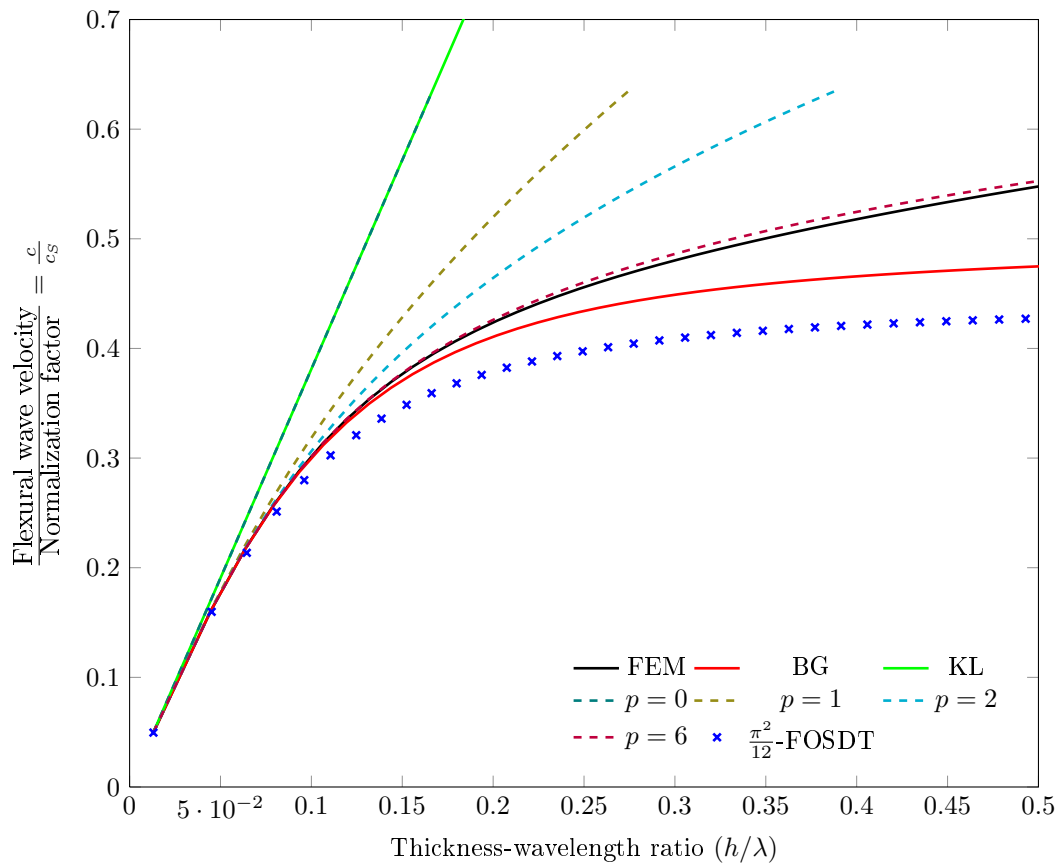


FIGURE 3.5 – Comparison of the flexural dispersion curves for a [GFRP, Al, GFRP, Al]_s ply

TABLE 3.3 – Elastic properties of aluminium material, E and G in Pa , ρ in kg/m^3 (Liu et al., 2016)

E	G	ν	ρ
7.20e+10	2.67e+10	0.35	2700

We check on figures 3.2, 3.3, 3.4 and 3.5 that the asymptotic expansion method with $p = 0$ coincides with the Kirchhoff-Love plate model which shows significant discrepancies with the reference solution for all plate configurations. Thus, solving higher-order problems ($p \geq 1$) is a must for the improvement of the asymptotic estimations.

Flexural velocities computed for $p = 1$ and $p = 2$ show minor improvement compared to Kirchhoff-Love solutions as depicted in figures 3.2, 3.3, 3.4 and 3.5. Thus, they do not yield accurate enough predictions.

It can be noticed that going further in the expansion allows refining the approximate solution. In fact, the computed results for a $[0^\circ, 90^\circ]_s$ ply reveal a good approximation of the solution for an order $p = 16$. When considering a $[-30^\circ, 30^\circ]_s$ and a $[0^\circ, -45^\circ, 90^\circ, 45^\circ]_s$ ply, figures 3.3 and 3.4 show a good accordance between the asymptotic expansion method and the finite element results for $p = 15$. According to figure 3.5, the computed results reveal great estimations of the flexural dispersion curve for a $[GFRP, Al, GFRP, Al]_s$ ply for $p = 6$.

Asymptotic expansions provide increasingly better approximations of flexural dispersion curves as the order p increases. However, one is inclined to carry calculations to quite high orders (up to a power of 32 of the parameter k^*) to get a good degree of accuracy.

It should be pointed out that the asymptotic expansion method converges for much larger values of the small parameter ($k^* > 3$) when the Lagrange inversion theorem is used. Referring to Bejjani et al. (2019), the Bending-Gradient approach offers more rapidity and flexibility to compute the desired results in comparison with the asymptotic analysis.

3.5.2 In-plane membranal waves

By choosing $\alpha_0 \neq 0$ and $V_3^{-1} = 0$, we can derive dispersion curves corresponding to the in-plane modes. In this case, $\alpha_0 = \frac{A_1}{\rho}$ or $\alpha_0 = \frac{A_2}{\rho}$ as stated in Section 3.4. The greatest value between A_1 and A_2 is the one that corresponds to longitudinal waves which are known to propagate faster than shear waves.

In figures 3.6, 3.7, 3.8 and 3.9 are depicted the longitudinal dispersion curves. Those of the in-plane shear mode are plotted in figures 3.11, 3.12, 3.13 and 3.14.

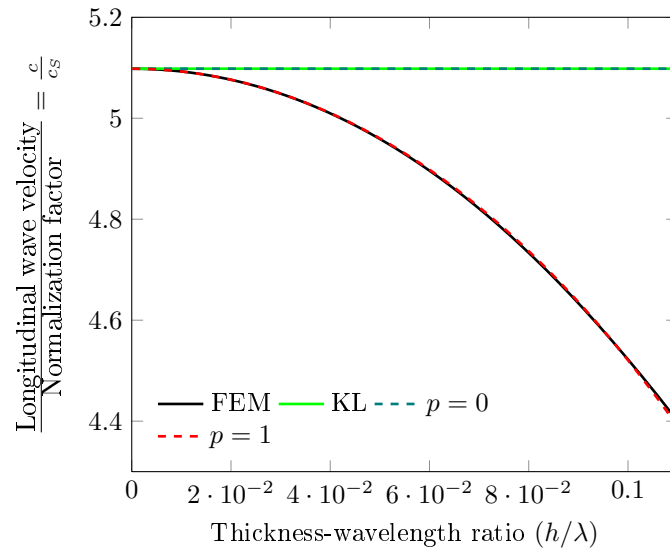


FIGURE 3.6 – Comparison of longitudinal dispersion curves for a $[0^\circ, 90^\circ]_s$ ply

3.5.2.1 Longitudinal waves

It is seen on figures 3.6, 3.7, 3.8 and 3.9 that a great approximation of the reference solution is acquired for $p = 1$. In fact, one can clearly observe slight variations of the longitudinal velocities. The asymptotic expansion method does not hence bring a drastic improvement of the approximation of in-plane dispersion curves compared to the Kirchhoff-Love model, which coincide with the zeroth-order approximations.

It is important to note that simulations were presented only for thickness-wavelength ratios smaller than 0.15 since in this case Poisson's effect can be neglected. For higher thickness-wavelength ratios, it is expected that the asymptotic expansion method will fail to provide accurate results. This is illustrated in figure 3.10 for example where a strong dispersion of the longitudinal mode is observed for $0.15 < \lambda < 0.5$ in the case of a $[\text{GFRP}, \text{Al}, \text{GFRP}, \text{Al}]_s$ ply.

3.5.2.2 In-plane shear waves

As for the case of flexural waves, the simulations presented hereafter are obtained using Lagrange (1770) inversion theorem (Appendix 3.6).

For a $[0^\circ, 90^\circ]_s$ ply, figure 3.11 shows that the in-plane shear curve obtained by the asymptotic expansion method for $p = 0$ is practically identical to the Kirchhoff-Love and the finite element solution.

As shown in figure 3.12, the approximation of the dispersion curve is considerably close to the reference solution for $p = 11$ in the case of a $[-30^\circ, 30^\circ]_s$ ply.

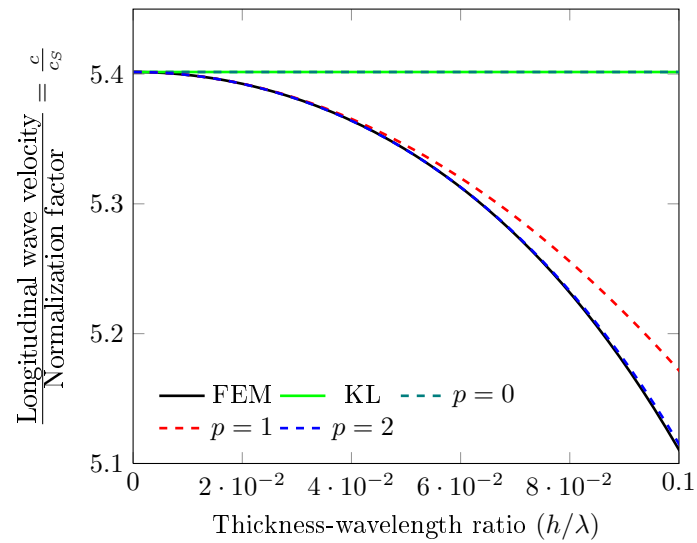


FIGURE 3.7 – Comparison of longitudinal dispersion curves for a $[-30^\circ, 30^\circ]_s$ ply

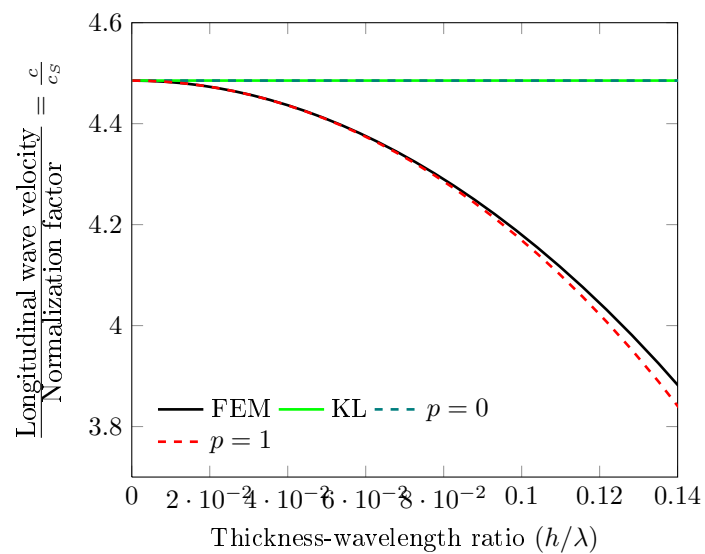


FIGURE 3.8 – Comparison of longitudinal dispersion curves for a $[0^\circ, -45^\circ, 90^\circ, 45^\circ]_s$ ply

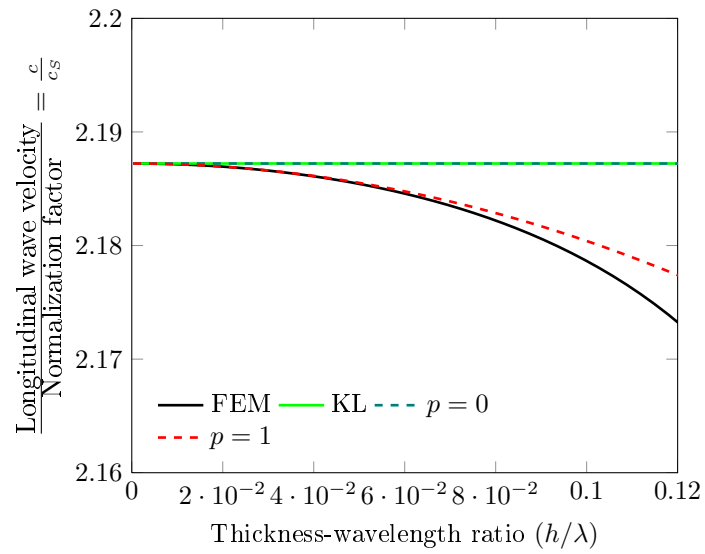


FIGURE 3.9 – Comparison of longitudinal dispersion curves for a [GFRP, Al, GFRP, Al]_s ply

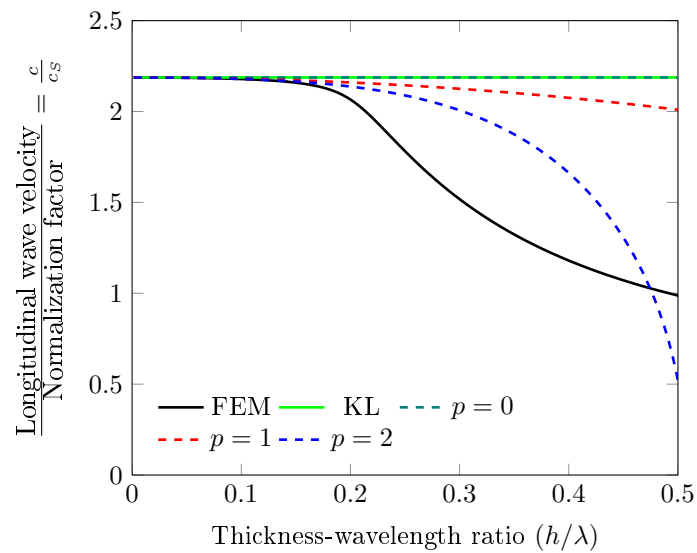


FIGURE 3.10 – Comparison of longitudinal dispersion curves for a [GFRP, Al, GFRP, Al]_s ply

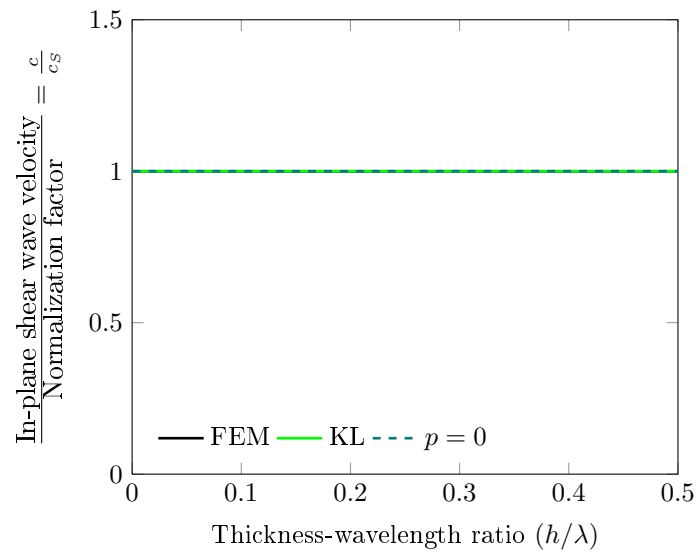


FIGURE 3.11 – Comparison of in-plane shear dispersion curves for a $[0^\circ, 90^\circ]_s$ ply

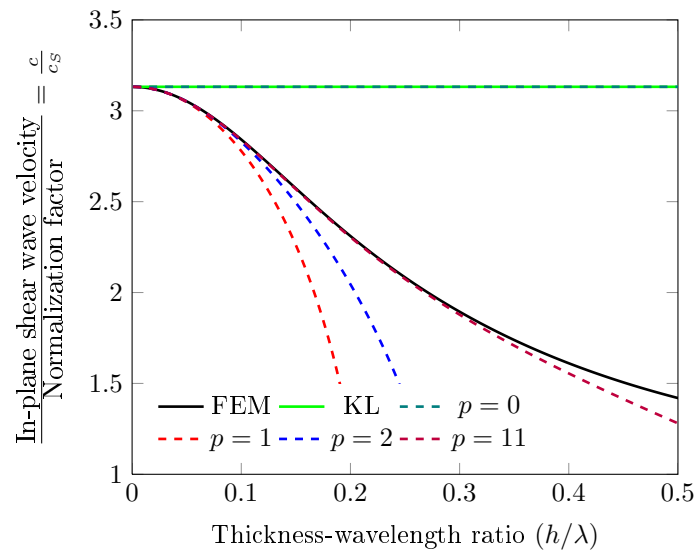


FIGURE 3.12 – Comparison of in-plane shear wave dispersion curves for a $[-30^\circ, 30^\circ]_s$ ply

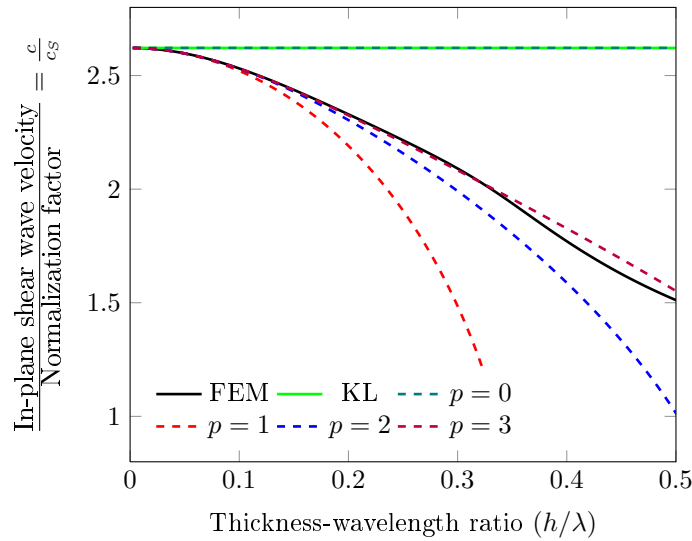


FIGURE 3.13 – Comparison of in-plane shear wave dispersion curves for a $[0^\circ, -45^\circ, 90^\circ, 45^\circ]_s$ ply

It is observed on figure 3.13 that the predicted dispersion curve is well correlated with the finite element solution for $p = 3$ in the case of a $[0^\circ, -45^\circ, 90^\circ, 45^\circ]_s$ ply.

According to figure 3.14, the in-plane shear dispersion curve is accurately captured for $p = 1$ compared to the finite element results for a $[\text{GFRP}, \text{Al}, \text{GFRP}, \text{Al}]_s$ ply.

Through the asymptotic expansion method and the Lagrange inversion theorem, we were able to estimate the dispersion curves of only three of all the wave modes obtained through the finite element method. What is interesting is that the domain of validity of the method is not limited to the vicinity of zero.

Using asymptotic expansions to model the propagation of flexural waves turns out to be complicated in comparison with the Bending-Gradient theory. Surprising is the fact that using Lagrange inversion theorem and carrying out calculations to high orders is a must to obtain good approximations of the flexural dispersion relations, as those obtained with the Bending-Gradient theory. Based on the obtained results, the domain of application of the asymptotic expansion method is clearly limited to the in-plane modes.

3.6 Conclusion

This paper is concerned with the prediction of the propagation of waves in composite plates by means of the asymptotic expansion method. In its initial version, this method exploits the existence of a small parameter corresponding to the thickness-to-wavelength ratio. The displacement, the strain and the stress solutions of the wave propagation problem are searched under the form of power series of the small parameter. Inserting these series

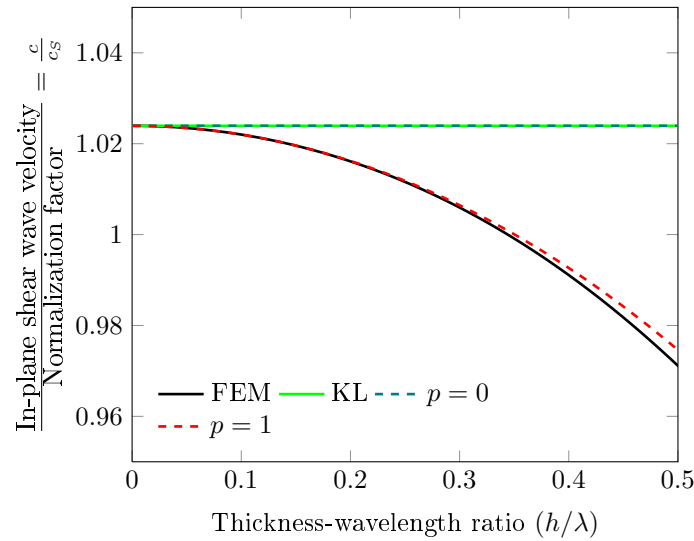


FIGURE 3.14 – Comparison of in-plane shear dispersion curves for a [GFRP, Al, GFRP, Al]_s ply

in the original problem and gathering terms which correspond to the same power of the small parameter yields an infinite sequence of problems to be solved recursively.

To assess the asymptotic expansions capability for estimating dispersion relations, numerical calculations were carried out. It was shown that the asymptotic expansion method provides identical solutions with the Kirchhoff-Love theory solutions for the zeroth-order. The Kirchhoff-Love theory gives results far from the actual ones when the thickness-to-wavelength ratio increases. Seeking higher orders in the expansion was hence a must to obtain better predictions of the flexural, compressional and in-plane shear wave modes. It was also shown that the convergence of the dispersion curves calculated as Taylor series of the thickness-to-wavelength ratio was limited to small values of this ratio (less than 0.06). In order to enhance the convergence, the Lagrange's inversion theorem has been used leading to convergence of the series for all the considered values of the thickness-to-wavelength ratio (up to 0.5). *This is an important theoretical result indicating that the asymptotic expansion method can be sometimes applied even when the assumed small parameter is not so small.*

Numerical results were compared to the finite element method for verification purposes. The in-plane shear mode was accurately estimated in general. Good approximations of the longitudinal mode were obtained, yet in a limited range of thickness-wavelength ratios.

The approximations of the flexural dispersion curves were in particular compared to the Bending-Gradient theory and to the first-order shear deformation theory ($\frac{\pi^2}{12}$ -FOSDT). Good agreement between the calculated results, the reference results and those of the Bending-Gradient and $\frac{\pi^2}{12}$ -FOSDT was found. Unexpectedly, it was necessary to take into consideration much higher order terms of the expansion in order to achieve a similar accuracy as that of plate models. In addition, the procedure is somehow cumbersome and

complicated which means that the asymptotic expansions lack effectiveness in approximating flexural dispersion curves.

Conclusions et perspectives

Ce travail de thèse s'inscrit dans le cadre de l'étude de la propagation des ondes dans les plaques multicouches hétérogènes et anisotropes, un sujet qui a été abordé largement dans la littérature. Toute la problématique est de trouver une bonne estimation analytique ou semi-analytique des relations de dispersion décrivant l'évolution de la fréquence angulaire en fonction du nombre d'onde. Les équations qui régissent ce type de problèmes sont bien connues et peuvent être résolues numériquement. On cite par exemple la méthode des éléments finis qui, malgré le fait qu'elle permet de représenter facilement des domaines de géométrie compliquée, s'avère complexe de point de vue mise en oeuvre et coûteuse en temps de calcul et en mémoire.

Dans ce contexte, deux approches ont été proposées pour l'estimation des relations de dispersion des ondes se propageant dans une plaque symétrique infinie dans le cadre de l'élasticité linéaire : la théorie du Bending-Gradient et la méthode des développements asymptotiques. Le présent document est une évaluation du compromis entre la simplicité et l'exactitude de ces méthodes pour le problème de la propagation des ondes.

Avant de répondre au problème posé, il semblait pertinent de commencer par une justification mathématique du modèle du Bending-Gradient dans le cadre statique (Chapitre 1). Après avoir explicité les formulations en déplacement et en contrainte, nous avons défini les espaces fonctionnels auxquels appartiennent les variables du modèle. Ceci nous a permis d'établir et de prouver l'existence et l'unicité de la solution du problème dans le cas où la plaque est encastrée ou libre. Une brève discussion a été menée pour les plaques dont le bord est simplement appuyé.

Le Chapitre 2 a été consacré à tester la validité de la théorie du Bending-Gradient pour la propagation des ondes de flexion dans les plaques composites. Les équations du mouvement ont été formulées en tenant compte des déformations du cisaillement transverse et en négligeant les effets d'inertie rotatoire. Nous avons montré que, pour retrouver les relations de dispersion, il suffit d'annuler le déterminant d'une matrice dont on a explicité les composantes. Dans ce cadre, nous avons créé un code permettant d'obtenir facilement ces relations en utilisant le langage de programmation Matlab. Le code est simple à utiliser et a été mis à la disposition des étudiants et des chercheurs. Les résultats obtenus par la méthode des éléments finis ont servi de référence pour la vérification de la pertinence de la théorie du Bending-Gradient. Nous avons comparé nos résultats aussi à ceux des modèles de Kirchhoff-Love et de Reissner-Mindlin. Le résultat principal de ce chapitre sti-

pule que les résultats obtenus par le Bending-Gradient sont les plus robustes et les moins sensibles à la configuration de la plaque. Il serait intéressant de pouvoir adapter la théorie du Bending-Gradient afin de permettre la caractérisation du comportement dynamique des plaques composites non nécessairement symétriques.

Le Chapitre 3 s'est attaché à tester l'efficacité de la méthode des développements asymptotiques pour modéliser le comportement dynamique linéaire des plaques multicouches infinies, avec le rapport épaisseur sur longueur d'onde comme petit paramètre. Après avoir exprimé les champs solutions sous forme de séries en puissance du petit paramètre, nous les avons injectés dans le problème initial. En rassemblant les termes de même puissance, nous avons obtenu une cascade de problèmes dont la résolution à l'ordre zéro nous a permis d'obtenir les trois modes de compression, de cisaillement dans le plan et de flexion du modèle de Kirchhoff-Love. La comparaison des résultats avec ceux de la méthode des éléments finis montre une bonne approximation du mode de cisaillement dans le plan en général et du mode de compression dans un domaine limité de rapports épaisseur-longueur d'onde. Un bon accord entre les résultats obtenus, ceux du Bending-Gradient et des éléments finis est indiqué pour les ondes de flexion. Cependant, il s'avère nécessaire de prendre en compte des termes d'ordres supérieurs pour améliorer la précision de la solution. La méthode des développements asymptotiques, bien que rigoureuse, semble être compliquée à mettre en oeuvre en comparaison à la théorie du Bending-Gradient.

Annexes

Annexe A

In the sequel we use the symbol "c" to denote a generic positive constant. In other words, the constant c takes different values at successive occurrences, even in the same equation.

A.1

We denote by $\|\bullet\|_{SC(0)}$ the norm associated with the scalar product $\langle \bullet, \bullet \rangle_{SC(0)}$. Let $\underline{\mu}_n \in SC(0), n \in \mathbb{N}$ be a Cauchy sequence in the norm $\|\bullet\|_{SC(0)}$. Then, $(\underline{\mu}_n)$ is a Cauchy sequence in $\underline{L}^2(\omega)$ and $(\underline{\mu}_n \otimes \underline{\nabla})$ is a Cauchy sequence in $\underline{L}^2(\omega)$. Therefore, there exists $\underline{\mu} \in \underline{L}^2(\omega)$ and $\underline{R} \in \underline{L}^2(\omega)$ such that $\underline{\mu}_n$ and $\underline{\mu}_n \otimes \underline{\nabla}$ converge to $\underline{\mu}$ in $\underline{L}^2(\omega)$ and to \underline{R} in $\underline{L}^2(\omega)$, respectively. We thus have that $\underline{\mu}_n$ converges to $\underline{\mu}$ in $\underline{D}'(\omega)$. Consequently, $\underline{\mu}_n \otimes \underline{\nabla}$ converges to $\underline{\mu} \otimes \underline{\nabla}$ in $\underline{D}'(\omega)$. Since $\underline{\mu}_n \otimes \underline{\nabla}$ also converges to \underline{R} in $\underline{D}'(\omega)$, then we have that $\underline{R} = \underline{\mu} \otimes \underline{\nabla}$. This proves that $\underline{\mu}$ is in $\underline{H}^1(\omega)$. We are left with proving that $\underline{i} \div ((\underline{\mu} \otimes \underline{\nabla}) \otimes \underline{\nabla}) = 0$. As the gradient operator is continuous, then $(\underline{\mu}_n \otimes \underline{\nabla}) \otimes \underline{\nabla}$ converges to $(\underline{\mu} \otimes \underline{\nabla}) \otimes \underline{\nabla}$ in the sense of distributions. We also have that $\underline{\mu}_n \in SC(0)$. Therefore, $\underline{i} \div ((\underline{\mu}_n \otimes \underline{\nabla}) \otimes \underline{\nabla}) = 0$. We have proved that $SC(0)$ equipped with the scalar product $\langle \bullet, \bullet \rangle_{SC(0)}$ is hence a Hilbert space.

A.2

Let $(\underline{M}, \underline{M}')$ be in $\underline{H}^1(\omega) \times \underline{H}^1(\omega)$. Then, using properties (1.44) and (1.45) and the Cauchy–Schwarz inequality, we have that :

$$\begin{aligned}
 |a_s(\underline{M}, \underline{M}')| &\leq c \left(\left| \int_{\omega} \underline{M}' : \underline{M} \right| + \left| \int_{\omega} {}^T(\underline{M}' \otimes \underline{\nabla}) \div (\underline{M} \otimes \underline{\nabla}) \right| \right) \\
 &\leq c \left(\|\underline{M}'\|_{\underline{L}^2(\omega)} \|\underline{M}\|_{\underline{L}^2(\omega)} + \|\underline{M}' \otimes \underline{\nabla}\|_{\underline{L}^2(\omega)} \|\underline{M} \otimes \underline{\nabla}\|_{\underline{L}^2(\omega)} \right) \\
 &\leq c \left(\|\underline{M}'\|_{\underline{L}^2(\omega)}^2 + \|\underline{M}' \otimes \underline{\nabla}\|_{\underline{L}^2(\omega)}^2 \right)^{1/2} \left(\|\underline{M}\|_{\underline{L}^2(\omega)}^2 + \|\underline{M} \otimes \underline{\nabla}\|_{\underline{L}^2(\omega)}^2 \right)^{1/2} \\
 &\leq c \|\underline{M}'\|_{\underline{H}^1(\omega)} \|\underline{M}\|_{\underline{H}^1(\omega)}
 \end{aligned}$$

We thus have proved that the bilinear form a_s is continuous on $SC(0)$ and the linear map $\underline{\mu} \rightarrow a_s(\underline{P}, \underline{\mu})$ is also continuous on $SC(0)$.

A.3

We have :

$$\begin{aligned}
|b(W, \underline{\Phi})| &= \left| \int_{\omega} pW \right| \\
&\leq \|p\|_{H^{-1}(\omega)} \|W\|_{H_0^1(\omega)} \\
&\leq \|p\|_{H^{-1}(\omega)} \|W, \underline{\Phi}\|_{KC_0}
\end{aligned}$$

Consequently, the linear form b is continuous on KC_0 .

A.4

Using properties (1.44) and (1.45) then the Cauchy-Schwarz inequality leads to

$$\begin{aligned}
|a((W, \underline{\Phi}), (W', \underline{\Phi}'))| &\leq \left| \int_{\omega} (\underline{\Phi} \cdot \underline{\nabla}) : \underline{D} : (\underline{\Phi}' \cdot \underline{\nabla}) \right| + \left| \int_{\omega}^T (\underline{\Phi} + \underline{\mathbf{i}} \cdot \underline{\nabla} W) : \underline{H} : (\underline{\Phi}' + \underline{\mathbf{i}} \cdot \underline{\nabla} W') \right| \\
&\leq c \left(\left| \int_{\omega} (\underline{\Phi} \cdot \underline{\nabla}) : (\underline{\Phi}' \cdot \underline{\nabla}) \right| + \left| \int_{\omega}^T (\underline{\Phi} + \underline{\mathbf{i}} \cdot \underline{\nabla} W) : (\underline{\Phi}' + \underline{\mathbf{i}} \cdot \underline{\nabla} W') \right| \right) \\
&\leq c \left(\|\underline{\Phi} \cdot \underline{\nabla}\|_{\underline{L}^2(\omega)} \|\underline{\Phi}' \cdot \underline{\nabla}\|_{\underline{L}^2(\omega)} + \|\underline{\Phi} + \underline{\mathbf{i}} \cdot \underline{\nabla} W\|_{\underline{L}^2(\omega)} \|\underline{\Phi}' + \underline{\mathbf{i}} \cdot \underline{\nabla} W'\|_{\underline{L}^2(\omega)} \right)
\end{aligned}$$

Since $\|\underline{\mathbf{i}} \cdot \underline{\nabla} W\|_{\underline{L}^2(\omega)}^2 = \frac{3}{2} \|\underline{\nabla} W\|_{\underline{L}^2(\omega)}^2$, using the Poincaré inequality yields :

$$|a((W, \underline{\Phi}), (W', \underline{\Phi}'))| \leq c \|W, \underline{\Phi}\|_{KC_0} \|W', \underline{\Phi}'\|_{KC_0}$$

This ends the proof.

Annexe B

B.1

Let $\underline{\mathbb{R}}$ be the space of 2D third order tensors which comply with the following symmetries :

$$(1) \quad \underline{\mathbb{R}} = \{(X_{\alpha\beta\gamma}) \in \mathbb{R}^8 \mid X_{\alpha\beta\gamma} = X_{\beta\alpha\gamma}\}.$$

Sab and Lebée (2015) orthogonally decomposed the vector space $\underline{\mathbb{R}}$, endowed with the scalar product $X_{\alpha\beta\gamma}X'_{\alpha\beta\gamma}$, into $\text{Im } h$ and its orthogonal $\text{Ker } h$:

$$\underline{\mathbb{R}} = \text{Ker } h \oplus \text{Im } h,$$

where \oplus is the direct sum operator (Section 3.2), $\text{Im } h$ is the image of the sixth-order shear force compliance tensor $h_{\alpha\beta\gamma\delta\epsilon\zeta}$:

$$\text{Im } h = \{h_{\alpha\beta\gamma\delta\epsilon\zeta}X_{\zeta\epsilon\delta}, \quad X_{\zeta\epsilon\delta} \in \underline{\mathbb{R}}\},$$

and $\text{Ker } h$ denotes its kernel :

$$\text{Ker } h = \{X_{\alpha\beta\gamma} \in \underline{\mathbb{R}} \mid h_{\alpha\beta\gamma\delta\epsilon\zeta}X_{\zeta\epsilon\delta} = 0\}.$$

Sab and Lebée (2015) have proved that the shear force compliance tensor $h_{\alpha\beta\gamma\delta\epsilon\zeta}$ is definite only on the subspace $\text{Im } h$ whose dimension is between two and six, depending on the elastic properties of the plate. When the plate is homogeneous, the dimension of $\text{Im } h$ is exactly two and in this case the Bending-Gradient theory degenerates into the Reissner-Mindlin theory. When $h_{\alpha\beta\gamma\delta\epsilon\zeta}$ is definite and therefore invertible, $\text{Im } h$ is equal to $\underline{\mathbb{R}}$ of dimension six.

B.2

For the particular case of homogeneous plates, we recall that the Bending-Gradient shear compliance tensor $h_{\alpha\beta\gamma\delta\epsilon\zeta}$ is of the form (2.11). Contracting three times the left and the right of both sides of the above equation with $\frac{2}{3}i_{\alpha\beta\gamma\delta}$, we obtain the expression of $f_{\alpha\beta}^{\text{R}}$ in terms of $h_{\alpha\beta\gamma\delta\epsilon\zeta}$ (see equation (2.14)). In view of the positive definiteness of $f_{\alpha\beta}^{\text{R}}$, we define its inverse $F_{\alpha\beta}^{\text{R}}$.

Propagation of elastic waves is governed by the equations of the Bending-Gradient theory, which for homogeneous plates write :

$$(2) \quad \begin{cases} Q_{\alpha} - M_{\alpha\beta,\beta} = 0, \\ Q_{\alpha,\alpha} = \ddot{U}_3\bar{\rho}. \end{cases}$$

In terms of displacements (U_3, φ_{α}) , the above equations are revised as :

$$(3a) \quad \begin{cases} F_{\alpha\beta}^{\text{R}}(\varphi_{\beta} + U_{3,\beta}) - D_{\alpha\beta\xi\eta}\varphi_{\eta,\xi\beta} = 0, \\ F_{\alpha\beta}^{\text{R}}(\varphi_{\beta,\alpha} + U_{3,\beta\alpha}) = \ddot{U}_3\bar{\rho}. \end{cases}$$

The displacements $(U_3, \varphi_\alpha)(x_1, t)$, solution to the wave equations (3), have the general following form :

$$(4a) \quad \begin{cases} U_3(x_1, t) = \Re \left(\hat{U}_3 e^{j(\omega t - kx_1)} \right), \\ (4b) \quad \varphi_\alpha(x_1, t) = \Re \left(\hat{\varphi}_\alpha e^{j(\omega t - kx_1)} \right), \end{cases}$$

where \hat{U}_3 and $\hat{\varphi}_\alpha$ are constants. Plugging these functions into equations (3), it follows that :

$$(5a) \quad \begin{cases} F_{\alpha\beta}^R \left(\hat{\varphi}_\beta - jk\delta_{\beta 1} \hat{U}_3 \right) + k^2 D_{\alpha 11 \eta} \hat{\varphi}_\eta = 0, \\ (5b) \quad F_{1\beta}^R \left(-jk\hat{\varphi}_\beta - k^2\delta_{\beta 1} \hat{U}_3 \right) + \omega^2 \hat{U}_3 \bar{\rho} = 0. \end{cases}$$

We denote by $[\delta^h]$ the vector of dimension 3 representing the generalized displacements :

$$(6) \quad [\delta^h]^T = \left[\hat{U}_3, \hat{\varphi}_1, \hat{\varphi}_2 \right].$$

Equations (5) can be rewritten as :

$$(7) \quad [\mathcal{B}] \cdot [\delta^h] = 0,$$

where $[\mathcal{B}]$ is a 3×3 matrix identified as :

$$(8) \quad [\mathcal{B}] = \begin{bmatrix} \omega^2 \bar{\rho} - k^2 F_{11}^R & -jk F_{11}^R & -jk F_{12}^R \\ -jk F_{11}^R & F_{11}^R + k^2 D_{1111} & F_{12}^R + k^2 D_{1121} \\ -jk F_{21}^R & F_{21}^R + k^2 D_{2111} & F_{22}^R + k^2 D_{2121} \end{bmatrix}.$$

The dispersion relation of flexural waves for homogeneous plates is deduced from solving :

$$(9) \quad \det[\mathcal{B}] = 0,$$

which yields

$$(10) \quad \omega^2 = \frac{k^6 F_{11}^R (D_{1111} D_{2121} - D_{1121}^2) + k^4 D_{1111} (F_{11}^R F_{22}^R - (F_{12}^R)^2)}{\bar{\rho} \left((F_{11}^R + k^2 D_{1111}) (F_{22}^R + k^2 D_{2121}) - (F_{12}^R + k^2 D_{2111})^2 \right)}.$$

The tensors $F_{\alpha\beta}^R$ and $D_{\alpha\beta\gamma\delta}$, being positive definite respectively imply that :

$$F_{11}^R > 0, \quad F_{11}^R F_{22}^R - (F_{12}^R)^2 > 0$$

and

$$D_{1111} > 0, \quad D_{1111} D_{2121} - D_{1121}^2 > 0.$$

Furthermore, the wavenumber k being real implies that the matrix $\begin{pmatrix} F_{11}^R + k^2 D_{1111} & F_{12}^R + k^2 D_{2111} \\ F_{12}^R + k^2 D_{2111} & F_{22}^R + k^2 D_{2121} \end{pmatrix}$ is positive definite. Therefore, its determinant is always positive. Namely,

$$(F_{11}^R + k^2 D_{1111}) (F_{22}^R + k^2 D_{2121}) - (F_{12}^R + k^2 D_{2111})^2 > 0.$$

As a consequence, equation (10) admits two real roots corresponding to the forward and backward flexural waves.

Annexe C

C.1

In this section, we present the numerical computation of the functions \mathbb{P} and \mathbb{Q} introduced previously in Sect. 3.4.

Let f denote a function defined on the interval $[-\frac{1}{2}, \frac{1}{2}]$ and $\{x_i\}_{i=0}^n$ a sequence of $n + 1$ increasing numbers in $[-\frac{1}{2}, \frac{1}{2}]$ with

$$(11) \quad x_0 = -\frac{1}{2}, \quad x_n = \frac{1}{2}, \quad x_{k+1} = x_k + \frac{1}{n}.$$

The following notation is used for clarity purposes :

$$(12) \quad f_k = f(x_k) = f\left(x_0 + \frac{k}{n}\right).$$

Let $g = \mathbb{Q}(f) = \int_{-\frac{1}{2}}^z f(y)dy$. The discretized function of g is expressed as :

$$(13) \quad g_0 = 0, \quad g_{k+1} = g_k + \frac{1}{n} \frac{f_{k+1} + f_k}{2}, \quad k = 0, 1, \dots, n-1.$$

The definite integral I_g of g on $[-\frac{1}{2}, \frac{1}{2}]$ writes :

$$(14) \quad I_g = \int_{-\frac{1}{2}}^{\frac{1}{2}} g(t)dt = \sum_{k=0}^{n-1} \frac{1}{n} \frac{g_{k+1} + g_k}{2}.$$

We recall that $\mathbb{P}(g)$ designates the unique primitive of the function g such that $\langle \mathbb{P}(g) \rangle = 0$. We have that :

$$(15) \quad \mathbb{P}(g) = g - I_g.$$

The discretized function of $\mathbb{P}(g)$ is given by :

$$(16) \quad g_k - I_g, \quad k = 0, 1, \dots, n.$$

C.2

Lagrange (1770) inversion theorem reads as follows :

Suppose that $Y = f(X)$, $X \in \mathbb{R}$, is a real smooth function which admits a power series expansion

$$(17) \quad Y = a_1X + a_2X^2 + \dots + a_nX^n + \dots$$

where the coefficients a_1, a_2, a_n, \dots are known real numbers and $a_1 \neq 0$. Then, it is possible to express X in terms of powers of Y by :

$$(18) \quad X = b_1 Y + b_2 Y^2 + \dots + b_n Y^n + \dots$$

where the coefficients b_n are given by the explicit formula :

$$(19) \quad b_n = \frac{1}{n!} \left[\frac{d^{n-1}}{dx^{n-1}} \left(\frac{1}{a_1 + a_2 X + \dots + a_n X^{n-1}} \right)^n \right]_{|X=0}.$$

for any order n .

More details on the Lagrange inversion theorem can be found in G. De Bruijn (1958).

When considering flexural waves ($\alpha_0 = 0$), we have that :

$$Y = c^2, \quad \text{and} \quad X = k^{*2},$$

whereas for in-plane shear waves, $\alpha_0 \neq 0$ yields :

$$Y = c^2 - \alpha_0, \quad \text{and} \quad X = k^{*2}.$$

C.3

Inspired by ideas from Reissner (1945), Lebée and Sab (2011) suggested a new plate model, known as the Bending-Gradient theory, dedicated to thick and heterogeneous plates. This theory replaces the classical Reissner-Mindlin out-of-plane shear forces by the generalized shear force related to the first gradient of the bending moment. Furthermore, six rotations are introduced instead of only two. This is why the Bending-Gradient theory is considered as an extension of the Reissner-Mindlin theory to laminated plates. In general, the Bending-Gradient model cannot be replaced by a Reissner-Mindlin model unless the constitutive material of the plate is homogeneous. In this case, the two models strictly coincide. For further details on the Bending-Gradient theory, the reader may refer to Lebée and Sab (2011), Lebée and Sab (2013), Lebée and Sab (2015), Lebée and Sab (2015), Sab and Lebée (2015) and Bejjani et al. (2018).

In a recent paper (Bejjani et al., 2019), the validity of the Bending-Gradient theory regarding plane wave propagation in composite plates was tested. Numerical simulations were carried out on different plate configurations and it was shown that the Bending-Gradient approximation of the dispersion curve associated to flexural waves is the most robust one and the less sensitive to the ply configuration.

Wave propagation in an infinite composite plate is governed by the full set of equations of the Bending-Gradient theory, which write :

$$(20a) \quad \left\{ \begin{array}{l} \underline{\mathbf{R}} - \underline{\mathbf{P}}^S : (\underline{\mathbf{M}} \otimes \underline{\nabla}) = 0, \quad \underline{\mathbf{Q}} = \underline{\mathbf{i}} : \underline{\mathbf{R}} \quad \text{and} \quad \underline{\mathbf{Q}} \cdot \underline{\nabla} = \ddot{U}_3 \bar{\rho}, \\ (20b) \quad \left\{ \begin{array}{l} \underline{\mathbf{x}} = \underline{\mathbf{d}} : \underline{\mathbf{M}} \quad \text{and} \quad \underline{\mathbf{\Gamma}} = \underline{\mathbf{h}} : \underline{\mathbf{R}}, \\ (20c) \quad \left\{ \begin{array}{l} \underline{\mathbf{x}} = \underline{\mathbf{\Phi}} \cdot \underline{\nabla} \quad \text{and} \quad \underline{\mathbf{\Gamma}} = \underline{\mathbf{\Phi}} + \underline{\mathbf{i}} \cdot \underline{\nabla} U_3. \end{array} \right. \end{array} \right. \end{array} \right.$$

Equations (20)a, (20)b and (20)c respectively designate the equations of motion, the constitutive equations and the compatibility conditions.

U_3 is the out-of-plane displacement and $\underline{\Phi}$ is the Bending-Gradient generalized third-order rotation tensor.

The second order tensor $\underline{\chi}$ is the curvature tensor, while the third-order tensor Γ is the Bending-Gradient generalized shear strain.

The second-order tensor $\underline{\mathbf{M}}$ and the vector $\underline{\mathbf{Q}}$ designate the conventional bending moment tensor and shear force respectively, related to the 3D local stress (σ_{ij}) by :

$$(21) \quad M_{\alpha\beta} = \langle x_3 \sigma_{\alpha\beta} \rangle \quad \text{and} \quad Q_\alpha = \langle \sigma_{\alpha 3} \rangle.$$

The third-order tensor $\underline{\mathbf{R}}$ represents the Bending-Gradient generalized shear force.

Here, $\underline{\underline{\mathbf{d}}}$ is the classical bending compliance fourth-order tensor, always positive and definite. The sixth-order tensor $\underline{\underline{\mathbf{h}}}$ is the generalized shear compliance which is positive but definite only on its image $\text{Im } h$. The projection operator onto $\text{Im } h$ is denoted by $\underline{\underline{\mathbf{P}}}^S$.

Finally, $\bar{\rho}$ is given by :

$$(22) \quad \bar{\rho} = \int_{-\frac{h}{2}}^{\frac{h}{2}} \rho(x_3) dx_3.$$

The derivation and the implementation of the Bending-Gradient equations of motion is wholly described in Bejjani et al. (2019).

Bibliographie

- J. Renno, E. Manconi, B. Mace, A finite element method for modelling waves in laminated structures, *Advances in Structural Engineering* 16 (2013) 61–76.
- Z. Liu, M. Fard, J. Davy, Prediction of the effect of porous sound-absorbing material inside a coupled plate cavity system, *International Journal of Vehicle Noise and Vibration* 12 (2016) 314.
- A. Lebée, K. Sab, On the generalization of reissner plate theory to laminated plates, part ii : Comparison with the bending-gradient theory, *Journal of Elasticity* 126 (2015).
- N. Pagano, Exact solutions for composite laminates in cylindrical bending, *Journal of Composite Materials* 3 (1969) 398–411.
- A. Lebée, K. Sab, Justification of the Bending-Gradient Theory Through Asymptotic Expansions, Springer Berlin Heidelberg, Berlin, Heidelberg, pp. 217–236.
- N. Bejjani, K. Sab, J. Bodgi, A. Lebée, The bending-gradient theory for thick plates : Existence and uniqueness results, *Journal of Elasticity* 133 (2018) 37–72.
- D. Morgenstern, Herleitung der plattentheorie aus der dreidimensionalen elastizitätstheorie, *Archive for Rational Mechanics and Analysis* 4 (1959) 145–152.
- W. Prager, J. Synge, Approximations in elasticity based on the concept of function space, *Quarterly of Applied Mathematics* V (1947).
- P. Ciarlet, P. Destuynder, Justification of the two-dimensional linear plate model., *Journal de mecanique* 18 (1979) 315–344.
- P. G. Ciarlet, Plates and junctions in elastic multi-structures : An asymptotic analysis (1990).
- P. G. Ciarlet, *Mathematical Elasticity - Volume II : Theory of Plates*, Elsevier Science Bv, 1997.
- E. Reissner, On the theory of bending of elastic plates, *International Journal of Solids and Structures* 12 (1976) 545–554.

-
- H. Hencky, Über die berücksichtigung der schubverzerrung in ebenen platten, *Ingenieur-Archiv* 1 (1947) 72–76.
- L. Bollé, Contribution au problème linéaire de flexion d'une plaque élastique, *Bulletin technique de la Suisse Romande* 73 (1947) 281–285.
- E. Reissner, Reflections on the theory of elastic plates, *Applied Mechanics Reviews - APPL MECH REV* 38 (1985).
- T. Hughes, *The Finite Element Method : Linear Static and Dynamic Finite Element Analysis*, volume 78, 2000.
- D. Arnold, R. Falk, Asymptotic analysis of the boundary layer for the plate model, *SIAM Journal on Mathematical Analysis* 27 (1996) 486–514.
- S. Alessandrini, D. Arnold, R. Falk, A. Madureira, Derivation and justification of plate models by variational methods, *Plates and Shells* 21 (1999).
- D. Arnold, A. Madureira, S. Zhang, On the range of applicability of the reissner–mindlin and kirchhoff–love plate bending models, *Journal of Elasticity* 67 (2002) 171–185.
- D. Braess, S. Sauter, C. Schwab, On the justification of plate models, *Journal of Elasticity* 103 (2009) 53–71.
- R. Paroni, P. Podio-Guidugli, G. Tomassetti, A justification of the reissner-mindlin plate theory through variational convergence, *Analysis and Applications (Singapore)* 5 (2007).
- P. Neff, K. Hong, The Reissner-Mindlin plate is the Gamma-limit of linear Cosserat elasticity, pp. 91–94.
- J. M. Whitney, Stress analysis of thick laminated composite and sandwich plates, *Journal of Composite Materials* 6 (1972) 426–440.
- J. N. Reddy, On refined computational models of composite laminates, *International Journal for Numerical Methods in Engineering* 27 (1989) 361–382.
- A. K. Noor, M. Malik, An assessment of five modeling approaches for thermo-mechanical stress analysis of laminated composite panels, *Computational Mechanics* 25 (2000) 43–58.
- A. D. Diaz, J.-F. Caron, R. P. Carreira, Un modèle de stratifiés, *Comptes Rendus de l'Académie des Sciences - Series IIB - Mechanics* 329 (2001) 873 – 879.
- E. Carrera, Theories and finite elements for multilayered, anisotropic, composite plates and shells, *Archives of Computational Methods in Engineering* 9 (2002) 87–140.

-
- E. Reissner, The effect of transverse shear deformation on the bending of elastic plates, *J. Appl. Mech. Eng. ASME* 12 (1945) A69–A77.
- A. Lebée, K. Sab, A bending-gradient model for thick plates. part i : Theory, *International Journal of Solids and Structures* 48 (2011) 2878–2888.
- N. Pagano, Influence of shear coupling in cylindrical. bending of anisotropic laminates, *Journal of Composite Materials* 4 (1970) 330–343.
- A. Lebée, K. Sab, A bending-gradient model for thick plates, part ii : Closed-form solutions for cylindrical bending of laminates, *International Journal of Solids and Structures* 48 (2011) 2889–2901.
- A. Lebée, K. Sab, Homogenization of thick periodic plates : Application of the bending-gradient plate theory to a folded core sandwich panel, *International Journal of Solids and Structures* 49 (2012a) 2778 – 2792.
- A. Lebée, K. Sab, Homogenization of cellular sandwich panels, *Comptes Rendus Mécaniques* 340 (2012b) 320–337.
- A. Lebée, K. Sab, Homogenization of a space frame as a thick plate : Application of the bending-gradient theory to a beam lattice, *Computers and Structures* 127 (2013).
- K. Sab, A. Lebée, Homogenization of Heterogeneous Thin and Thick Plates, 2015.
- K. Sab, F. Legoll, S. Forest, Stress gradient elasticity theory : Existence and uniqueness of solution, *Journal of Elasticity* 123 (2015).
- A. Lebée, K. Sab, On the generalization of reissner plate theory to laminated plates, part i : Theory, *Journal of Elasticity* 126 (2015).
- N. Bejjani, P. Margerit, K. Sab, J. Bodgi, A. Lebée, The bending-gradient theory for flexural wave propagation in composite plates, *International Journal of Solids and Structures* (2019).
- G. Kirchhoff, Über das gleichgewicht und die bewegung einer elastischen scheibe., *Journal für die reine und angewandte Mathematik* 40 (1850a) 51–88.
- G. Kirchhoff, Ueber die schwingungen einer kreisförmigen elastischen scheibe, *Annalen der Physik* 157 (1850b) 258–264.
- A. E. H. Love, I. the small free vibrations and deformation of a thin elastic shell, *Proceedings of the Royal Society of London* 43 (1888) 352–353.
- R. D. Mindlin, Influence of rotatory inertia and shear flexural motions of isotropic elastic plates, *Journal of Applied Mechanics* 18 (1951) 31 – 38.

-
- P. C. Yang, C. H. Norris, Y. Stavsky, Elastic wave propagation in heterogeneous plates, *International Journal of Solids and Structures* 2 (1966) 665 – 684.
- J. M. Whitney, N. J. Pagano, Shear deformation in heterogeneous anisotropic plates, *Journal of Composite Materials* 6 (1970) 30.
- O. Perret, A. Lebé, C. Douthe, K. Sab, The bending-gradient theory for the linear buckling of thick plates : Application to cross laminated timber panels, *International Journal of Solids and Structures* 87 (2016) 139 – 152.
- E. Kausel, Wave propagation in anisotropic layered media, *International Journal for Numerical Methods in Engineering* 23 (1986) 1567–1578.
- S. K. Datta, A. H. Shah, R. L. Bratton, T. Chakraborty, Wave propagation in laminated composite plates, *The Journal of the Acoustical Society of America* 83 (1988) 2020–2026.
- H. Gravenkamp, C. Song, J. Prager, A numerical approach for the computation of dispersion relations for plate structures using the scaled boundary finite element method, *Journal of Sound and Vibration* 331 (2012) 2543 – 2557.
- P. Margerit, Caractérisation large bande du comportement dynamique linéaire des structures hétérogènes viscoélastiques anisotropes. Application à la table d’harmonie du piano, Ph.D. thesis, Université Paris-Est, 2018.
- H. Lamb, On waves in an elastic plate, *Proceedings of the Royal Society of London. Series A, Containing Papers of a Mathematical and Physical Character* 93 (1917) 114–128.
- W. T. Thomson, Transmission of elastic waves through a stratified solid medium, *Journal of Applied Physics* 21 (1950) 89 – 93.
- N. Haskell, The Dispersion of Surface Waves on Multilayered Media, *American Geophysical Union (AGU)*, pp. 86–103.
- H. Schmidt, G. Tango, Efficient global matrix approach to the computation of synthetic seismograms, *Geophysical Journal of the Royal Astronomical Society* 84 (2007) 331 – 359.
- A. H. Nayfeh, The general problem of elastic wave propagation in multilayered anisotropic media, *The Journal of the Acoustical Society of America* 89 (1991) 1521–1531.
- S. Rokhlin, L. Wang, Stable recursive algorithm for elastic wave propagation in layered anisotropic media : Stiffness matrix method, *The Journal of the Acoustical Society of America* 112 (2002) 822–34.
- S. Dong, R. B. Nelson, On natural vibrations and waves in laminated orthotropic plates, *Journal of Applied Mechanics* 39 (1972).

-
- Z. C. Xi, G. R. Liu, K. Y. Lam, H. M. Shang, Dispersion and characteristic surfaces of waves in laminated composite circular cylindrical shells, *The Journal of the Acoustical Society of America* 108 (2000) 2179–2186.
- P. J. Shorter, Wave propagation and damping in linear viscoelastic laminates, *Journal of The Acoustical Society of America - J ACOUST SOC AMER* 115 (2004).
- E. Barbieri, A. Cammarano, S. D. Rosa, F. Franco, Waveguides of a composite plate by using the spectral finite element approach, *Journal of Vibration and Control* 15 (2009) 347–367.
- I. Bartoli, A. Marzani, F. L. di Scalea, E. Viola, Modeling wave propagation in damped waveguides of arbitrary cross-section, *Journal of Sound and Vibration* 295 (2006) 685–707.
- N. Bejjani, The Bending-Gradient flexural dispersion curves, 2019. <https://github.com/Nadinebejjani/Bending-Gradient.git>.
- G. Green, On the propagation of light in crystallized media, *Transactions of the Cambridge Philosophical Society* 7 (1839) 121–140.
- E. B. Christoffel, Über die fortpflanzung von stäben durch elastische feste körper, *Annali Mat. pura appl* 8 (1970) 193–243.
- L. Rayleigh, On the free vibrations of an infinite plate of homogeneous isotropic elastic matter, *Proceedings of the London Mathematical Society* s1-20 (1888) 225–237.
- M. J. S. Lowe, Plate waves for the NDT of diffusion bonded titanium, Ph.D. thesis, Imperial College London (University of London), 1993.
- K. F. Graff, *Wave motion in elastic solids*, New York : Dover Publications, 1991.
- J. Miklowitz, *Theory of Elastic Waves and Waveguides*, North-Holland, Amsterdam, 1978.
- D. Chimenti, Guided waves in plates and their use in materials characterization, *Applied Mechanics Reviews* 50 (1997).
- J. D. D. Achenbach, Wave propagation in elastic solids, *Journal of Applied Mechanics* 16 (1974).
- R. D. Mindlin, *Waves and vibrations in isotropic elastic plates*, Structural mechanics, Pergamon Press, New York (1960).
- J. N. Reddy, A simple higher-order theory for laminated composite plates, *Journal of Applied Mechanics*, *Transactions ASME* 51 (1984) 13–19.
- G. Turvey, M. Osman, Large deflection analysis of orthotropic mindlin plates, *proceedings of the 12th Energy resource technology conference and exhibition*, Houston, Texas (1989) 163–172.

-
- G. Turvey, M. Osman, Elastic large deflection analysis of isotropic rectangular mindlin plates, *International Journal of Mechanical Sciences* 32 (1990) 315 – 328.
- G. J. Turvey, M. Y. Osman, *Large Deflection Effects in Antisymmetric Cross-Ply Laminated Strips and Plates*, Springer Netherlands, Dordrecht, pp. 397–413.
- J. Whitney, Shear correction factor for orthotropic laminates under static loads, *Journal of Applied Mechanics* 40 (1991) 302–304.
- J. Whitney, C. Sun, A higher order theory for extensional motion of laminated composites, *Journal of Sound and Vibration* 30 (1973) 85 – 97.
- J. Whitney, C. Sun, A refined theory for laminated anisotropic, cylindrical shells, *Journal of Applied Mechanics* 41 (1974) 471–476.
- B. Gautham, N. Ganesan, Free vibration analysis of thick spherical shells, *Computers and Structures* 45 (1992) 307 – 313.
- S. Ambartsumyan, *Theory of anisotropic plates : Strength, Stability and Vibration*, Technomic Publishing Co., 1970.
- R. Nelson, D. Lorch 41 (1974).
- K. Lo, R. Christensne, E. Wu, A high order theory of plate deformation. part i : homogeneous plates, *Journal of Applied Mechanics* 44 (1977a) 663–668.
- K. Lo, R. Christensne, E. Wu, A high-order theory of plate deformation-part ii : Laminated plates 44 (1977b) 669–676.
- J. N. Reddy, A generalization of two-dimensional theories of laminated plates, *Communications in Applied Numerical Methods* 3 (1987) 173 – 180.
- J. N. Reddy, *Mechanics of laminated composite plates : theory and analysis*, CRC Press, Boca Raton (1997).
- G. Liu, J. Tani, K. Watanabe, T. Ohyoshi, Lamb wave propagation in anisotropic laminates, *Journal of Applied Mechanics-transactions of The Asme - J Appl Mech* 57 (1990) 923–929.
- G. Liu, Z. Xi, Y. Horie, Elastic waves in anisotropic laminates, *Applied Mechanics Reviews - Appl Mech Rev* 56 (2002).
- H. Poincaré, Sur les intégrales irrégulières : Des équations linéaires, *Acta Math.* 8 (1886) 295–344.
- K. O. Friedrichs, R. F. Dressler, A boundary-layer theory for elastic plates, *Communications on Pure and Applied Mathematics* 14 (1961) 1–33.

-
- A. Goldenveizer, Derivation of an approximate theory of bending of a plate by the method of asymptotic integration of the equations of the theory of elasticity, *Journal of Applied Mathematics and Mechanics* 26 (1962) 1000 – 1025.
- A. Goldenveizer, The principles of reducing three-dimensional problems of elasticity to two-dimensional problems of the theory of plates and shells (1966).
- E. Reissner, J. L. Synge, On the derivation of boundary conditions for plate theory, *Proceedings of the Royal Society of London. Series A. Mathematical and Physical Sciences* 276 (1963) 178–186.
- H. Le Dret, *Problèmes Variationnels dans les Multi-Domaines : Modélisation des Jonctions et Applications*, Masson, 1991.
- M. Dauge, E. Faou, Z. Yosibash, *Plates and Shells : Asymptotic Expansions and Hierarchical Models*, American Cancer Society, pp. 1–39.
- E. Sanchez-Palencia, *Non-Homogenous Media and Vibration Theory*, volume 127, 1980.
- J. Sanchez-Hubert, E. Sanchez-Palencia, *Introduction aux Méthodes Asymptotiques et à l’Homogénéisation*, pp. xiv+266.
- D. Caillerie, J. C. Nedelec, Thin elastic and periodic plates, *Mathematical Methods in the Applied Sciences* 6 (1984) 159–191.
- T. Lewinski, Effective models of composite periodic plates-i. asymptotic solution, *International Journal of Solids and Structures* 27 (1991) 1155 – 1172.
- N. Bejjani, Implementation of the asymptotic expansion method, 2019. <https://github.com/Nadinebejjani/Asymptotic-Expansions.git>.
- J.-L. Lagrange, Nouvelle méthode pour résoudre les équations littérales par le moyen des séries., Chez Haude et Spener, Libraires de la Cour et de l’Académie royale, 1770.
- N. G. De Bruijn, *Asymptotic Methods in Analysis*, North Holland Publishing Co. - Amsterdam, 1958.